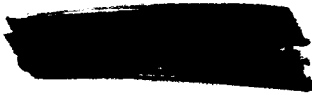


MASTER COPY



ORNL-4018

C-93a - Advanced Concepts for Future

AEC RESEARCH AND DEVELOPMENT REPORT

Application - Reactor Experiments

M-3679 (46th ed., Rev.)

Classification Cancelled  
Or Changed To  
By Authority Of AEC  
Date SEP 13 1971

MEDIUM-POWER REACTOR EXPERIMENT

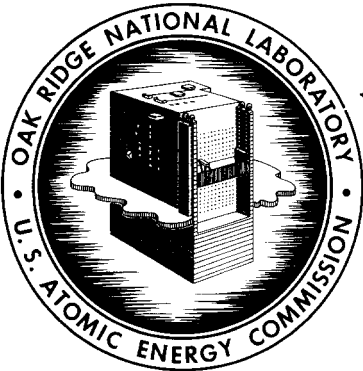
QUARTERLY PROGRESS REPORT

FOR PERIOD ENDING JUNE 30, 1966

SPECIAL REREVIEW FINAL DETERMINATION

CLASS. \_\_\_\_\_ AUTH. \_\_\_\_\_

REVIEWERS/VERIFYERS	CLASS.	DATE
(1) <u>Pd Baker</u>	<u>U</u>	<u>6-30-80</u>
(2) <u>At Goresky</u>	<u>U</u>	<u>7-7-80</u>



**OAK RIDGE NATIONAL LABORATORY**

operated by

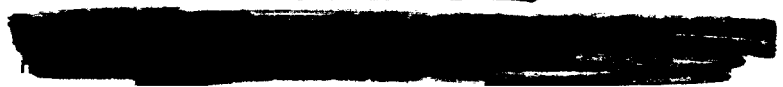
**UNION CARBIDE CORPORATION**

for the

**U.S. ATOMIC ENERGY COMMISSION**

GROUP 1

Excluded from Automatic  
Downgrading and Declassification



*U-2503 6/30/80*

LEGAL NOTICE

This report was prepared as an account of Government sponsored work. Neither the United States, nor the Commission, nor any person acting on behalf of the Commission:

- A. Makes any warranty or representation, expressed or implied, with respect to the accuracy, completeness, or usefulness of the information contained in this report, or that the use of any information, apparatus, method, or process disclosed in this report may not infringe privately owned rights; or
- B. Assumes any liabilities with respect to the use of, or for damages resulting from the use of any information, apparatus, method, or process disclosed in this report.

As used in the above, "person acting on behalf of the Commission" includes any employee or contractor of the Commission, or employee of such contractor, to the extent that such employee or contractor of the Commission, or employee of such contractor prepares, disseminates, or provides access to, any information pursuant to his employment or contract with the Commission, or his employment with such contractor.

ORNL-4018

Contract No. W-7405-eng-26

MEDIUM-POWER REACTOR EXPERIMENT  
QUARTERLY PROGRESS REPORT  
for Period Ending June 30, 1966

A. P. Fraas, Project Manager

DECEMBER 1966

OAK RIDGE NATIONAL LABORATORY  
Oak Ridge, Tennessee  
operated by  
UNION CARBIDE CORPORATION  
for the  
U.S. ATOMIC ENERGY COMMISSION

~~RESTRICTED DATA~~

This document contains Restricted Data as defined in the Atomic Energy Act of 1954. Its transmission or the disclosure of its contents in any manner to an unauthorized person is prohibited.

GROUP 1

Excluded from Automatic Downgrading and Declassification

~~RESTRICTED DATA~~



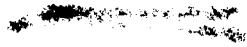
## FOREWORD

A program for investigating the feasibility of a boiling-potassium reactor was initiated at ORNL in FY 1962. Perhaps the most promising application for this reactor is for power plants designed to produce electricity in space using a potassium Rankine cycle with a single working fluid to cool the reactor, carry out the thermodynamic cycle, lubricate the bearings in the turbine and generator, and cool the generator. It also shows promise for other mobile power plant applications. In FY 1962 and FY 1963, work on this program was covered in the Space Power Program Semiannual Progress Reports. In FY 1964, the reporting was supplemented by two additional quarterly reports, entitled "Medium-Power Reactor Experiment Progress Report."

By the latter part of FY 1964 favorable results of the feasibility investigation led to the decision to proceed with a program to run a reactor experiment designed primarily to investigate the feasibility of operating a boiling-potassium reactor, particularly its stability and control characteristics. The work has been largely completed and reported in some 96 technical papers and reports.

The program was sharply curtailed early in 1966, and only a small close-out effort has been budgeted for FY 1967.





CONTENTS

	<u>Page</u>
FOREWORD .....	iii
SUMMARY .....	vii
1. MPRE DESIGN .....	1
Summary of Principal Accomplishments and Current Status of Effort on MPRE Program .....	1
Program Literature -- Reports and Papers Prepared in the Course of the MPRE Program .....	8
Dimensional and Performance Data .....	16
MPRE Hot-Channel Analysis .....	16
Analysis Conditions .....	16
Discussion of Computer Results .....	23
Zero-Gravity Boiler Recirculation System .....	26
Stress Analyses of MPRE Pressure Vessel .....	28
2. REACTOR PHYSICS .....	33
Transient Analysis .....	33
Reference Reactor .....	50
3. DEVELOPMENT TESTS .....	52
Liquid-Metal Jet Pump Test Loop .....	52
Tests of Ultrasonic Nucleation in Potassium .....	55
Liquid-Metal Flowmeter Calibration Facility .....	63
Single-Rod Capsule Tests with Potassium .....	64
Critical-Heat-Flux Tests of Seven-Rod Boiler with Water ..	66
Small Water System .....	67
Small Potassium Systems .....	68
System No. 1 .....	68
System No. 2 .....	68
Tests of Turbine Pumps for Boiling-Potassium Systems .....	69
Tests of Nozzle and Turbine-Blade Materials in Forced- Circulation Boiling-Potassium Loop .....	76
Intermediate Water System Operation .....	77
Intermediate Potassium System .....	77
Large Potassium System .....	79
Reactor Control-Plug Drive System .....	79

Fuel Element Irradiation Tests .....	84
Zero-Gravity Experiments .....	86
Flight Objectives .....	87
May 17 Flight Results .....	88
Conclusions .....	89
4. MATERIALS .....	91
Natural-Circulation Boiling-Potassium Loop Tests .....	91
Loop NCL-10 .....	91
Loop NCL-11 .....	92
Brazing Alloy Development .....	95
Behavior of Stainless Steel Welds Under Cyclic Loading ....	96
Bore-Seal Development .....	99
Analysis of IPS Filter Deposit .....	100

SUMMARY

1. MPRE Design

Summary of Principal Accomplishments and Current Status of Effort on MPRE Program. Inasmuch as the abrupt cancellation of the MPRE program makes this the last quarterly progress report, the first section is devoted to a summary of the principal accomplishments and current status of the effort. The work is divided into ten major problem areas, which are used as headings in a table that traces the chronological development of the work. A second table summarizes the accumulated operating time with potassium systems at ORNL. The section closes with a summary of the work that would have to be carried out before a unit could be launched if the program were to be reinstated. A list of 94 reports and technical papers published in the course of the MPRE program is appended at the end of the section.

MPRE Hot-Channel Analysis. The hot-spot problem in a boiling reactor is very different from that in a liquid- or gas-cooled reactor, particularly if (as in the MPRE) lateral flow between the fuel rods is possible. The special problems of a boiling reactor are outlined, an analysis technique is developed, and the results of typical calculations are summarized. These indicate that the hot-channel and hot-spot effects are very much less severe in a boiling reactor than in a liquid- or gas-cooled reactor.

Zero-Gravity Boiler Recirculation System. A new approach to the vapor separation and boiler recirculation problems was devised. This makes use of a free-turbine-driven centrifuge that also acts as the expansion tank and the boiler recirculating pump. The proportions of a typical unit together with its principal advantages and disadvantages are outlined.

Stress Analysis of MPRE Pressure Vessel. The effects of nozzle penetrations for the jet pumps and instrumentation in the head of the MPRE reactor pressure vessel were investigated by reworking the plain-carbon-steel model to include these components. Strain gages were installed where high stresses seemed likely, and the vessel was pressurized

hydraulically. Results show an increase of only about 10% in the maximum stresses found; hence no change in the vessel design appears to be required.

## 2. Reactor Physics

Transient Analysis. A mathematical model of the MPRE reactor was elaborated to include all of the major elements of the system, and the model was used to examine the dynamic response of the system to a number of extreme hypothetical perturbations. It was found that if all the 0.5%  $\Delta k$  available in the control rods under the clean, hot condition were inserted rapidly, severe overshoots in power and temperature would occur, but it appears that the reactor might survive such accidents. When a scram was included in the program with a 10-msec delay between initiation of the scram signal and the onset of motion of the control mechanism, the reactor conditions scarcely departed from the steady-state values before the excursion was terminated and the power dropped to a negligible value.

Reference Reactor. A detailed examination of the power distribution around the irregular parameter of the core was carried out with a DDK calculation. The analysis indicated that no serious hot spots would be produced by the irregularities.

## 3. Development Tests

Liquid-Metal Jet-Pump Test Loop. The system for testing potassium jet pumps was completed, and initial tests in the noncavitating region were carried out. A comparison of the results with data for water show excellent agreement.

Tests of Ultrasonic Nucleation in Potassium. A single Firerod capsule fitted with pressure, temperature, and sound monitoring instrumentation showed that an ultrasonic nucleation device was very effective in initiating and maintaining good nucleation in boiling potassium with no nucleation sites present.

Liquid-Metal Flowmeter Calibration Facility. Tests to investigate improved techniques for manufacturing heaters indicate that the manufacturer has achieved better compaction of the electrical insulation and

that good joints can be obtained between Nichrome-5 heater element wires and Nichrome-5 leads by simple compaction.

Critical-Heat-Flux Tests of Seven-Rod Boiler with Water. A comparison was made of the relative effectiveness of a thermocouple in the center of the rod and the leakage current to ground as indicators of burnout. Both were found to give excellent indications of incipient burnout conditions.

Small Water System. The system was modified to incorporate the vapor and liquid piping configuration planned for the installation of the Mark-2 turbine pump in the second small potassium system (SPS-2). Tests were run to determine the performance of the turbine pump and the system as a whole. Excessive lubricant leakage to the turbine cavity required reworking of parts to reduce the bearing running clearances at the turbine end.

Small Potassium Systems. A series of tests to determine burnout heat-flux limitations in the SPS-1 boiler was terminated after 241 hr because of thermocouple failures in all seven heater rods, electrical failures in two heater rods, and a high leakage current to ground in one of the remaining rods. The system was shut down for installation of new heater rods that had been fabricated with improved techniques and installed in a new boiler assembly designed for a 1/16-in. rod spacing.

After 71 hr of boiling operation, SPS-2 was shut down as a consequence of internal failures in the heater rods. A new rod bundle is being fabricated with the new improved heater rods, and the Mark-2 turbine pump is being installed in the system.

Tests of Turbine Pumps for Boiling-Potassium Systems. The Mark 1 turbine pump was removed from the IPS system after 2586 hr of operation with 46 starts and stops. On disassembly it was found that there was no sign of either turbine-bucket erosion or cavitation damage in the impeller. No difficulties were experienced with galling of the parts in the course of the disassembly, possibly as a consequence of the use of Aquadag in the assembly of close-fitting parts such as threads.

Tests of Nozzle and Turbine-Blade Materials in Forced-Circulation Boiling-Potassium Loop. The test was interrupted after a total of 3600 hr because of a potassium leak to the atmosphere. This stemmed from an

improper mounting of an electric heater, which caused a leak through the joint between the thermocouple and the adapter sleeve used to attach it to the boiler. The leak has been repaired, and operation will continue.

Intermediate Water System Operation. A new dummy heater rod was installed in the center of the rod bundle to obtain better data on the boiler pressure drop.

Intermediate Potassium System. Because of the relatively long period required to obtain a new rod bundle, the first rod bundle used in the IPS system was reinstalled in an effort to operate the system for a time while a new rod bundle with heater rods fabricated by improved techniques was being prepared. The test was terminated after 6 1/2 hr of operation because it became evident that the rods had deteriorated further. The rod bundle was removed, and the new bundle of improved rods was installed. Testing will resume early in July to determine the performance characteristics of the system up to the full-rated output of 4 kw/rod.

Large Potassium System. Work on the system was stopped at the beginning of the previous quarter as a consequence of the budget cut. The fabricated components have been stored.

Reactor Control-Plug Drive System. Detailed measurements of the velocity and deceleration characteristics of the control-plug drive mechanism under scram conditions were carried out, and satisfactory performance was demonstrated.

Fuel Element Irradiation Tests. Irradiation is continuing on an extensometer test assembly and on two MPRE prototype fuel element capsules. Measurements with the extensometer capsule show that the UO<sub>2</sub> is continuing to expand and contract with temperature as if it were a monolithic column independent of the cladding.

Zero-Gravity Experiments. Flight tests in the KC-135 airplane at Wright Field demonstrated that the revised separator-expansion tank assembly is basically sound in design. Difficulty was experienced with air-bubble entrainment in the liquid in the expansion tank, but it is believed that this would be corrected if a liquid-vapor system were employed rather than the air-water system used in the test because subcooling of the tank by heat losses or by subcooled liquid in the swirl

jets would more than suffice to condense vapor bubbles entrained at the rate shown in the flight test. The obvious next step in the program is to repeat the test with steam in place of air, an approach that appears to be quite feasible and consistent with the flight-test limitations of the KC-135.

#### 4. Materials

Natural-Circulation Boiling-Potassium Loop Tests. The effects of various amounts of oxygen contamination in the potassium were investigated in natural-convection loops.

Brazing Alloy Development. Tests of a series of Ni, Ge, Fe, Cr, and Si brazing alloys show good strength both in the as-brazed condition and after aging for 1000 hr at 1500°F.

Behavior of Stainless Steel Welds Under Cyclic Loading. Tests of welded stainless steel specimens indicate a greatly reduced resistance to strain cycling in the base metal adjacent to the weld. It was also found that the effect can be greatly reduced by a postweld heat treatment.

Bore-Seal Development. Capsule tests for 1000 hr at both 600 and 1000°F indicate that an 82% Ti-18% Cu braze is resistant to attack by potassium vapor. The tests also indicate that, while a layer of nickel plating is not effective in protecting a copper-brazed joint, a 3-mil vapor-deposited tungsten layer appears to provide adequate protection.

Analysis of IPS Filter Deposit. Examination of the filter from the IPS system after 2600 hr of testing showed that a thin layer of a fine-grained grayish deposit covered most of the filter-screen surface. Examination of this deposit indicates that a small amount of oxygen entered the system during some phase of the repair and cleanup operations, and this led to a small amount of corrosion that caused the deposit.

1. MPRE DESIGN

A. P. Fraas

Inasmuch as the abrupt cancellation of the MPRE program makes this the last quarterly progress report, it appears in order to begin with a brief summary of the more significant accomplishments to date in the MPRE program and the current status of the design and development effort. Subsequent sections present the progress during the quarter.

Summary of Principal Accomplishments and Current  
Status of Effort on MPRE Program

A. P. Fraas

A convenient way to summarize the accomplishments of the MPRE program and to indicate the status of the development effort at the point where the program is being closed is to make use of tables and a list of reports on the program (see Refs. 1-94 in following Section, pp. 8-15.

The most significant accomplishments are listed below:

1. The compatibility of stainless steel with boiling potassium was demonstrated.<sup>54</sup>
2. Sufficient data on the heat transfer and burnout limitations was obtained with boiling potassium to validate the boiling potassium reactor concept.<sup>31,43,45</sup>
3. Calculations and critical experiments showed that boiling potassium reactors can be proportioned to give both a good power distribution and good nuclear stability and control characteristics.<sup>17,23</sup>
4. Good boiling flow stability and good flow distribution were demonstrated in electrically heated core mockups.<sup>43,71</sup>
5. Nucleation rings were developed that serve to initiate and maintain smooth nucleate boiling of potassium.<sup>43,93</sup>
6. A new single-loop Rankine cycle system was devised in which the only electronic control equipment is that required to couple the reactor to the generator output.<sup>69,71,72</sup> Studies and system tests showed that it has excellent stability and control characteristics.<sup>70,72,73</sup>

7. A 37%-scale electrically heated mockup of the MPRE was operated 2500 hr with a potassium-vapor turbine-driven feed pump.<sup>92,93</sup>

8. A full-scale electrically heated mockup of the MPRE is about two-thirds completed.<sup>92,93</sup>

9. Two full-scale MPRE fuel elements were operated in-pile for 10,000 hr with no sign of difficulty. One has been removed for inspection and the test is continuing on the other as of July 1966.

10. A light-weight tapered-tube direct condenser designed for space operation was developed and shown to give a uniform flow distribution with good flow stability.<sup>16,67</sup>

11. A new type of compact vapor separator-expansion tank assembly was developed and operated under zero-gravity conditions.<sup>46,94</sup>

12. Studies showed that a single-loop Rankine cycle system is much superior to two- or three-loop systems from the standpoint of both performance and reliability and may be scaled readily to meet the range of requirements from 30 kw(e) to 5 Mw(e).<sup>16,17</sup>

Table 1.1 presents a considerably more detailed picture than that given above of the steps in the program and is a modification of a table prepared early in the MPRE development program (and referred to briefly in Ref. 80, p. 71) to highlight the principal feasibility problems and to indicate the principal experiments planned to cope with them. Most of these problems have been solved (with about the effort originally contemplated), and the work carried out is covered in the reports listed in the next section. In view of the large number of reports and the many cross references required to relate them, it appeared best to compile these in a list rather than to present them at the bottom of each page as is normally done with references in ORNL quarterly reports and is done elsewhere in this report. This approach also provides a convenient means for referencing the cryptic statements in Table 1.1. To facilitate use of this list of references, it is divided into categories that correspond with the column headings of Table 1.1. In addition, the quarterly progress reports are included at the end of the list. Within each category the reports are listed essentially in the order in which the work was carried out; thus the order does not always correspond with the order of the dates of publication.

Table 1.1. Summary of Major Steps in the MPRE Program

Year	General Design and Analysis	Reactor Core Evaluation	Boiler	Vapor Separator and Expansion Tank	Corrosion, Mass Transfer, and Materials Problems	Turbine Pump and Turbine-Generator	Jet Pumps	Condenser Radiator	System Stability and Control	System Endurance Tests
FY-59 -60 -61	Ten working fluids evaluated. <sup>1,2,3</sup> One-loop, stainless steel-UO <sub>2</sub> -potassium system devised and found to give smallest radiator, lowest specific weight, and highest reliability. <sup>1,2,3</sup> Boiling flow stability requirements defined. <sup>30</sup> Preliminary calculations indicated small negative void coefficient possible in a boiling-potassium reactor.		Heat transfer and burnout data from single-tube boiler showed potassium boiling heat transfer performance similar to that of water. <sup>31</sup>		Capsule and natural-convection loop tests showed stainless steel compatible with boiling potassium. <sup>47</sup>			Tests showed high effectiveness for proposed radiator tube-reflector assembly.		
FY-62	Basic development program outlined and preliminary layouts for 7- and 91-rod test rigs prepared. <sup>79</sup> Reactor-vapor separator-expansion tank assembly and basic system layout evolved. <sup>79</sup> Flow in tapered-tube condenser analyzed. <sup>65</sup>	Reactor calculations defined 241-rod MPRE core with good power distribution and negligible void coefficient. <sup>79</sup>	Four-rod water and seven-rod Freon boilers showed excellent internal flow stability consistent with analyses. <sup>79,80</sup> First Firerods tested in boiling potassium. <sup>80</sup>	99% efficient liquid removal demonstrated with small toroidal air-water separator. <sup>80,81</sup>		Small turbine pump for seven-rod boiler built and tested with steam. <sup>80</sup> Tungsten carbide bearings run 4000 hr in potassium with 350 starts and stops under load. <sup>80,81</sup>	Water tests showed that a jet pump operated with cavitation suppression head <1 in. H <sub>2</sub> O. <sup>79</sup>			Small water-steam system with boiler and turbine pump gave smooth bootstrap start and stable operation over entire power range. <sup>80</sup>
FY-63	Effectiveness of capillary forces for controlling free liquid surfaces analyzed. <sup>81</sup> Analytical solution of system performance characteristics, flow distribution, and component matching requirements worked out. <sup>82</sup>	Critical experiments verified calculated critical mass, power distribution, and negative void coefficient for potassium in coolant passages. <sup>19,20,81,82</sup>	Good stable flow distribution demonstrated in 91-rod water boiler. <sup>81</sup> Explosive boiling problems evaluated; <sup>81</sup> hot fingers and nucleation rings found to be good solutions. <sup>82</sup>	Greater than 99% removal of water demonstrated with toroidal vapor separators for 7- and 91-rod boilers using both air-water and steam-water mixtures. <sup>46</sup>		Brittleness of molybdenum required design refinements in turbine pumps with carbide bearings for SPS-1 and IPS. <sup>58</sup> Little erosion of simulated turbine bucket was found after 750 hr in 3000 fps jet of 84%-quality potassium vapor. <sup>58</sup>	Noncavitating performance determined for jet pumps for 7- and 91-rod boiler systems.	Zero-gravity tests of free liquid surfaces in tapered tubes run in NASA drop-test tower. <sup>81</sup> Test of 12-tapered-tube condenser with steam checked analysis. <sup>81</sup>	Seven-rod water boiler system mockup showed good stability and control characteristics from bootstrap start to full power with cavitation control of liquid inventory distribution. <sup>81</sup>	Forced-convection boiling potassium corrosion loop operated for 1000 hr. <sup>82</sup>
FY-64	Launch package configuration evolved. <sup>10</sup> Preliminary design of test facility prepared. <sup>8</sup> Poor flow distribution at low condenser temperatures found in 12-tube potassium condenser corrected by deliberate design for choking at condenser tube inlets. <sup>67</sup>		Burnout limitation data obtained with 7- and 91-rod water boilers. <sup>43</sup>	Vapor separators developed for 91-rod potassium boilers and for zero-gravity test of air-water unit of seven-rod boiler size. <sup>46</sup>	Forced-convection corrosion loop tests showed that molybdenum parts in stainless steel systems are sensitive to O <sub>2</sub> contamination of potassium. The use of hot traps is suggested. <sup>54</sup>	World's first potassium vapor turbine operated in SPS-1. Tungsten carbide bearings did not scuff in 50 starts and stops. <sup>85</sup> No corrosion or erosion of molybdenum turbine pump or K-94 bearings. <sup>58,85,86</sup>	Technique for obtaining good cavitation performance test data developed. <sup>85</sup> Basic relations for cavitation performance developed and correlated with jet pump test data. <sup>59</sup>	Good flow distribution and good flow stability demonstrated with 144 tapered-tube condenser in water-steam system. <sup>70</sup>	91-rod water boiler system mockup demonstrated good stability and control characteristics from bootstrap start to 125% power. <sup>71</sup> Seven-rod potassium boiler system showed performance similar to that of seven-rod water boiler system. <sup>85</sup>	Forced-convection corrosion loops operated 2820 hr. <sup>54</sup> SPS-1 ran 170 hr. <sup>86</sup>
FY-65	Test facility designed and hazards report prepared. <sup>8,12</sup> Analytical design of MPRE and full-scale mockup largely completed. <sup>89,90</sup>	Fuel elements specified and procured for hot critical experiment. <sup>51</sup> In-pile fuel element tests started. Effects of local variations in potassium reactivity coefficients investigated and found to be small. <sup>23</sup>	Smooth initiation of nucleate boiling demonstrated in 91-rod potassium boiler both with hot fingers and with nucleation rings only. <sup>78</sup>	Vapor separator-expansion tank for full-scale MPRE developed to give ~99% quality in air-water tests. <sup>46</sup> Zero-gravity tests with seven-rod size air-water separator in KC-135 airplane showed that a strong swirl is required for low lateral acceleration. <sup>87</sup>	Specimens from loops showed that corrosion mechanism in a recirculating boiler system is quite different from that in all-liquid loops. Mass-transfer rates are much lower, and material moves from condenser to boiler. <sup>54</sup>	Bearing trouble in seven-rod potassium boiler system showed that filter is essential in lube supply. <sup>58</sup> Bearing trouble in 91-rod system showed loads should be in same direction at both ends of shaft to avoid edge loading. <sup>58</sup>	Extensive cavitation limit tests of jet pumps for MPRE show different types of cavitation and sensitivity to geometry. <sup>60</sup>	Infrared photos prove excellent for investigating flow and temperature distribution in potassium condenser-radiator. <sup>67</sup> Flow distribution stable and uniform in 144-tube potassium condenser. <sup>67</sup>	Electronic analog correlated well with 91-rod electrically heated mockups; <sup>70</sup> 91-rod potassium boiler system showed characteristics similar to those of water system. <sup>71</sup>	Forced-convection corrosion loops operated 1540 hr. <sup>54</sup> SPS-1 ran 1376 hr. IPS ran 400 hr. <sup>89</sup>
FY-66	Scale-up potential of MPRE to 30 Mw(t) and superiority of one-loop system in size, weight, and reliability shown. <sup>16,17</sup> Materials problems and limitations delineated in series of staff papers. <sup>49,51-53</sup> Variations of MPRE system delineated to show the many degrees of freedom available. <sup>16,18</sup> Stress analysis of reactor pressure vessel completed. <sup>19</sup>	Control-plug drive prototype completed 2000 scrams satisfactorily. <sup>26</sup> Fuel element in-pile tests show UO <sub>2</sub> expands and contracts as if monolithic and independent of cladding. <sup>93,94</sup> Two fuel elements completed 9500 hr in-pile at MPRE full-power design conditions. <sup>94</sup>	Preliminary tests with potassium in seven-rod boiler showed burnout limit at least as high as for water. <sup>92</sup> Seven-rod-boiler zero-gravity test rig designed, built, and run upside down.	Revised toroidal vapor separator-expansion tank zero-gravity design developed in 91-rod boiler size. Bench tests show insensitivity to attitude. <sup>92</sup> Zero-gravity tests in KC-135 airplane showed fairly good behavior of free surface. <sup>94</sup>	Tests showed that vapor-deposited tungsten protected brazed Al <sub>2</sub> O <sub>3</sub> -Covar joints better than nickel plate. <sup>94</sup> Specimens removed from seven-rod boiler system after 4500 hr showed little corrosion and mass transfer. <sup>94</sup>	No erosion found in IPS turbine and pump after 2500 hr with cavitation in pump operating at 2000 fps with 95%-quality vapor. <sup>94</sup> Cavitation limit in electromagnetic pump depends on inert-gas pressure in expansion tank. New brazing technique gives corrosion-resistant joint for generator bore seal. <sup>94</sup>	Compact jet pump layout developed for MPRE expansion tank. <sup>91</sup> Rig built for testing jet pumps in potassium. Test data correlated well with similar data for water. <sup>94</sup>	Transparent condenser designed for zero-gravity tests operated in seven-rod water boiler system. <sup>92</sup> Tests run with electrically heated rod with fins and reflector checked performance calculations. <sup>68</sup>	Good correlation between 91-rod potassium and water boiler systems and electronic analog, including control of liquid inventory distribution. <sup>70,71</sup> Good stability and control characteristics found for electronic analog of MPRE reactor and turbine generator. <sup>72</sup>	SPS ran 2900 hr. <sup>54</sup> IPS ran 2800 hr. <sup>77</sup> Completed 10,000 hr with forced-convection loops. <sup>54</sup>

The problem areas implicit in Table 1.1 were called out and listed explicitly in a program summary report prepared two years ago.<sup>11</sup> While in the interest of brevity this list is not included here, it is worth noting that only one major unforeseen problem was encountered in the five years of the program, that is, liquid superheating and explosive boiling in potassium.<sup>35-37,81</sup> Nucleation rings were found to provide adequate nucleation sites to initiate smooth nucleate boiling and maintain it over a broad range of operating conditions (Ref. 81, pp. 113-122; Ref. 82, pp. 54-65). Two other problems proved to be more difficult than anticipated; first, the system is quite sensitive to the presence of noncondensables,<sup>71</sup> and second potassium-lubricated bearings are very sensitive to fine particles down to diameters of about 5  $\mu$ .<sup>58</sup> Both these problems were resolved by refinements in design.<sup>58</sup> A fourth major problem that proved to be an obstacle in the test program, though not involved in the nuclear plant, was good quality control in the fabrication of the electric heater rods used to simulate fuel elements.<sup>92-94</sup> This prevented accumulation of the amount of endurance testing that would otherwise have been achieved.

A narrative summary follows to put the information presented above in perspective. As indicated in the first column of Table 1.1, a basic element in the MPRE program was a comprehensive review of nuclear electric space power plant applications so that performance, size, weight, reliability, and related requirements could be delineated for the principal types of space vehicle and mission.<sup>1,3,4,15</sup> A wide variety of thermodynamic cycles, power plant systems, and materials combinations was examined with a view to meeting these requirements, and both the initial work in the latter 1950's<sup>1,2</sup> and the recent critical reviews in the past year<sup>16-18</sup> indicate that a single-loop version of a Rankine cycle system employing potassium vapor as the working fluid promises both a higher performance potential and a greater system reliability than those of any other cycle or system that has been given serious consideration. Such a system built of stainless steel gives a sufficiently high performance to satisfy the requirements for most of the missions that are contemplated, and the cost and time required to develop it appear to be quite modest.

If such a system of stainless steel were proved out, extrapolation of this experience to the design and development of a similar refractory metal system that would meet the performance requirements for the more difficult missions should be relatively straightforward.<sup>16,17</sup>

The design of the reactor<sup>15,23,25,46</sup> and all the components, except the turbine generator, together with the integration of these components into a complete system was largely completed. This work included the design and most of the construction of a full-scale electrically heated mockup, extensive tests of the prototypes for the free-turbine-driven feed pump<sup>58</sup> and the tapered-tube direct condenser radiator,<sup>67</sup> critical experiments of the reactor,<sup>23</sup> stress analyses of the reactor pressure vessel,<sup>19</sup> development of the vapor separator and expansion tank,<sup>46</sup> and the design of the facility,<sup>8</sup> including a reactor safety analysis.<sup>12</sup> Problems of operating the system under zero-gravity conditions were studied,<sup>13</sup> and a series of experiments to investigate these problems was designed for flight tests in the KC-135 airplane at Wright Field. Ground tests of both a transparent boiler and a transparent condenser were conducted, and both ground and flight tests of a vapor separator-expansion tank unit were carried out with favorable results.<sup>94</sup>

Results of extensive endurance tests of reduced-scale electrically heated mockups of the MPRE system indicate that corrosion and mass transfer in a stainless steel system with molybdenum alloy turbine parts and tungsten carbide bearings lead to negligible amounts of mass transfer and a maximum intergranular penetration of only about 1/2 mil in 4500 hr. Extensive analyses and system tests indicate that single-loop systems can be designed and built so that they will operate stably over a wide range of powers<sup>69-73</sup> with only two simple basic control functions<sup>16</sup> and can be put through a bootstrap startup. Consequently, the single-loop system can be built with a sufficiently simple set of electronic instrumentation and control equipment for a high system reliability to be obtained.<sup>16</sup>

The amount of operating experience accumulated in the high-temperature endurance testing of both components and systems is summarized in Table 1.2. This work includes the completion of 10,000 hr of in-pile operation of two fuel elements at full design temperature and power conditions. As a matter of interest, an additional column is included to

Table 1.2. Summary of Operating Experience at ORNL  
with Potassium Systems up to June 1966

	Accumulated Operating Time (hr)	
	Stainless Steel Systems	Niobium Systems
Corrosion tests		
Thermal-convection loops	22,000	21,000
Forced-convection loops	12,000	3,000
Component tests		
Electric heater	95,000	
Simulated system	7,700	
Centrifugal pumps	(3,100) <sup>a</sup>	
Turbines	(3,100) <sup>a</sup>	
Bearing test rig	4,500	
Generators		
Heat exchangers	(11,000) <sup>a</sup>	
Heat transfer	2,800	
Miscellaneous	16,000	
Reactor tests	0	
Total	160,000	24,000
Fuel element in-pile tests (in NaK-filled capsules)	26,000	

<sup>a</sup>Parentheses around numbers indicate that there is duplication, e.g., the 11,000 hr of heat exchanger testing was part of the simulated system testing.

summarize the operating experience accumulated with potassium boiling in niobium systems in the high-temperature materials program.

If the program were to be reinstated, the major steps remaining before the first power plant could be launched are summarized below:

1. Determine the effects of rod size and spacing on the burnout-limited heat flux in boiling potassium.
2. Demonstrate the desired service life with high reliability by operating at least one full-scale and four reduced-scale systems for at least 10,000 hr each.

3. Demonstrate a low fission-product-release rate from a defective fuel element in potassium by an in-pile test, and subject four fuel elements to 10,000- to 20,000-hr tests.
4. Demonstrate good control of free liquid surfaces by zero-gravity tests of water mockups of both components and a complete system in a KC-135 airplane.
5. Demonstrate zero-gravity startup and restart capability of a small system mockup with all components in a horizontal plane.
6. Demonstrate by testing in a manned orbiting laboratory the startup and operating characteristics of a reduced-scale electrically heated steam-water mockup of the system.
7. Demonstrate the feasibility and reliability of a potassium vapor turbine-generator unit.
8. Demonstrate in a ground test (the MPRE) the stability and control characteristics of a complete system, including the reactor and turbine-generator, and run a 10,000-hr endurance test.
9. Demonstrate satisfactory system startup and free-liquid-surface control characteristics under zero-gravity conditions by orbiting a potassium-vapor power plant complete except for the reactor, which would be replaced by a chemically fueled heat source.
10. Demonstrate the reliability of a launch package power plant configuration by subjecting three complete nuclear plants to 10,000-hr endurance tests.
11. Demonstrate flight worthiness of a complete power plant launch package by testing in an environmental test chamber.

There are three major sets of problems. The first two are primarily concerned with feasibility and involve (1) extensive operation of systems already built or under construction at ORNL and (2) the construction and operation of the MPRE. The third is the demonstration of the reliability and flight worthiness of a complete flight-configured power plant. A small amount of work is continuing in FY 1967 under a closeout program.

Program Literature - Reports and Papers Prepared in  
the Course of the MPRE Program

Design and Analysis

1. A. P. Fraas, Fission Reactors as a Source of Electrical Power in Space, pp. 151-163 in Proceedings of Second Symposium on Advanced Propulsion Concepts, Boston, Oct. 7-8, 1959, Vol. III, AFRD-60-2519.
2. M. L. Myers, Study of Outage Experience with Selected Boiler and Turbine Generator Units, USAEC Report ORNL-CF-60-3-56, Oak Ridge National Laboratory, March 1960.
3. A. P. Fraas et al., A Comparative Study of Fission-Reactor-Turbine-Generator Power Sources for Space Vehicles, USAEC Report ORNL-2768, Oak Ridge National Laboratory, September 1961.
4. M. Blander, L. G. Epel, A. P. Fraas, and R. F. Newton, Aluminum Chloride as a Thermodynamic Working Fluid and Heat Transfer Medium, USAEC Report ORNL-2677, Oak Ridge National Laboratory, Sept. 21, 1959.
5. P. G. Lafyatis, Hazards of Nuclear Power Units in Space Applications, USAEC Report ORNL-CF-60-2-18, Oak Ridge National Laboratory, February 1960.
6. A. P. Fraas, Heat Transfer Limitations for Dynamic Converters, in Proceedings of the Sixth AGARD Combustion and Propulsion Colloquium on Energy Sources and Energy Conversion, Cannes, France, March 16-20, 1964, Peramon Press, Paris.
7. A. P. Fraas, Reliability as a Criterion in Nuclear Space Power-Plant Design, in Proceedings of the Air Transport and Space Meeting, New York, April 27-30, 1964, SAE-ASME Paper No. 861A.
8. Medium-Power Reactor Experiment (MPRE) Test Facility Preliminary Design Report, USAEC Report ORNL-TM-820, Oak Ridge National Laboratory, Apr. 27, 1964.
9. A. P. Fraas, Boiling Potassium Reactor for Space, Nucleonics, 22(1): 72-74 (1964).
10. A. P. Fraas, The MPRE - A Boiling Potassium Reactor System, Third AIAA Aerospace Power Systems Conference, Philadelphia, Sept. 1-4, 1964, USAEC Report TID-7703.
11. Oak Ridge National Laboratory and AEC-DRD, Answers to Questions on the MPRE Posed by the President's Science Advisory Committee, Report WASH-1050, Sept. 23, 1964.
12. S. J. Ditto et al., MPRE Safety Analysis Report, USAEC Report ORNL-TM-898, Oak Ridge National Laboratory (to be published).

13. R. B. Korsmeyer, The Rankine Cycle in a Zero-Gravity Environment, USAEC Report ORNL-TM-1137, Oak Ridge National Laboratory, July 1965.
14. A. P. Fraas, Survey of Operating Conditions and Requirements for Nuclear Reactor Turbine-Generator Space Power Plants for the 1970-1985 Period, USAEC Report ORNL-TM-1364, Oak Ridge National Laboratory, January 1966.
15. G. Samuels, Fuel Element Design for Boiling Potassium Reactors, USAEC Report ORNL-TM-1344, Oak Ridge National Laboratory, January 1966.
16. A. P. Fraas and J. W. Michel, Comparison of 1-, 2-, and 3-Loop Systems for Nuclear Turbine-Generator Space Power Plants of 300 kw to 5 Mw of Electrical Output, USAEC Report ORNL-TM-1366, Oak Ridge National Laboratory, February 1966.
17. J. W. Michel, A. M. Perry, O. L. Smith, and J. V. Wilson, Design Study of Boiling Potassium Reactors for Thermal Outputs of 1 Mw to 30 Mw, USAEC Report ORNL-TM-1365, Oak Ridge National Laboratory, April 1966.
18. J. W. Michel, Summary of Possible Improvements to the MPRE and of Alternate Systems, USAEC Report ORNL-TM-1491, Oak Ridge National Laboratory (to be published).
19. F. J. Witt, R. C. Gwaltney, J. E. Smith, and R. S. Valachovic, Stress Analyses of MPRE Pressure Vessel, USAEC Report ORNL-4022, Oak Ridge National Laboratory (to be published).

#### Reactor Core Evaluation

20. J. T. Mihalczko, A Small Graphite-Reflected UO<sub>2</sub> Critical Assembly, USAEC Report ORNL-TM-450, Oak Ridge National Laboratory, Dec. 28, 1962. (Classified)
21. J. T. Mihalczko, A Small Graphite-Reflected UO<sub>2</sub> Critical Assembly, Part II, USAEC Report ORNL-TM-561, Oak Ridge National Laboratory, Apr. 8, 1963. (Classified)
22. J. T. Mihalczko, A Small Beryllium-Reflected UO<sub>2</sub> Assembly, USAEC Report ORNL-TM-655, Oak Ridge National Laboratory, July 23, 1963. (Classified)
23. A. M. Perry, Status of MPRE Core Design, pp. 36-49 in AIAA Specialist Conference on Rankine Space Power Systems, Vol. II, USAEC Report TID-22508, October 1965.
24. J. Foster, The MPRE Reactor Control Mechanism, pp. 50-62 in AIAA Specialist Conference on Rankine Space Power Systems, Vol. II, USAEC Report TID-22508, October 1965.

25. J. Foster and J. T. Meador, Design and Development of the MPRE Reactor Control Drive System, USAEC Report ORNL-TM-1608, Oak Ridge National Laboratory (to be published).
26. O. L. Smith and A. M. Perry, Some Calculations Performed on a Series of Conceptual Fast-Neutron Reactors Fueled with Highly Enriched  $UO_2$  or  $PuO_2$  and Reflected with Carbon, Beryllium Metal, or Beryllium Oxide, USAEC Report ORNL-TM-1620, Oak Ridge National Laboratory (to be published).
27. O. L. Smith, TACS - A Code to Calculate Fast Reactor Group Cross Sections from Point Data for Primary Use in  $S_n$  Transport Codes, USAEC Report ORNL-TM-1610, Oak Ridge National Laboratory (to be published).
28. O. L. Smith and J. C. Robinson, Possible Control Mechanisms for the MPRE, USAEC Report ORNL-TM-1619, Oak Ridge National Laboratory (to be published).
29. H. C. Claiborne, Reactor Shielding for Nuclear Turbine-Generator Space Power Plants, USAEC Report ORNL-TM-1367, Oak Ridge National Laboratory (to be published).

#### Boiler

30. A. P. Fraas, Flow Stability in Heat Transfer Matrices Under Boiling Conditions, USAEC Report ORNL-CF-59-11-1, Oak Ridge National Laboratory.
31. H. W. Hoffman and A. I. Krakoviak, Forced Convection Saturation Boiling of Potassium at Near Atmospheric Pressure, p. 182 in Proceedings of the 1962 High-Temperature Liquid Metals Heat Transfer Technology Meeting, USAEC Report BNL-756, Brookhaven National Laboratory.
32. H. W. Hoffman and A. I. Krakoviak, Convective Boiling with Liquid Potassium, p. 19 in Proceedings of the 1964 Fluid Mechanics Institute, Stanford University Press, 1964.
33. J. W. Cooke, Thermophysical Property Measurements of Alkali Liquid Metals, pp. 66-87 in Proceedings of 1963 High-Temperature Liquid-Metal Heat Transfer Technology Meeting, USAEC Report ORNL-3605, Oak Ridge National Laboratory, November 1964.
34. H. W. Hoffman, Recent Experimental Results in ORNL Studies with Boiling Potassium, pp. 334-350 in Proceedings of 1963 High-Temperature Liquid-Metal Heat Transfer Technology Meeting, USAEC Report ORNL-3605, Oak Ridge National Laboratory, November 1964.
35. H. W. Hoffman and A. I. Krakoviak, Studies in Boiling with Liquid Potassium, pp. 3.5.1-3.5.12 in Proceedings of the Second Joint USAEC-EURATOM Two-Phase Flow Meeting, USAEC Report CONF-640507, November 1964.

36. A. I. Krakoviak, Notes on the Liquid-Metal Boiling Phenomenon, USAEC Report ORNL-TM-618, Oak Ridge National Laboratory, July 1963.
37. J. A. Edwards, Superheat with Boiling Alkali Metals, USAEC Report ORNL-CF-64-10-1, Oak Ridge National Laboratory, October 1964.
38. A. I. Krakoviak, Superheat Requirements with Boiling Liquid Metals, pp. 310-333 in Proceedings of 1963 High-Temperature Liquid-Metal Heat Transfer Technology Meeting, USAEC Report ORNL-3605, Oak Ridge National Laboratory, November 1964.
39. Studies of Heat Transfer and Fluid Mechanics, Progress Report for Period January 1 - September 30, 1963, USAEC Report ORNL-TM-915, Oak Ridge National Laboratory, October 1964: A. I. Krakoviak and H. W. Hoffman, Boiling Potassium Heat Transfer, pp. 5-26; J. L. Wantland, Water Boiling in a Multirod Geometry, pp. 27-30; J. W. Cooke, Thermophysical Properties, Alkali Liquid Metals, pp. 97-107.
40. Studies in Heat Transfer and Fluid Mechanics, Progress Report for Period October 1, 1963 - June 30, 1964, USAEC Report ORNL-TM-1148, Oak Ridge National Laboratory, August 1965: A. I. Krakoviak and H. W. Hoffman, Boiling Potassium Heat Transfer, pp. 2-28; L. G. Alexander, Boiling in Multirod Geometries, pp. 29-31; T. C. Min, Analysis of Parallel Flow in Rod Clusters, pp. 50-63; J. W. Cooke, Thermophysical Properties, Alkali Liquid Metals, pp. 114-123.
41. J. A. Edwards and H. W. Hoffman, Superheat with Boiling Alkali Metals, in Proceedings of Conference on Application of High-Temperature Instrumentation to Liquid Metal Experiments, USAEC Report ANL-7100, Argonne National Laboratory, December 1965.
42. R. P. Wichner and H. W. Hoffman, Pressure Drop with Forced-Convection Boiling of Potassium, in Proceedings of Conference on Application of High-Temperature Instrumentation to Liquid Metal Experiments, USAEC Report ANL-7100, Argonne National Laboratory, December 1965.
43. M. M. Yarosh, Boiling Studies for the Medium Power Reactor Experiment, pp. 88-104 in AIAA Specialist Conference on Rankine Space Power Systems, Vol. II, USAEC Report TID-22508, October 1965.
44. R. P. Wichner, Vapor-Bubble Growth Rates in Superheated Liquid Metals, USAEC Report ORNL-TM-1413, Oak Ridge National Laboratory, July 1966.
45. M. E. LaVerne, Analysis of the Hot Spot Problem in the MPRE, USAEC Report ORNL-TM-1371, Oak Ridge National Laboratory (to be published).

#### Vapor Separator and Expansion Tank

46. J. Foster and J. K. Jones, Development of an Entrainment Separator for the MPRE, USAEC Report ORNL-TM-1609, Oak Ridge National Laboratory (to be published).

Corrosion, Mass Transfer, and Materials Problems

47. D. H. Jansen and E. E. Hoffman, Type 316 Stainless Steel, Inconel, and Haynes Alloy No. 25 Natural-Circulation Boiling Potassium Corrosion Test Loops, USAEC Report ORNL-3790, Oak Ridge National Laboratory, June 1965.
48. C. W. Fox, Fabrication of Critical Assembly Calandria, USAEC Report ORNL-TM-779, Oak Ridge National Laboratory, March 1964.
49. C. W. Fox, Development of Procedure for Welding Fuel Element End Closures at Reduced Pressure, USAEC Report ORNL-TM-1130, Oak Ridge National Laboratory, June 1965.
50. S. C. Weaver and J. L. Scott, Comparison of Reactor Fuels for High-Temperature Applications, USAEC Report ORNL-TM-1360, Oak Ridge National Laboratory, December 1965.
51. G. M. Tolson, MPRE Fuel Elements: Manufacture, Inspection, Drawings, and Specifications, USAEC Report ORNL-3902, Oak Ridge National Laboratory, January 1966.
52. R. W. Swindeman, Fatigue of Austenitic Stainless Steels in the Low and Intermediate Cycle Range, USAEC Report ORNL-TM-1363, Oak Ridge National Laboratory, January 1966.
53. W. R. Martin, Factors Affecting the Mechanical Properties of Stainless Steels at MPRE Operating Temperatures, USAEC Report ORNL-TM-1362, Oak Ridge National Laboratory, February 1966.
54. J. H. DeVan, Compatibility of Potassium with Structural Materials, USAEC Report ORNL-TM-1316, Oak Ridge National Laboratory, April 1966.

Turbine Pump and Turbine-Generator

55. L. G. Epel and J. R. Simmons, Thermodynamic Diagrams for Lithium, Sodium, and Potassium, USAEC Report ORNL-CF-59-11-67, Oak Ridge National Laboratory, November 1959.
56. M. L. Myers, Study of Outage Experience with Selected Boiler and Turbine Generator Units, USAEC Report ORNL-CF-60-3-56, Oak Ridge National Laboratory, March 1960.
57. W. R. Chambers, A. P. Fraas, and M. N. Ozisik, A Potassium-Steam Binary Vapor Cycle for Nuclear Power Plants, USAEC Report ORNL-3584, Oak Ridge National Laboratory, May 1964.
58. L. V. Wilson, H. C. Young, and A. M. Smith, Experience with Turbine-Driven Potassium Boiler-Feed Pumps for the MPRE, pp. 258-282 in AIAA Specialists Conference on Rankine Space Power Systems, Vol. I, USAEC Report CONF-651026, October 1965.

Jet Pumps

59. M. E. LaVerne, A New Similarity Parameter for Correlation of Jet Pump Cavitation, Proceedings of the 1965 Symposium on Cavitation in Fluid Machinery, American Society of Mechanical Engineers, Chicago (to be published).
60. R. S. Holcomb, M. E. Lackey, and F. E. Lynch, Performance of Experimental Jet Pumps Under Noncavitating and Cavitating Conditions, USAEC Report ORNL-3745, Oak Ridge National Laboratory, January 1966.

Condenser Radiator

61. A. P. Fraas, Radiators for Space Power Plants, USAEC Report ORNL-CF-59-8-31, Oak Ridge National Laboratory, August 1959.
62. A. P. Fraas, Improved Heat Sink for Space Vehicles, USAEC Report ORNL-CF-59-1-21, Oak Ridge National Laboratory, January 1959.
63. R. J. Hefner and P. G. Lafyatis, Protection of Space Vehicles from Meteorite Penetration, USAEC Report ORNL-CF-60-1-67, Oak Ridge National Laboratory, January 1960.
64. P. G. Lafyatis, Effect of Temperature on Radiator Weight for Space Vehicle Power Plants, USAEC Report ORNL-CF-60-1-109, Oak Ridge National Laboratory, January 1960.
65. R. B. Korsmeyer, Condensing Flow in Finned, Tapered Tubes, USAEC Report ORNL-TM-534, Oak Ridge National Laboratory, May 1963.
66. E. A. Franco-Ferreira, Fabrication of Radiators for Boiling Heat-Transfer Experiments, USAEC Report ORNL-TM-602, Oak Ridge National Laboratory, August 1963.
67. A. P. Fraas, Design and Development Tests of Direct-Condensing Potassium Radiators, pp. 716-736 in AIAA Specialists Conference on Rankine Space Power Systems, Vol. I, USAEC Report CONF-651026, October 1965.
68. R. S. Holcomb and F. E. Lynch, Thermal Performance of a Finned-Radiator Tube with a Reflector, USAEC Report ORNL-TM-1613, Oak Ridge National Laboratory (to be published).

System Stability and Control

69. M. E. LaVerne, Control Concepts and Digital Computer Analysis of the MPRE Fluid System, USAEC Report ORNL-TM-1368, Oak Ridge National Laboratory, February 1966.

70. A. R. Barbin and M. M. Yarosh, An Analog Study of a Single-Loop Rankine Cycle System, USAEC Report ORNL-TM-1369, Oak Ridge National Laboratory, February 1966.
71. M. M. Yarosh, Stability and Control Characteristics of Electrically Heated Test Rigs Designed to Simulate the MPRE Fluid System, USAEC Report ORNL-TM-1370, Oak Ridge National Laboratory, February 1966.
72. O. W. Burke and S. J. Ditto, An Analog Computer Study of the Control Characteristics of the Medium-Power Reactor Experiment System Including the Turbine-Generator, USAEC Report ORNL-TM-1494, Oak Ridge National Laboratory, May 1966.
73. O. L. Smith and J. C. Robinson, A Theoretical Investigation of the Dynamic Characteristics of the Medium-Power Reactor Experiment, USAEC Report ORNL-TM-1611, Oak Ridge National Laboratory (to be published).

System Endurance Tests

74. P. G. Smith, J. H. DeVan, and A. G. Grindell, Cavitation Damage to Centrifugal Pump Impellers During Operation with Liquid Metals and Molten Salt at 1050-1400°F, pp. 329-337 in Trans. ASME, Series D, Journal of Basic Engineering, Vol. 85, Sept. 1963.
75. R. E. MacPherson and A. P. Fraas, Potassium Rankine Cycle Operating Experience for the Medium-Power Reactor Experiment, pp. 11-34 in AIAA Specialist Conference on Rankine Space Power Systems, Vol. II, USAEC Report TID-22508, October 1965.
76. H. J. Metz and M. M. Yarosh, Experiences and Developments in Instrumentation for Liquid Metal Experiments, Proceedings of the Fourth High-Temperature Liquid-Metal Heat Transfer Technology Conference held Sept. 28-29, 1965, at Argonne National Laboratory, USAEC Report ANL-7100.
77. M. M. Yarosh, P. A. Gnadl, and J. Zasler, The Intermediate Potassium System - A Rankine Cycle, Potassium Test Facility, USAEC Report ORNL-4025, Oak Ridge National Laboratory (to be published).
78. M. M. Yarosh and S. E. Bolt, The Intermediate Water System - A Rankine Cycle Test Facility, USAEC Report ORNL-TM-1614, Oak Ridge National Laboratory (to be published).

Program Progress Reports

79. Oak Ridge National Laboratory, Space Power Program Progress Report for Period Ending December 31, 1961, USAEC Report ORNL-3270.
80. Oak Ridge National Laboratory, Space Power Program Progress Report for Period Ending June 30, 1962, USAEC Report ORNL-3337.

81. Oak Ridge National Laboratory, Space Power Program Progress Report for Period Ending December 31, 1962, USAEC Report ORNL-3420.
82. Oak Ridge National Laboratory, Space Power Program Progress Report for Period Ending June 30, 1963, USAEC Report ORNL-3489.
83. Oak Ridge National Laboratory, Medium-Power Reactor Experiment Progress Report for Period July 1, 1963 to September 30, 1963, USAEC Report ORNL-3534.
84. Oak Ridge National Laboratory, Space Power Program Progress Report for Period Ending December 31, 1963, USAEC Report ORNL-3571.
85. Oak Ridge National Laboratory, Medium-Power Reactor Experiment Progress Report for Period January 1, 1964 to March 31, 1964, USAEC Report ORNL-3641.
86. Oak Ridge National Laboratory, Space Power Program Progress Report for Period Ending June 30, 1964, USAEC Report ORNL-3683.
87. Oak Ridge National Laboratory, Medium-Power Reactor Experiment Progress Report for Period Ending September 30, 1964, USAEC Report ORNL-3748.
88. Oak Ridge National Laboratory, Medium-Power Reactor Experiment Progress Report for Period Ending December 31, 1964, USAEC Report ORNL-3774.
89. Oak Ridge National Laboratory, Medium-Power Reactor Experiment Progress Report for Period Ending March 31, 1965, USAEC Report ORNL-3818.
90. Oak Ridge National Laboratory, Medium-Power Reactor Experiment Progress Report for Period Ending June 30, 1965, USAEC Report ORNL-3860.
91. Oak Ridge National Laboratory, Medium-Power Reactor Experiment Progress Report for Period Ending September 30, 1965, USAEC Report ORNL-3897.
92. Oak Ridge National Laboratory, Medium-Power Reactor Experiment Progress Report for Period Ending December 31, 1965, USAEC Report ORNL-3937.
93. Oak Ridge National Laboratory, Medium-Power Reactor Experiment Progress Report for Period Ending March 31, 1966, USAEC Report ORNL-3976.
94. Oak Ridge National Laboratory, Medium-Power Reactor Experiment Progress Report for Period Ending June 30, 1966, USAEC Report ORNL-4018 (this report).

Dimensional and Performance Data

Table 1.3 lists the dimensional and performance data for the MPRE. No changes in these data were made during this reporting period.

MPRE Hot-Channel Analysis

M. E. LaVerne

Concern over possible deleterious effects associated with nonuniform vapor generation in MPRE-type rod bundles prompted an analysis of flow distributions in such bundles.<sup>1</sup> A computer program embodying the analysis was written and tested. Results of computer runs indicate that the flow channel couplings characteristic of the MPRE-type core greatly diminish the effects of dissymmetry.

Analysis Conditions

Basic Assumptions. Three basic assumptions were made for derivation of the MPRE flow distribution model: (1) the core pressure drop is adequately correlated by the expression used in the analog report,<sup>2</sup> (2) the pressure is constant across any transverse cross section of the core, and (3) there is no interchange of liquid between channels. The validity of the first assumption is shown by Fig. 1.1, in which the analog expression  $W^2 \Delta X$  is plotted against  $\Delta P$  for the rod bundle of the intermediate water system. As will be seen, use of the analog expression is attractive in that it leads to a set of linear algebraic equations in the unknown vapor flows within the core.

The second assumption certainly would be valid at the ends of the core. Away from the edges of the core, both axially and radially, its plausibility is less clear. However, because of the high connectivity

---

<sup>1</sup>M. E. LaVerne, Analysis of the Hot Spot Problem in the MPRE, USAEC Report ORNL-TM-1371, Oak Ridge National Laboratory.

<sup>2</sup>A. R. Barbin and M. M. Yarosh, An Analog Study of a Single-Loop Rankine Cycle System, USAEC Report ORNL-TM-1369, Oak Ridge National Laboratory.

Table 1.3. Design Parameters for MPRE Reference Design 4

Reactor operating conditions	
Thermal power, Mw	1
Coolant	Potassium (boiling)
Inlet temperature, °F	1530
Outlet temperature, °F	1540
Inlet coolant pressure, psia	30
Outlet coolant pressure, psia	29
Reactor geometry	
Fuel element arrangement	Equilateral triangular pitch
Moderator	None in core
Core diameter (equivalent), in.	9.17
Distance across corners of core, in.	9.50
Core length, in.	11.625
Active core volume	
ft <sup>3</sup>	0.444
liters	12.58
Core free-flow area, ft <sup>2</sup>	0.130
Side reflector thickness, in.	3.0
Fluid flow data	
Core flow passage equivalent diameter, in.	0.198
Vapor flow at outlet	
lb/hr	4000
lb/sec	1.111
Liquid flow at outlet, lb/sec	4.444
Total liquid flow entering core	
lb/sec	5.555
ft <sup>3</sup> /sec	0.137
Total flow leaving core, ft <sup>3</sup> /sec	19.7
Vapor quality leaving core, %	20
Core exit vapor density, lb/ft <sup>3</sup>	0.058
Core inlet liquid density, lb/ft <sup>3</sup>	40.7
Core exit velocity, ft/sec	152
Core exit dynamic head, psi	0.144
Core inlet velocity, ft/sec	1.05
Core inlet dynamic head, psi	0.0048
Core circuit pressure drop, psi	1.0
Heat transfer data	
Power density (core average), w/cm <sup>3</sup>	79.5
Heat transfer surface area, ft <sup>2</sup>	30.55
Heat flux, Btu/hr.ft <sup>2</sup>	
Average	111,700
Maximum	146,000
Fuel element cladding temperature, °F	
Average	1555
Maximum (hot spot)	1580
Fuel central temperature, °F	
Average	2400
Maximum	2700
Fuel element data	
Configurations	Rods
Fuel form	UO <sub>2</sub> pellets in metal capsules
Number of fuel elements	241
Overall length, in.	19.875

Table 1.3 (continued)

---

Fuel element data (continued)	
Fueled length, in.	11.625
Fuel enrichment, %	93
Cladding material	Type 316 stainless steel
Cladding thickness, in.	0.020
Fuel element outside diameter, in.	0.50
Centerline spacing, in.	0.5625
Burnup at end of life, % of total U atoms	0.76
Core composition	
Stainless steel, volume fraction	0.11006
UO <sub>2</sub> , volume fraction	0.59598
Void inside fuel elements, volume fraction	0.01052
Coolant flow passages, volume fraction	0.28344
Control element data	
Type for normal control	Four movable BeO plugs (quadrants of the bottom reflector)
Mode of reactivity reduction	Vertical displacement parallel to axis of reactor; total travel 8 in.
Vertical height of control plugs, in.	8.5
Sheath material	Type 304 stainless steel
Combined worth of control plugs, % $\Delta k/k$	$\sim 5.0$
Pressure vessel data	
Material	Type 304 stainless steel
Shell outside diameter, in.	10.5
Wall thickness, in.	0.25
Overall length (with expansion tank and vapor separator), in.	34
Physics data	
Mass of UO <sub>2</sub> , kg	78.0
Mass of <sup>235</sup> U, kg	63.8
Effective delayed neutron fraction	0.0075
Median energy for fission, kev	840
Prompt neutron lifetime, sec	$3 \times 10^{-7}$
Reactivity worth of control plugs	0.05
Isothermal temperature coefficient of reactivity, (1/k)(dk/dt), °C <sup>-1</sup>	$-1.6 \times 10^{-5}$
Fuel reactivity coefficient, ( $\Delta k/k$ )/( $\Delta m/m$ )	0.545
Loss in k, fuel burnup for 1 Mwyr	0.0040
Reactivity effect of potassium filling coolant passages (relative to normal operating condition)	0.0014
Maximum excess k from control plug insertion	
At full power	0.006
Cold, clean	0.020
Neutron flux at outer surfaces of core, neutrons/cm <sup>2</sup> ·sec	
Fast (0.9-10 Mev)	$0.41 \times 10^{14}$
Thermal (0-1 ev)	$3.4 \times 10^{11}$

---

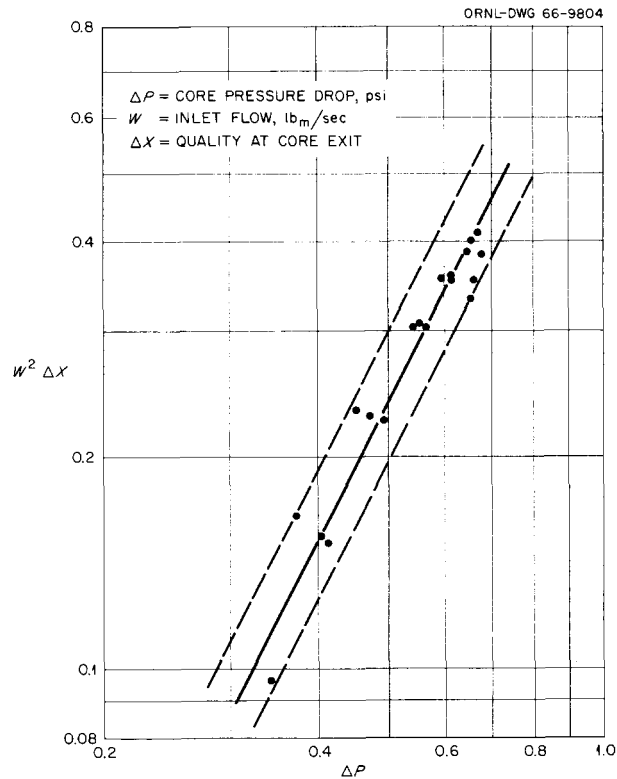


Fig. 1.1. Correlation of Core Pressure Drop Data for Intermediate Water System with Line Defined by the Analog Expression.

of adjacent channels (even for the closely packed MPRE core, the radial-to-axial equivalent-diameter ratio is 5:8), the discrepancy should be small even there. In any event, it would be expected that a large fraction of the transverse pressure variation that would exist if there were no vapor interchange between channels would wash out. In the absence of better information, this large fraction has been assumed to be one.

The final assumption arises primarily from the experimental observation that the liquid tends to flow as a film straight up the heater rods. Thus assumptions two and three are compatible in that there is no lateral force impelling the liquid sidewise. Further, any drag forces on the liquid arising from lateral diffusion of vapor will be small because of the small transverse vapor velocities. This, coupled with the large ratio of liquid density to vapor density leads to a negligible lateral transport of liquid. This assumption does not preclude interchange of vapor between adjacent channels.

Input Restrictions. In addition to the above assumptions, several restrictions were placed on the input parameters to the computer program. As a result, the problem was reduced from three to two dimensions with little loss in generality; however, the savings both in problem preparation and in volume of output are considerable.

Figure 1.2 shows a cross section through the core model. Fuel (or heater) rods may be added only in complete hexagonal rows. Similarly, radial power variations may occur only in complete rows. Axial power variations have the same shape for all rods in the core. Finally, the inlet flows may vary only with radial position of the channels and not with circumferential position. Channel characteristics (i.e., size, shape, power input, flow) thus are dependent only on radial location and independent of circumferential location.

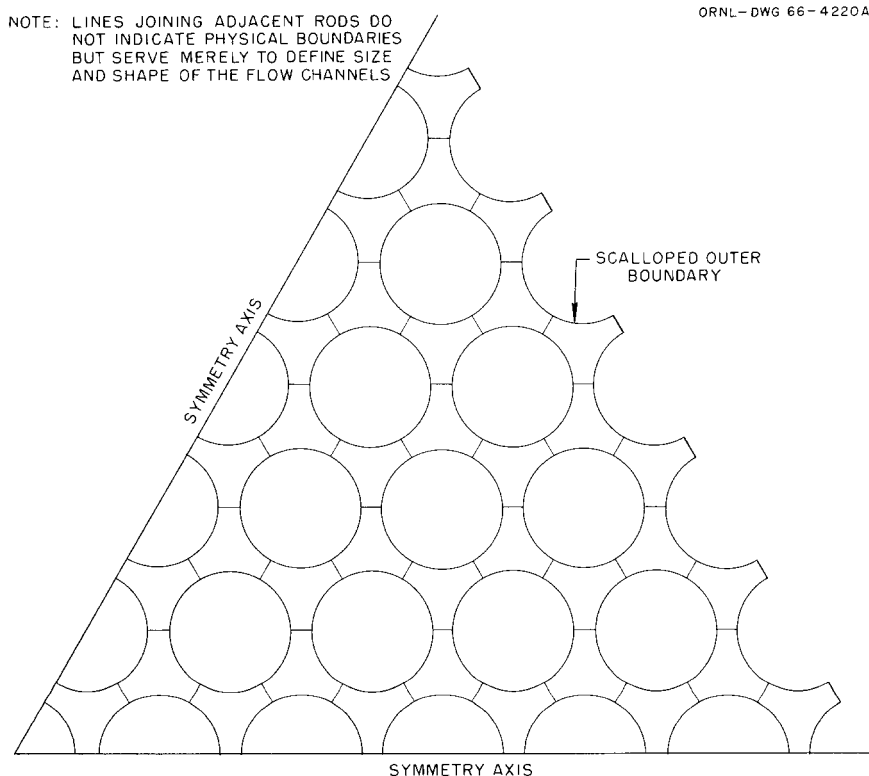


Fig. 1.2. One-Sixth Cross Section Through Typical Rod Matrix on Equilateral Triangular Pitch.

Vapor Flow Equations. Figure 1.1 shows that we may write, for segment I of channel j,

$$W_{I,j}^2 \Delta X_{I,j} = f(\Delta P) . \tag{1}$$

(The terms used in this and the following equations are defined on p. 23.) Equating the pressure drops for adjacent channels then gives

$$W_{I,j}^2 \Delta X_{I,j} = W_{I,j+1}^2 \Delta X_{I,j+1} . \tag{2}$$

Expressing the quality change as

$$\Delta X_{I,j} = (G_{I+1,j} - G_{I,j})/W_{I,j} \tag{3}$$

finally yields

$$\begin{aligned} W_{I,j} G_{I+1,j} - W_{I,j+1} G_{I+1,j+1} &= W_{I,j} G_{I,j} - W_{I,j+1} G_{I,j+1} \\ &= C_j \end{aligned} \tag{4}$$

for  $1 \leq j < N_c$ . The foregoing results in  $N_c - 1$  equations relating the  $N_c$  unknown vapor flows.

The remaining equation needed for determination of the vapor flows is obtained from a mass-flow balance. We have

$$\begin{aligned} 6G_{I+1,1} + 6G_{I+1,2} + 12G_{I+1,3} + 12G_{I+1,4} + \dots \\ + 3(N_c - 1)G_{I+1,N_c-2} + 3(N_c - 1)G_{I+1,N_c-1} \\ + 3(N_c + 1)G_{I+1,N_c} &= \sum_{i=1}^I \Delta G_i \\ &= C_{N_c} . \end{aligned} \tag{5}$$

The left side of Eq. (5) is, of course, the appropriately weighted sum of the individual channel flows and the right side is simply the total vapor generated (through the current segment).

Solution of the Vapor Flow Equations. Equations (4) are in bidiagonal form, so specification of any one flow uniquely determines the remaining flows. Elimination of the first  $N_c - 1$  flows between Eqs. (4) and (5)

yields an equation having only  $G_{I+1, N_c}$  as unknown. Solving explicitly for  $G_{I+1, N_c}$  then gives

$$G_{I+1, N_c} = \frac{C_{N_c} - \sum_{j=1}^{N_c-1} C_j \sum_{k=1}^j B_k/W_{I, k}}{W_{I, N_c} \sum_{j=1}^{N_c} B_j/W_{I, j}}, \quad (6)$$

where  $B_j$  has been written for the coefficient of  $G_{I+1, j}$  in Eq. (5).

Back substitution in Eq. (4) then yields, in succession, the remaining vapor flows. Explicitly, we have

$$G_{I+1, j} = (C_j + W_{I, j+1} G_{I+1, j+1})/W_{I, j} \quad (7)$$

for  $1 \leq j < N_c$ .

Vapor Generation in a Segment. As may be seen by reference to Fig. 1.2, any pair of adjacent rows of rods defines two distinct types of channel, which will be designated as inner and outer channels. An inner channel is defined by two rods from the inner row and one rod from the outer row of a pair, while an outer channel is defined by two rods from the outer row and one rod from the inner row. With these definitions we have

$$\Delta G_{I, j} = f_I (k_1 q_{I, r} + k_2 q_{I, r+1})/h_{fg}, \quad (8)$$

where  $k_1 = 2.0$  and  $k_2 = 1.0$  for an inner channel and  $k_1 = 1.0$  and  $k_2 = 2.0$  for an outer channel. The total vapor generated in segment  $i$  is, then,

$$\Delta G_i = \sum_{j=1}^{N_c} \Delta G_{i, j}. \quad (9)$$

Liquid Flow Equations. By virtue of assumption three, the liquid flows in adjacent channels are uncoupled, so

$$F_{I+1, j} = F_{I, j} - \Delta G_{I, j} \quad (10)$$

for  $1 \leq j \leq N_c$ .

Initial Conditions. In order to start the calculation, initial values are required for vapor and liquid flows and for pressure in the core. At

the beginning of the heated length, no vapor has yet been generated and the core pressure is equal to the inlet pressure. Hence, we have, for  $1 \leq j \leq N_c$ ,

$$\begin{aligned}
 G_{1,j} &= X_{1,j} = 0.0, \\
 F_{1,j} &= W_{1,j}, \\
 P_{1,j} &= P_{in}.
 \end{aligned}
 \tag{11}$$

Nomenclature. The following terms may be used with any consistent set of units:

<u>Quantity</u>	<u>Definition</u>
C	Constant defined by Eqs. (4) or (5)
f	Axial fraction of rod heat output
F	Channel liquid weight flow
G	Channel vapor weight flow
$\Delta G$	Generated vapor increment
$h_{fg}$	Heat of vaporization
k	Constant defined in Eq. (8)
$N_c$	Total number of channels
P	Pressure
$\Delta P$	Pressure drop
q	Rod heat output to channel
W	Channel total weight flow
X	Channel quality
$\Delta X$	Channel quality increment

<u>Subscript</u>	<u>Definition</u>
I	Current segment number
i	General segment number
j,k	General channel numbers

Discussion of Computer Results

Interchannel mixing in the physical core occurs continuously; in the computational model, the mixing occurs at the ends of discrete segments.

It is to be expected, then, that the number of axial segments used in a calculation will affect the results. A series of calculations was therefore made both with 7-rod and 91-rod cores having uniform power distribution to assess this effect. Figure 1.3 shows the effect on channel exit quality of varying the number of segments into which the heated length of the seven-rod core was divided. It is apparent from the figure that the major portion of the quality variation is accounted for by the time ten segments have been used. Beyond 20 segments, the change is negligible. Similar results were observed for the 91-rod core. Subsequent calculations were made for 25 segments.

An interesting abstraction from Fig. 1.3 is the observed quality decrease from the center to the outside of the core despite the uniform power distribution. This decrease can be explained on a purely geometric basis. As Fig. 1.2 shows, each flow channel is defined by three curved wall sections. In the outermost channel, only one of those sections is heated. The next channel in has two heated walls, while the third has three heated walls. Thus, the relative power inputs to the same three channels are as 1:2:3. In the absence of interchannel mixing, then, the qualities would be expected to vary in the same proportions. The observed

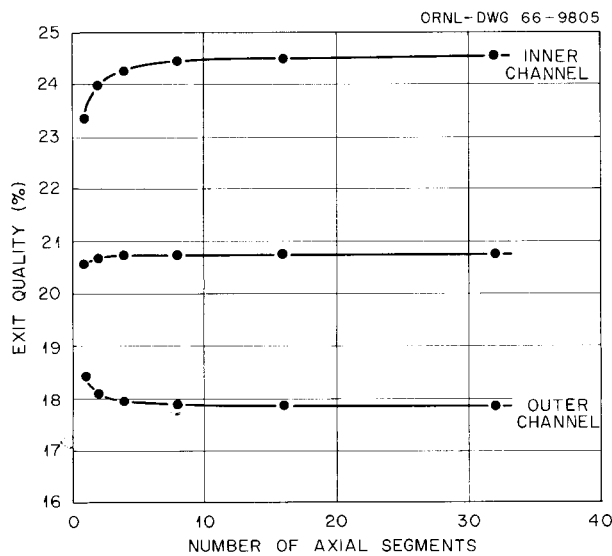


Fig. 1.3. Effect of Core Axial Subdivision on Calculated Exit Quality Distribution. Seven-rod bundle; uniform power, 3 kw per rod.

reduction to a variation of roughly 35% is attributable to the cross channel coupling characteristic of the MPRE-type core.

Figure 1.4 shows radial quality distributions at five axial locations in the MPRE core. The core power is 1 Mw, and the mean exit quality is 20%. Radial and axial power distributions were obtained from Figs. 2.4 and 2.5, respectively, of ORNL-3683.<sup>3</sup>

The effectiveness of the flow channel coupling in reducing the effects of power dissymmetry is readily apparent from the figure. What may not be so obvious is the reason for the quality dropoff at the core edge where the radial power distribution peaks. The explanation is twofold. First, the power spike of Ref. 3 has been integrated over the last row of fuel

---

<sup>3</sup>A. M. Perry, O. L. Smith, and J. V. Wilson, Revision and Further Study of Reference Reactor, pp. 38-39, Space Power Program Semiann. Progr. Rept. June 30, 1964, USAEC Report ORNL-3683, Oak Ridge National Laboratory.

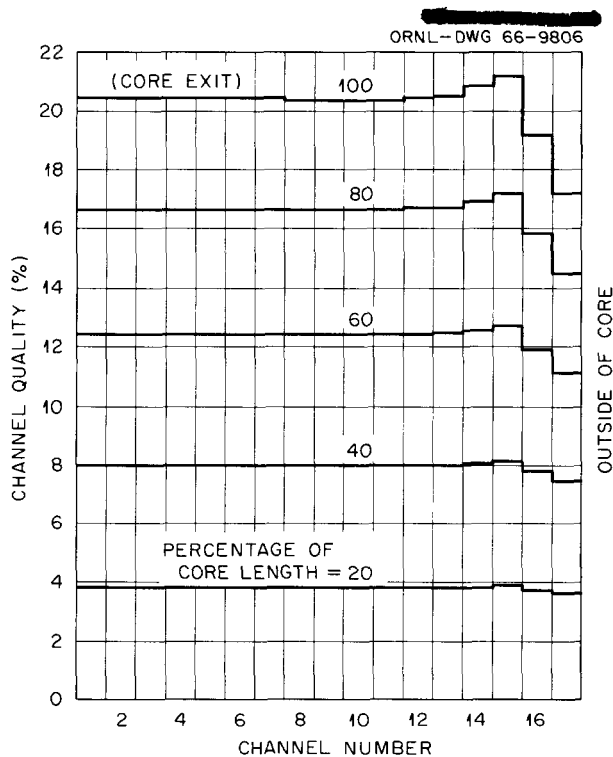


Fig. 1.4. Radial Quality Distribution at Several Axial Positions in the MPRE Core. Power, 1 Mw; mean exit quality, 20%.

rods and the resultant mean power assumed to be uniformly rejected around the rod periphery. Calculations by Jung<sup>4</sup> show that although the peripheral heat rejection varies, the variation is substantially reduced below that of the power generation across a fuel rod. To a first approximation, this variation has been taken as negligible. Second, the geometric effect explained above with reference to Fig. 1.3 then comes into play and results in the observed quality decrease in the outermost channels.

A more nearly precise calculation would allow peripheral variation in individual rod output. Radial power peaking would thus give more nearly uniform heat inputs to the outer channels and result in a lessened quality variation. It may be concluded that the present calculation actually gives a somewhat pessimistic estimate of the radial quality variation.

#### Zero-Gravity Boiler Recirculation System

M. E. Lackey

A concept for a new approach to the design of the vapor separator was evolved. It employs a free-turbine-driven centrifugal vapor-separator and expansion-tank combination for use in a zero-gravity environment. A preliminary layout is shown in Fig. 1.5. The separator complex consists of a centrifuge, a centrifuge feed pump, and a drive turbine mounted on a common shaft.

The centrifuge serves three separate but interdependent functions. The centrifugal force field developed by the centrifuge separates the liquid and the vapor and in the process develops sufficient head to serve as the boiler recirculating pump. The centrifuge is sized to allow the liquid-vapor interface to shift sufficiently to accommodate changes in the liquid volume, and hence the unit also serves as the expansion tank for the system. A centrifugal impeller serves to pump a uniform mixture of vapor and liquid from the boiler exit to the centrifuge inlet. The drive turbine is supplied with the entire vapor flow from the boiler, and it

---

<sup>4</sup>J. K. T. Jung, Temperature Distribution in Fuel Rods Near Core-Reflector Interface, pp. 10-12, Space Power Program Semiann. Progr. Rept. June 30, 1963, USAEC Report ORNL-3489, Oak Ridge National Laboratory.

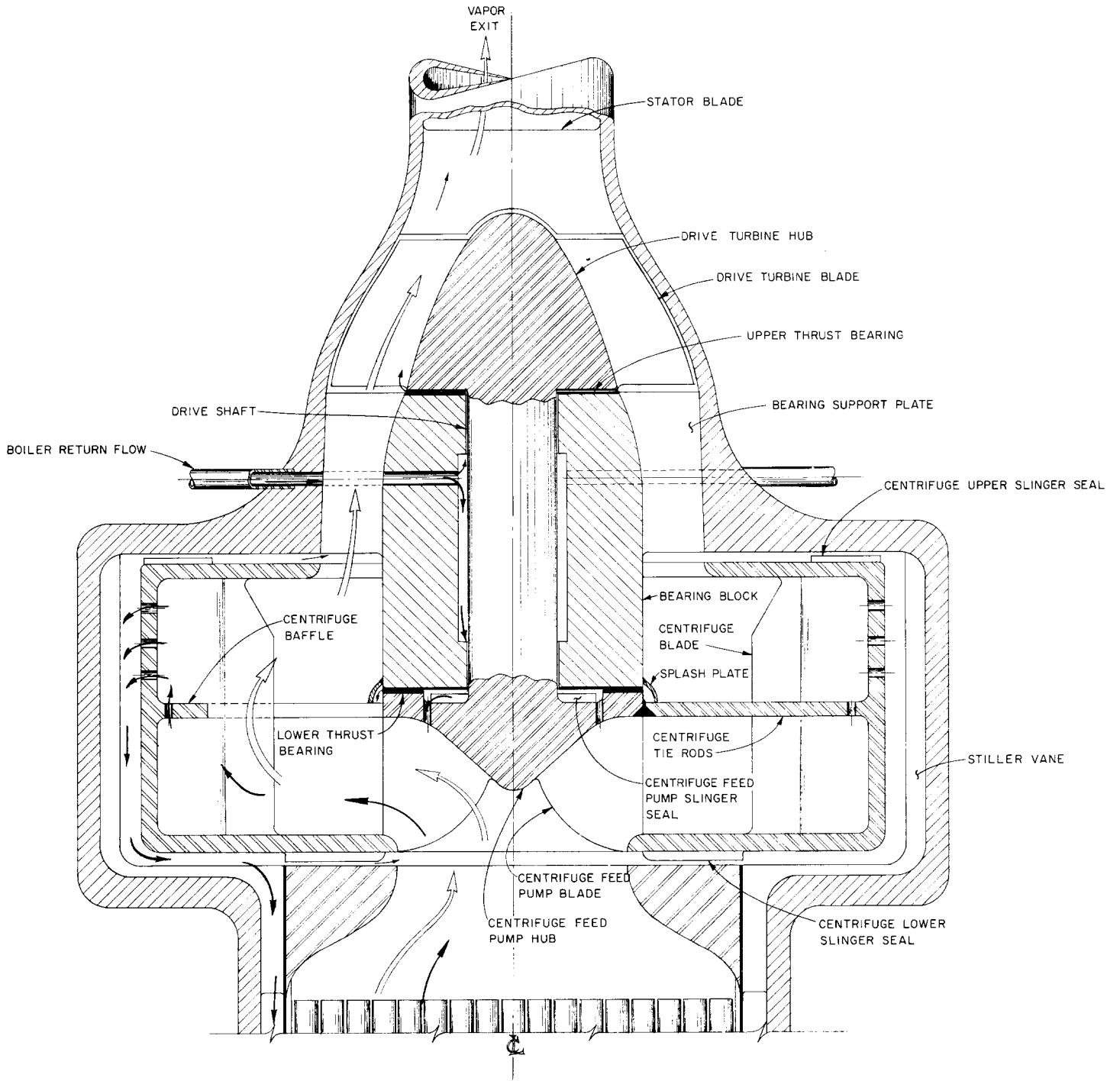


Fig. 1.5. Zero-Gravity Boiler Recirculation System.

provides the power requirements of the centrifuge and centrifuge feed pump.

The main advantages of this system are that

1. A positive separation of the liquid and vapor is effected by the centrifuge.
2. A stable liquid-vapor interface is maintained by the centrifugal field.
3. The centrifuge will supply sufficient head to overcome the boiler flow resistance over a wide range of boiler powers.
4. The design boiler pressure drop is not limited to the low values necessitated by the use of jet pumps for boiler recirculation. The centrifuge head can be matched to the desired boiler resistance by a proper selection of the centrifuge speed and diameter. The system shown in Fig. 1.5 will supply a pressure rise of approximately 5 psi at a centrifuge speed of 1100 rpm.

The main disadvantages of this system are that

1. The system requires the use of rotating machinery.
2. The interdependence of the various components of the system complicates the overall system development.
3. The leakage from the downstream thrust bearing is added to the exit vapor stream and it degrades the exit quality. However, this is not believed to be a very serious limitation, since the separation efficiency of the free-turbine-driven centrifugal separator will probably be high enough to allow a reasonable bearing leakage.

The high centrifugal force field afforded by this system as compared with gravity should negate the effects of gravity upon the system performance. This would allow complete component development to be performed in the laboratory, with only the final proof testing requiring operation under zero-gravity conditions.

Stress Analyses of MPRE Pressure Vessel

F. J. Witt      R. C. Gwaltney  
J. E. Smith    R. S. Valachovic

One cluster of nozzles consisting of the jet pump, thermocouple, and jet pump feed-flow nozzles was attached to the experimental model of

the MPRE pressure vessel.<sup>5</sup> The outer surfaces of the nozzles and adjoining regions were strain gaged and the vessel was again tested under internal pressure. The nozzle region is shown in Fig. 1.6. In the cluster shown the jet pump nozzle is not dimensionally correct. Hence, an additional nozzle having correct dimensions was placed in a region well away from the cluster. This nozzle is shown in the insert. Only the nozzle with the correct dimensions was strain gaged. The nozzles were placed near a section that was already gaged inside the vapor separator tank, and some significant readings near nozzle penetrations were obtained on the inner surface of the vessel. Some gages were also placed on the plate containing the inlet ports and the nearby outer cylinder region.

The results obtained are shown in Figs. 1.7 and 1.8 and supplement those previously reported.<sup>6</sup> These figures show that there are no serious stress concentrations in the nozzles. However the maximum stress obtained for the vessel at the test pressure increased about 10% to 11,000 psi at the inner surface near the junction region of the outer cylinder and the bottom plate. The addition of the penetrations also increased the stresses on the outer surface of the cylinder near the jet pump feed flow nozzle.

The region midway between the inlet ports was also examined. These results are summarized in the section identified as Section C-C in Fig. 1.8. In particular the maximum stress of about 10,000 psi for this region obtained in prior tests was not exceeded. It is still significant, however, that the maximum stress for the plate containing the inlet ports occurs well away from the ports.

In summary, the presence of the nozzles increases the stresses but not by a really significant amount. The data are being studied further; however, the general discussion concerning the integrity of the vessel will probably not be altered until additional information relating to high-temperature behavior of the material is obtained.<sup>6</sup> A final report is being prepared.

---

<sup>5</sup>F. J. Witt et al., Stress Analysis of Pressure Vessel, pp. 15-16, Medium-Power Reactor Experiment Quart. Progr. Rept. Mar. 31, 1966, USAEC Report ORNL-3976, Oak Ridge National Laboratory.

<sup>6</sup>F. J. Witt et al., Stress Analyses of the Pressure Vessel, pp. 6-16, Medium-Power Reactor Experiment Quart. Progr. Rept. Dec. 31, 1965, USAEC Report ORNL-3937, Oak Ridge National Laboratory.

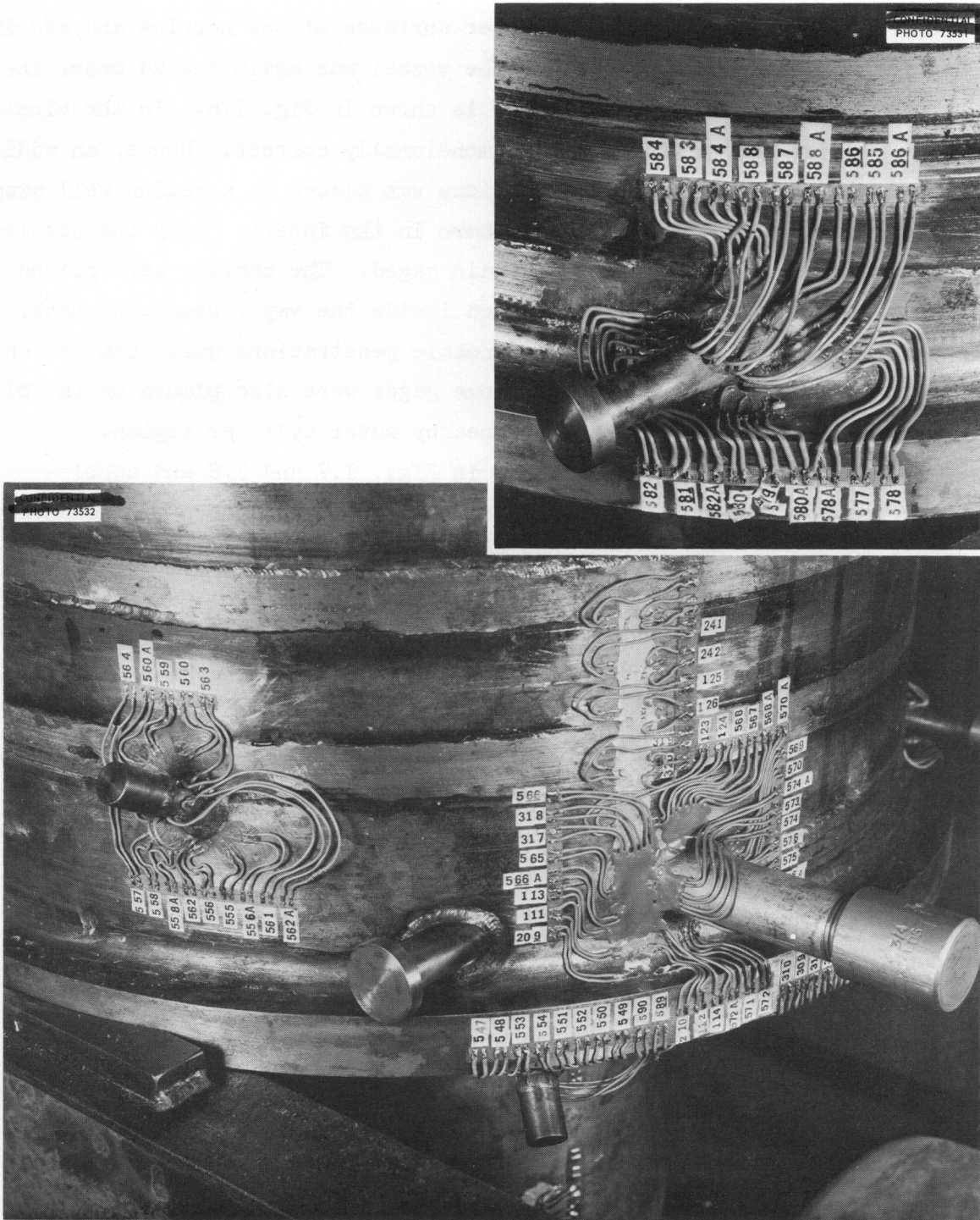


Fig. 1.6. Nozzle Cluster Region of the Vapor-Separator Tank Attached to Experimental Model of Pressure Vessel.

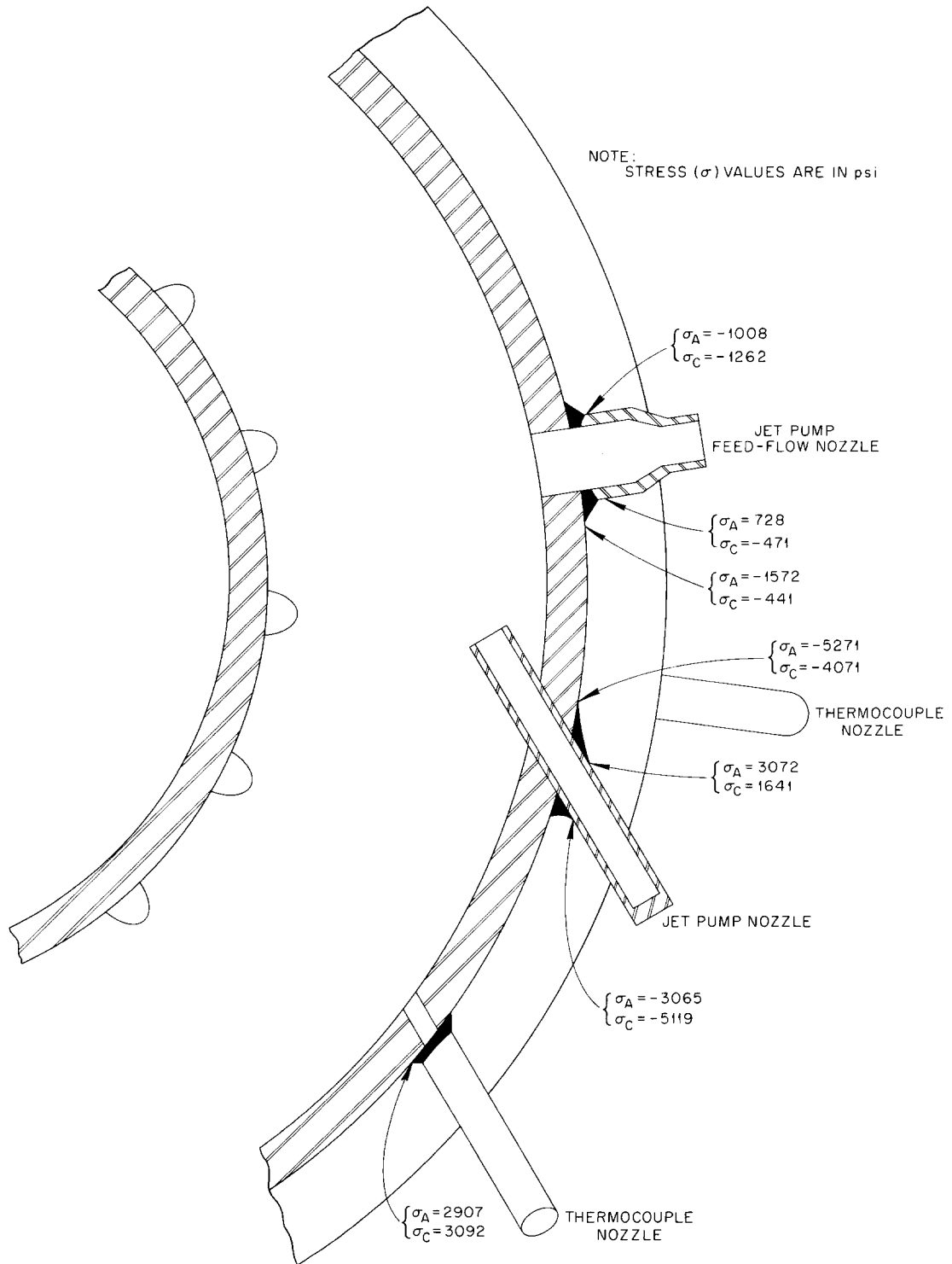


Fig. 1.7. Experimental Stresses Obtained in a Nozzle Cluster Region of the Vapor-Separator Tank (Plan View) Attached to Pressure Vessel with the Vessel Pressurized to 200 psig.

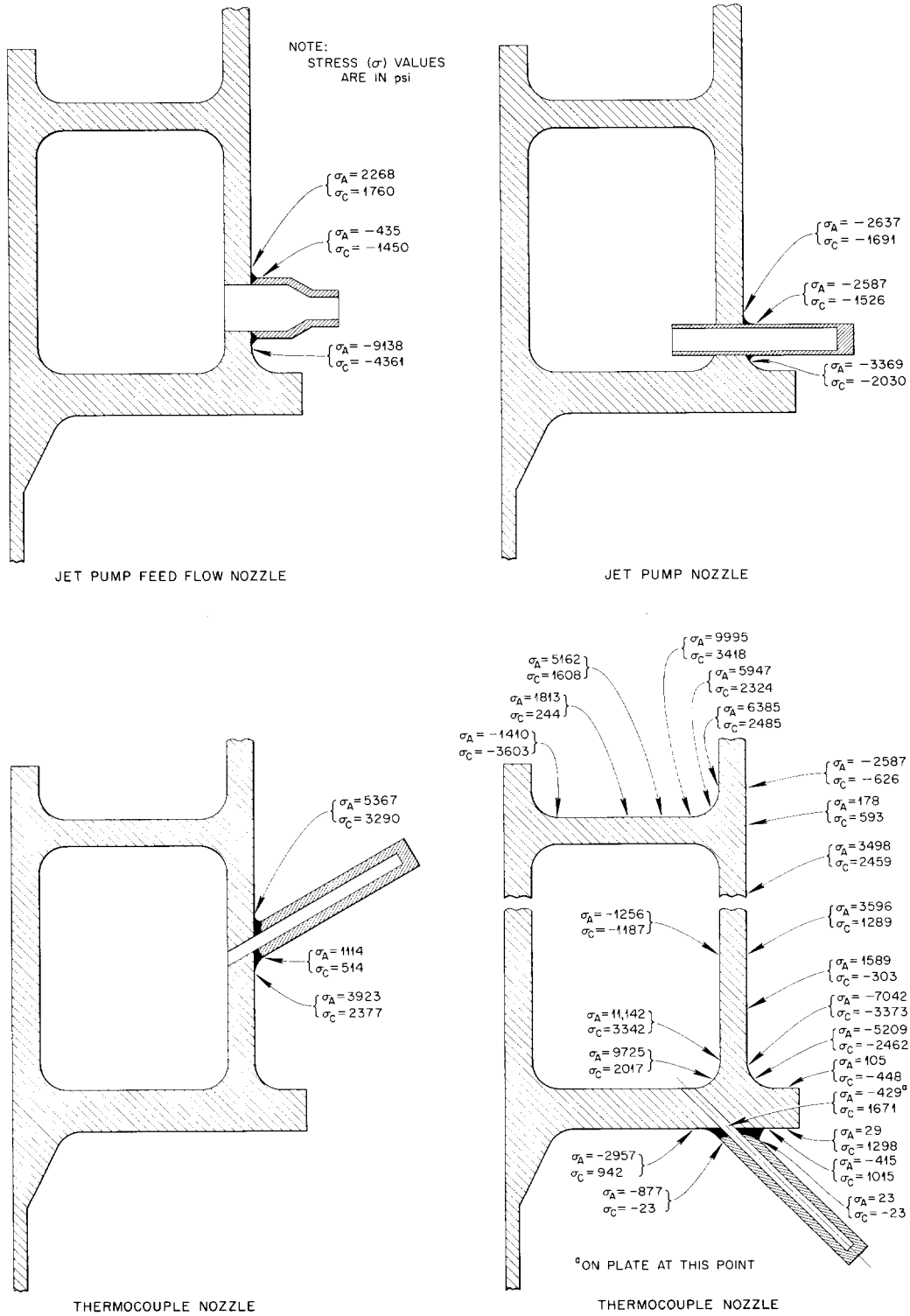


Fig. 1.8. Experimental Stresses Obtained in a Nozzle Cluster Region of the Vapor-Separator Tank (Elevation) Attached to Pressure Vessel with the Vessel Pressurized to 200 psig.

## 2. REACTOR PHYSICS

A. M. Perry

Transient Analysis

O. L. Smith

The mathematical model of the MPRE that was discussed in earlier progress reports<sup>1,2,3</sup> was extended to incorporate the parts of the system that were previously represented by boundary conditions at the outlet of the vapor separator and at the sideport of the boiler jet pump. The new features of the model include detailed descriptions of the performance of the turbine pump, condenser jet pump, and the condenser. The inclusion of these components extends the range of application of the model to significantly longer time intervals than those for which the previously used boundary conditions were valid.

Figure 2.1 shows a schematic representation of the system described by the model. The symbols used in the figure and in the text are defined in Table 2.1. A complete discussion of the model as it currently exists is presented in a topical report<sup>4</sup> and will not be given here.

The model was used to examine the dynamic response of the system to a number of nonequilibrium conditions. The cases studied are listed in Table 2.2. In each case the reactor is initially operating at some steady-state power level and the system is perturbed by the insertion of a ramp or step change in reactivity. The mechanism that causes the particular

---

<sup>1</sup>O. L. Smith and J. C. Robinson, Reactor Transient Analysis, pp. 17-19, Medium-Power Reactor Experiment Quart. Progr. Rept. Sept. 30, 1964, USAEC Report ORNL-3748, Oak Ridge National Laboratory.

<sup>2</sup>O. L. Smith and J. C. Robinson, Reactor Transient Analysis, p. 28, Medium-Power Reactor Experiment Quart. Progr. Rept. Mar. 31, 1965, USAEC Report ORNL-3818, Oak Ridge National Laboratory.

<sup>3</sup>O. L. Smith, Reactor Transient Analysis, pp. 35-39, Medium-Power Reactor Experiment Quart. Progr. Rept. Sept. 30, 1965, USAEC Report ORNL-3897, Oak Ridge National Laboratory.

<sup>4</sup>O. L. Smith and J. C. Robinson, A Theoretical Investigation of the Dynamic Characteristics of the Medium-Power Reactor Experiment (to be published), Oak Ridge National Laboratory.

Table 2.1. Definition of Symbols Used in Text and Figures

Symbol	Definition
$c_{cav}$	Turbine pump cavitation coefficient
$F_2$	Volumetric flow rate of liquid at inlet of boiler
$F_3$	Average longitudinal volumetric flow rate of liquid at top of inventory in expansion tank
$F_6$	Volumetric flow rate in driving stream of boiler jet pump (and in sideport of condenser jet pump)
$F_7$	Volumetric flow rate in driving stream of condenser jet pump
$F_9$	Volumetric flow rate of liquid discharged from condenser jet pump (and turbine pump)
$\Delta h_t(p_2, p_8)$	Change in enthalpy of vapor in passing through turbine of turbine pump
$H$	Fueled length of boiler
$H_w$	Suppression head (in inches of $H_2O$ ) at condenser jet pump sideport (proportional to $L_p$ )
$L_p$	Length (in inches) of static column of liquid at condenser jet pump sideport
$N$	Turbine pump speed
$p_2$	Average (spatial) boiler pressure
$p_6$	Boiler jet pump driving stream pressure (same as turbine pump discharge pressure and condenser jet pump driving stream pressure)
$p_8$	Condenser pressure
$p_9$	Condenser jet pump discharge pressure
$q$	Coolant quality
$q_e$	Boiler exit quality
$Q_f$	Total power generated in fuel
$r$	Radial position in a fuel pin
$r_k$	Radius of a fuel pin
$R$	Ratio of jet pump side-stream pressure rise to nozzle-stream pressure drop
$T$	Temperature in a fuel pin
$T_{cool}$	Temperature of coolant in boiler
$T_I$	Temperature at inner surface of pin cladding
$T_J$	Temperature at outer surface of pin cladding
$T_1$	Temperature at center of a pin
$T_8$	Temperature of coolant in condenser
$V_l$	Velocity of liquid
$V_v$	Velocity of vapor
$z$	Axial position relative to inlet of boiler
$\rho$	Total reactivity $(k_{eff} - 1)/k_{eff}$
$\rho_p$	Input reactivity perturbation
$\phi$	Ratio of jet pump sideport flow to nozzle flow

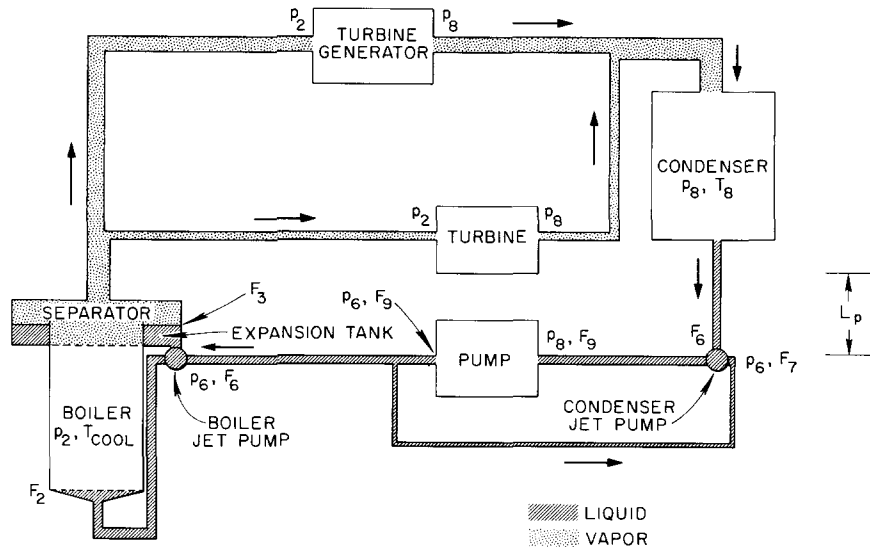


Fig. 2.1. Schematic Model of the MPRE System.

Table 2.2. Conditions of Reactor Transient Studied with Mathematical Model

Case	Initial Thermal Power Level	Reactivity Perturbation	Result
1	Full (1 Mw)	0.05% $\Delta k$ /sec ramp; 0.5% $\Delta k$ total insertion	No scram
2	Full	0.1% $\Delta k$ /sec ramp; 0.5% $\Delta k$ total insertion	No scram
3	Full	0.1% $\Delta k$ /sec ramp	Scram (150% power)
4	Full	10% $\Delta k$ /sec ramp	Scram (200% power)
5	Half (0.5 Mw)	0.1% $\Delta k$ step	No scram

reactivity perturbation need not be specified, and in fact it may well be physically impossible. The point here is simply to show how the system would react to such a perturbation if it occurred.

In case 1 the reactor is initially operating at full design thermal power of 1 Mw. The system is perturbed by inserting reactivity  $\rho_0$  at a

rate of  $0.05 \% \Delta k/\text{sec}$  until a total of  $0.5\% \Delta k$  has been added. No further external action is taken, and the response of the system is determined entirely by its inherent dynamic characteristics. The behavior of many of the system variables as a function of time is shown in Fig. 2.2. After approximately 30 sec the inserted reactivity is compensated by thermal expansion of the core (note the total reactivity in Fig. 2.2) and a new equilibrium thermal power level of about 2 Mw is achieved. The equilibrium value of the boiler pressure  $p_2$  is about 68 psia. The system temperatures achieve new equilibrium values, with the exception of the radiator temperature  $T_8$ , which is still rising slowly. It is noteworthy that no unacceptable temperatures occur during the transient. The melting point of the fuel is taken as  $5300^\circ\text{R}$ , and the maximum pin temperature in the fuel, given by the peak value of  $T_1$ , falls short of this value. The maximum cladding temperature, given by the peak value of  $T_I$ , is also well below the melting point for stainless steel ( $\sim 3100^\circ\text{R}$ ). The boiler exit quality  $q_e$  has a maximum value of about 54%, which is well below the approximately 70% level at which an abrupt drop in the heat transfer coefficient would occur at full power. It is possible that burnout might occur at the greater heat fluxes corresponding to the high power levels achieved in the transient but experimental data are insufficient for a determination. All the results are based on the assumption that burnout does not occur.

The pumping system maintains an adequate inventory of liquid potassium in the boiler and expansion tank assembly at all times. During the initial 16 sec of the transient the turbine pump responds to the demands of the system by rising partially out of cavitation (note the cavitation coefficient  $c_{\text{cav}}$  in Fig. 2.2), increasing the pump head  $p_6$  (actually  $p_6 - p_9$ ), and maintaining the flow to the boiler. This is an important feature during the early stages of the transient before the pump has a chance to speed up. As a consequence there is only a slight dip in the boiler inlet flow rate  $F_2$  and in the liquid inventory in the expansion tank. After the first 16 sec the pump speed  $N$  begins to increase appreciably; this provides additional head to increase the boiler flow rate and the pump goes back into cavitation that is actually deeper than initially.

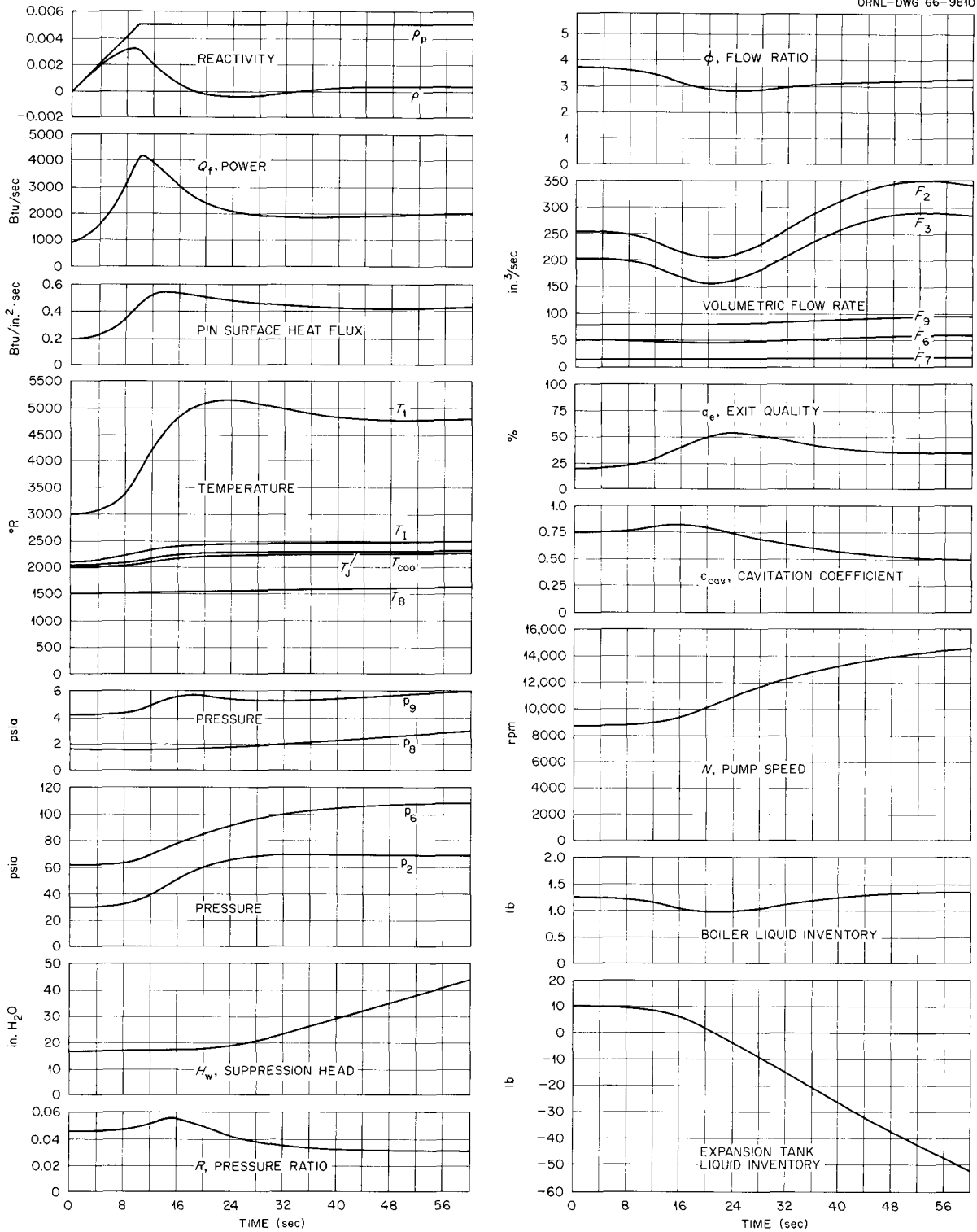


Fig. 2.2. System Variables as a Function of Time; Case 1.

The behavior of the turbine pump is controlled by the action of the condenser jet pump. During the initial 16 sec of the transient the condenser jet pump comes partially out of cavitation (note the pressure ratio  $R$  in Fig. 2.2) in response to the decreasing flow ratio  $\phi$  and the increasing suppression head  $H_w$ . The pump should continue this action until the return flow  $F_6$  from the turbine pump to the boiler jet pump matches the equilibrium vaporization rate in the boiler. In the present case this does not occur.

It can be seen in Fig. 2.2 that the flow to the boiler jet pump increases but does not double its initial value as do the boiler power and vaporization rate. Although the feed rate  $F_2$  to the bottom of the boiler increases adequately, it is at the expense of the liquid inventory in the expansion tank, which steadily decreases. The relatively small increase in  $F_6$  implies that liquid is accumulating in the condenser, since the supply rate of coolant to the condenser has doubled. This inadequacy of the pumping system may be characteristic of the system, since the MPRE is not designed to operate at the 200% power level considered here. On the other hand, it is possible that the difficulty lies in the model, because cavitation of the pump in the present model is controlled by the suppression head  $H_w$ , the nozzle-stream flow rate  $F_7$ , and the pump flow ratio  $\phi$ . An increase in suppression head or a decrease in flow ratio tends to drive the pump out of cavitation. An increase in nozzle-stream flow tends to drive the pump deeper into cavitation. During the first 16 sec of the transient of case 1 the effect of increasing suppression head and decreasing flow ratio controls the overall behavior of the pump, and it tends to rise out of cavitation. Then the effect of increasing nozzle flow becomes the controlling factor, and the pump is driven back into cavitation. However, the effects of coolant temperature changes on the suppression head have been neglected in the model (only the changes in static head are considered), and they probably become quite important in the calculation of case 1. The buildup of inventory in the condenser would cause the liquid to accumulate at the outlet end. Condensation would cease there and a large thermal gradient in the liquid would occur near the outlet. Consequently the liquid leaving the condenser would

arrive at the condenser jet pump greatly subcooled, perhaps by several hundred degrees. This addition to the sideport suppression head  $H_w$  should strongly tend to drive the jet pump out of cavitation and hence increase the pumping power of the system. This effect might be sufficient to re-balance the flow rates at the boiler and separator.

It should be pointed out that the calculation is not affected by the loss of liquid inventory in the expansion tank. The assumption is made that sufficient potassium for the boiler recirculation loop is available at all times. The calculation merely keeps track of the liquid inventory that would actually exist with the given flow into and out of the expansion tank. Starting with 10 lb of liquid in the tank, the inventory is depleted in about 22 sec, and the negative inventory shown in Fig. 2.2 indicates the additional amount of potassium that would have been removed from the tank if it has been present initially.

Several of the coolant characteristics are shown in Fig. 2.3 as a function of fractional axial position along the length of the core. By definition the coolant slip ratio is independent of time. The other quantities in Fig. 2.3 are shown at two times: at steady state,  $t = 0$ , and at the time of maximum departure from steady-state conditions,  $t = 24$  sec. It may be noted that the coolant properties deviate by relatively small amounts from steady-state conditions. Figure 2.4 shows the radial distribution of temperatures in the fuel pin, also at  $t = 0$  and at the time of maximum departure from steady-state conditions,  $t = 24$  sec.

Case 2 is identical with case 1 except that the reactivity ramp rate is twice as rapid in case 2, being  $0.1\% \Delta k/\text{sec}$  instead of  $0.05\% \Delta k/\text{sec}$ . The variables for this case are plotted in Figs. 2.5, 2.6, and 2.7. Only the first 30 sec of the transient is shown, since it is during this phase that the important aspects of the transient appear. The equilibrium conditions for case 2 are the same as for case 1, since the equilibrium power level is the same. The most noteworthy aspect of case 2 is that it is very similar to case 1. The peak power level and pin temperatures are slightly higher in case 2, and the maximum departures of the system variables from steady-state values occur 4 or 5 sec sooner in case 2. However, the overall response of the system to the doubled ramp rate is much like

~~CONFIDENTIAL~~  
ORNL-DWG 66-9811

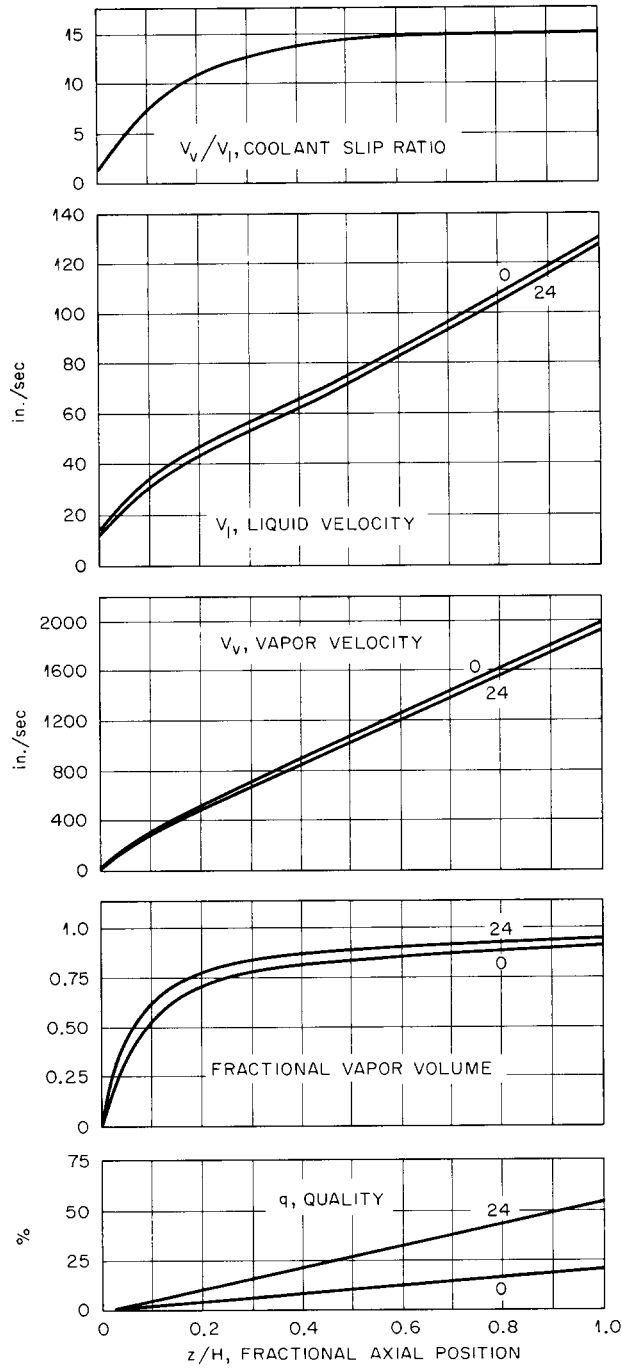


Fig. 2.3. System Variables as a Function of Axial Position at Times  $t = 0$  and  $t = 24$  sec; Case 1.

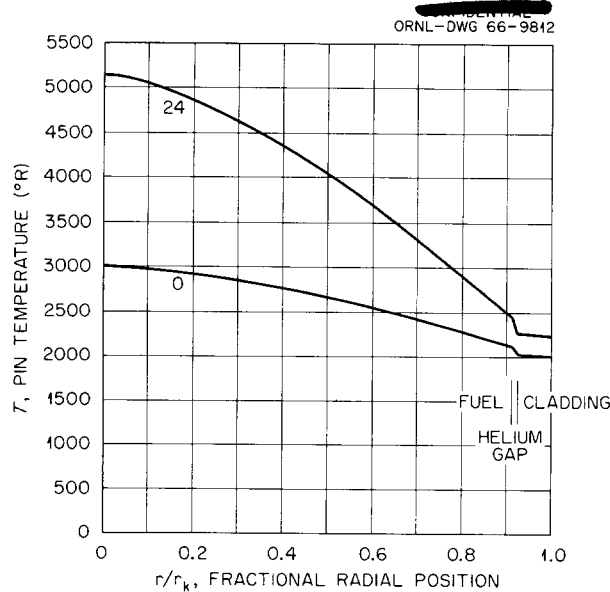


Fig. 2.4. Pin Temperature as a Function of Radial Position at Times  $t = 0$  and  $t = 24$  sec; Case 1.

that of case 1. In the hot full-power configuration at the start of the transient, the control plugs have about 0.5% excess reactivity available in them, and the control mechanism is capable of inserting this reactivity at the rate of about 0.1%  $\Delta k$ /sec. Thus case 2 essentially shows the response of the system if, for some reason, the control plugs are run all the way in and no safety action is taken.

We also considered two cases in which the reactor is scrammed when the power exceeds a given limit. Case 3 is identical with case 2 except that the reactor is scrammed when the power level in the fuel reaches 150% of initial power (see Fig. 2.8). A 10-msec time delay between the initiation of the scram signal and the onset of motion of the scram mechanism was assumed. The scram device is intended to be the bottom reflector, which is dropped and accelerated by the force of gravity. The most important observation from this case is that the reactor scarcely departs from steady-state conditions before the excursion is terminated and the power is reduced to a negligible value. Most of the system variables do not change before the reactor is shut down. A measure of the departure from steady state is given by the change in the central pin temperature,  $T_1$ . The value of  $T_1$  rises about 35°R and then begins to decrease, as

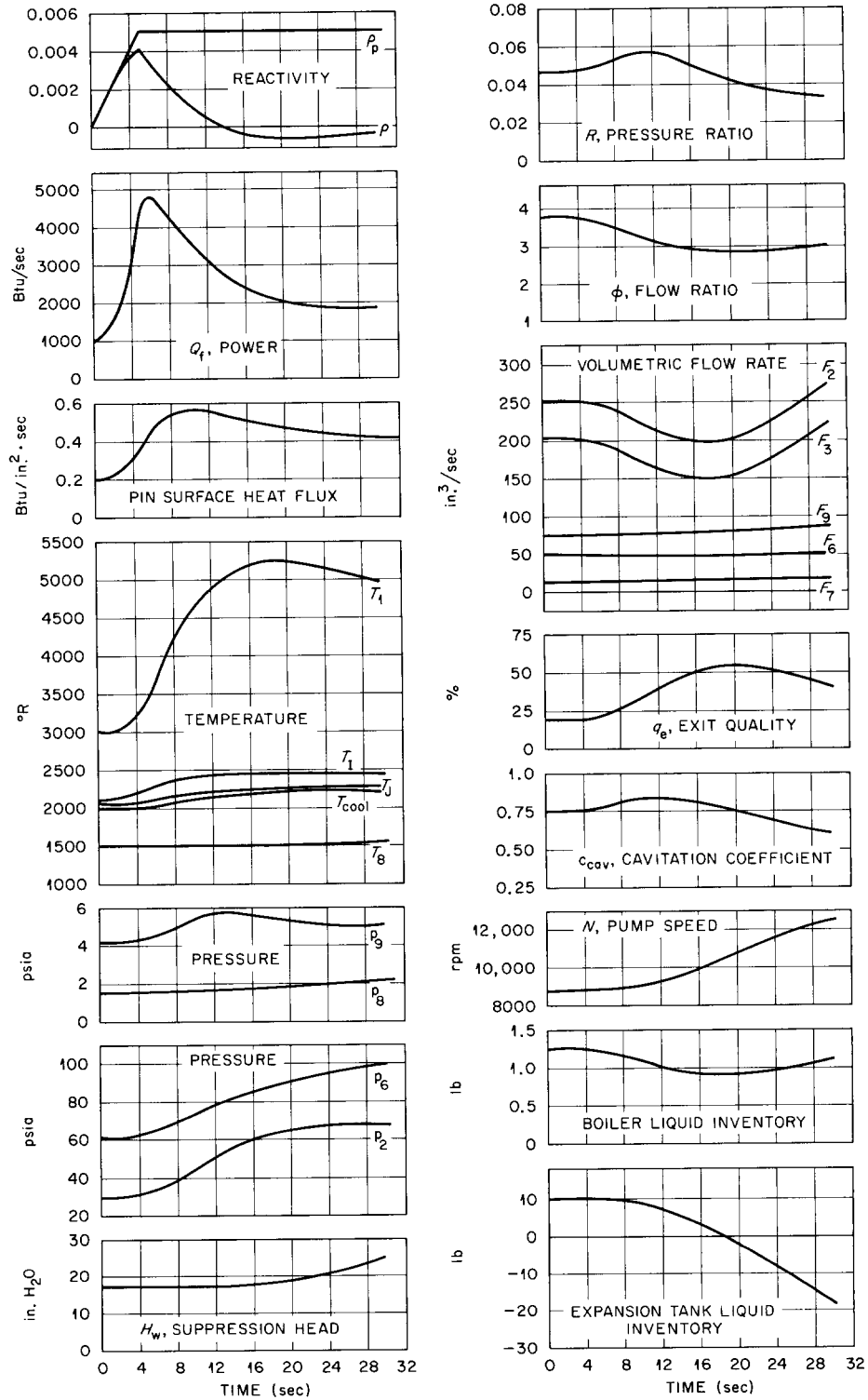


Fig. 2.5. System Variables as a Function of Time; Case 2.

ORNL-DWG 66-9814

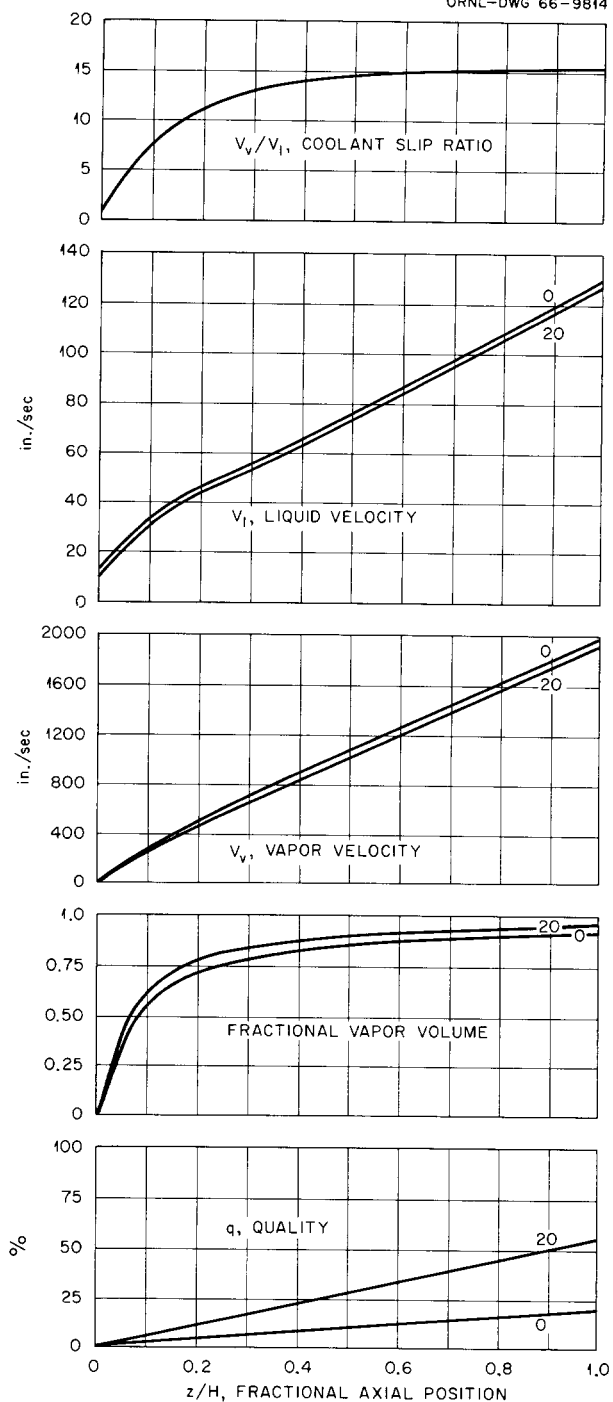


Fig. 2.6. System Variables as a Function of Axial Position at Times  $t = 0$  and  $t = 20$  sec; Case 2.

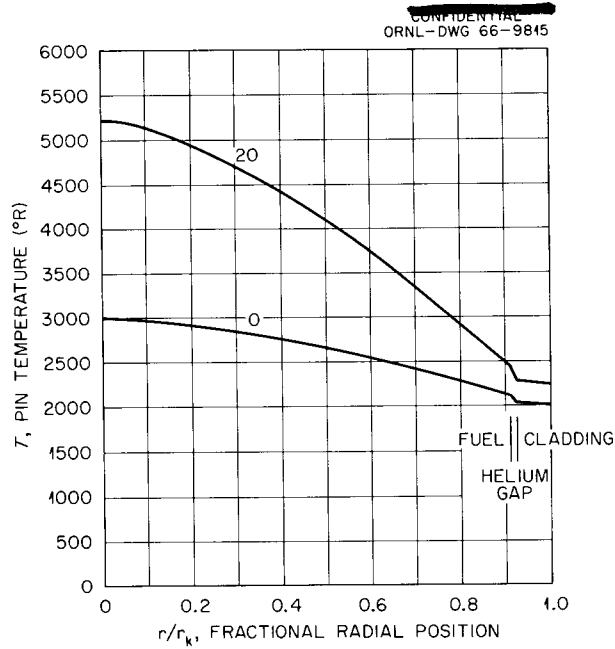


Fig. 2.7. Pin Temperature as a Function of Radial Position at Times  $t = 0$  and  $t = 20$  sec; Case 2.

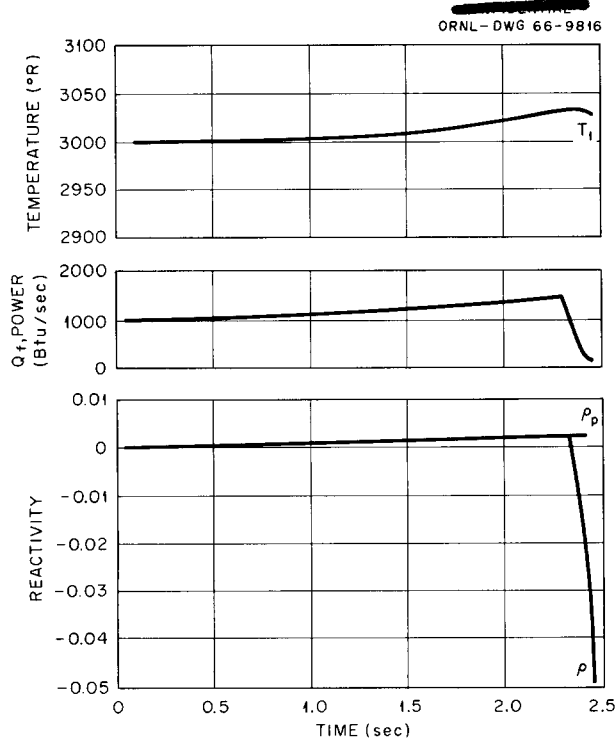


Fig. 2.8. System Variables as a Function of Time; Case 3.

shown in Fig. 2.8. Clearly the system is quite adequately guarded against this excursion by the postulated control system.

Case 4 is similar to case 3 except that the ramp rate is increased by two orders of magnitude to  $10\% \Delta k/\text{sec}$ . The reactor is scrammed when the thermal power level in the fuel reaches  $200\%$  of the starting power, that is, 2 Mw. The significant aspects of the transient are shown in Fig. 2.9. The net effect is much like that of case 3. The power level reaches a somewhat higher value, but the time interval over which it is above the initial value is much smaller. In this case the central pin temperature only increases  $10^\circ\text{R}$  before it begins to decrease. This latter

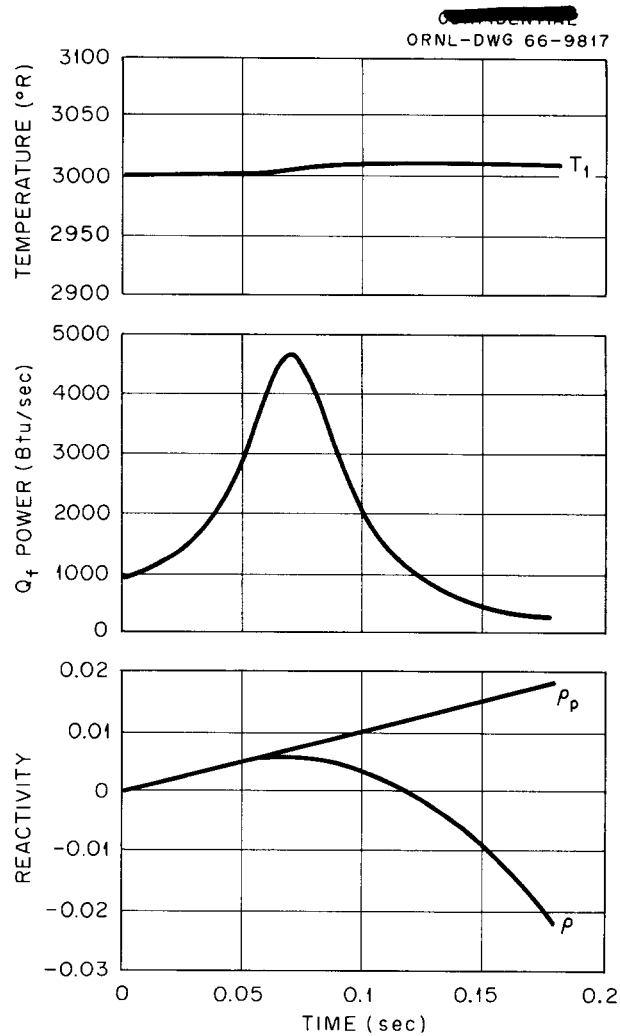


Fig. 2.9. System Variables as a Function of Time; Case 4.

case is clearly an extremely severe ramp. Thus the scram system appears to be adequate against virtually any type of ramp that is initiated at full power. On the other hand it is evident from cases 1 and 2 that the reactor cannot absorb a total reactivity insertion greater than about  $0.5\% \Delta k$  without serious melting of the core if safety action is not taken.

Case 5 represents a much less severe excursion than cases 1 and 2. The reactor is initially at half power and is brought up to about two-thirds of full power by adding a reactivity step of  $0.1\% \Delta k$ . The power delivered to the coolant, which is approximately proportional to  $p_2$ , increases at the rate of about  $0.5\%/sec$ . This rate of change is not greatly different from the rates that are proposed for actual operation of the reactor. Thus this case might, for example, represent part of the startup operation of the system, except that the reactivity would be ramped in rather than stepped. The system variables for this case are shown in Figs. 2.10, 2.11, and 2.12. It may be noted in this case that the suppression head of the condenser jet pump controls the cavitating performance of the jet pump throughout the transient. The pump is driven completely out of cavitation after 120 sec (see pressure ratio  $R$  in Fig. 2.10). There again appears to be some difficulty in balancing the flow rates and in maintaining the inventory in the expansion tank. Possibly some adjustment of the turbine pump and condenser jet pump characteristics is needed.

There is, however, a second possible cause of the difficulty. It may be noted that after 80 sec the pump speed begins to fall off, with a resultant loss in pumping power. This is caused by the rise in condenser pressure. The change in enthalpy across the turbine  $\Delta h_t(p_2, p_8)$  is a very steep function of the condenser pressure  $p_8$ , and a less steep function of boiler pressure  $p_2$ . As the condenser pressure rises the fractional decrease in enthalpy drop across the turbine is greater than the fractional increase in vapor flow through the turbine; consequently there is a net decrease in energy transferred to the turbine and a loss in pumping power. This sensitivity to the condenser pressure  $p_8$  in the mathematical model is probably not realistic. The sensitivity of  $\Delta h_t(p_2, p_8)$  to  $p_8$  increases with decreasing values of  $p_8$ . The condenser pressure at half power is

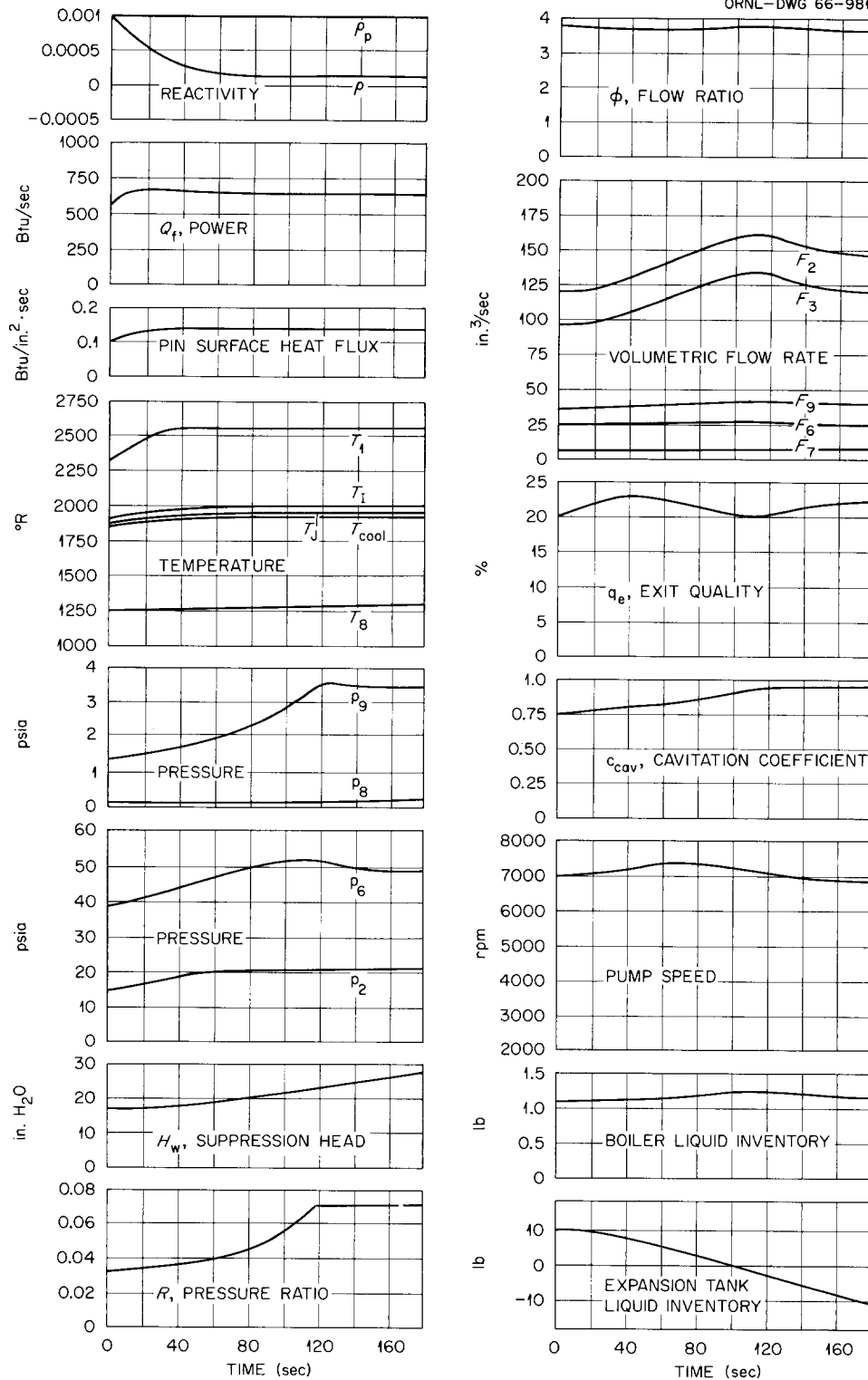


Fig. 2.10. System Variables as a Function of Time; Case 5.

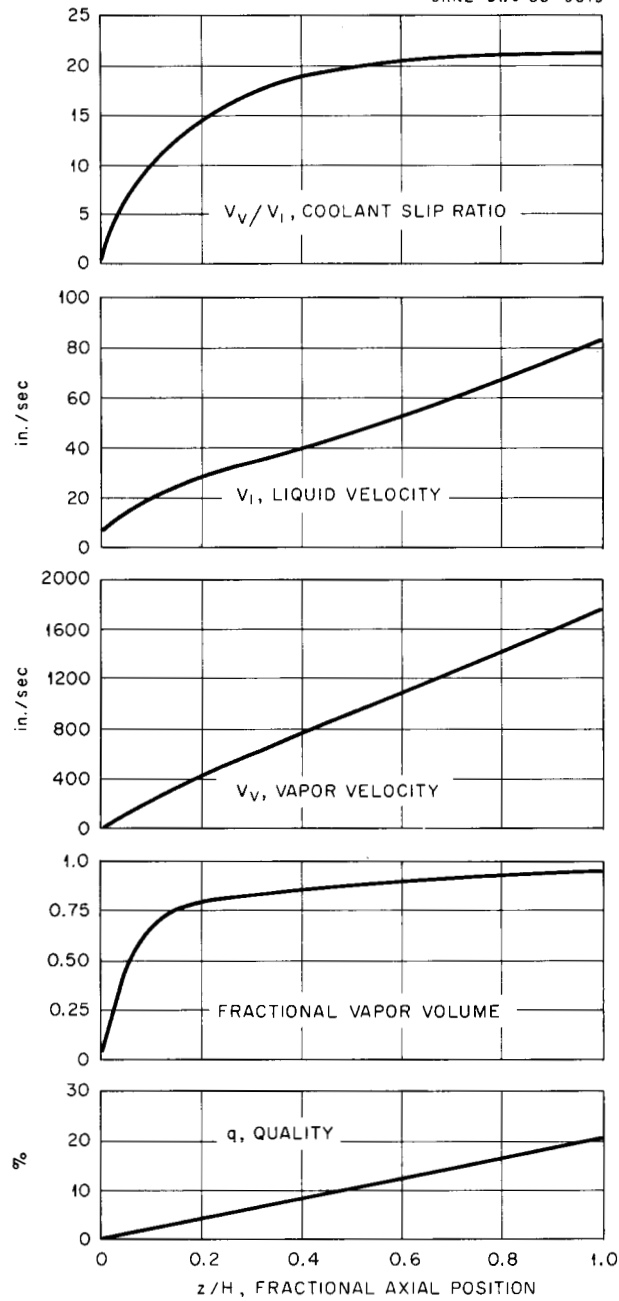


Fig. 2.11. System Variables as a Function of Axial Position; Case 5.

only about 0.15 psi, and very small changes in condenser pressure imply large changes in enthalpy.

In practice, losses between the turbine and the condenser should markedly increase the effective turbine discharge pressure and greatly reduce the sensitivity of the turbine to changes in condenser pressure.

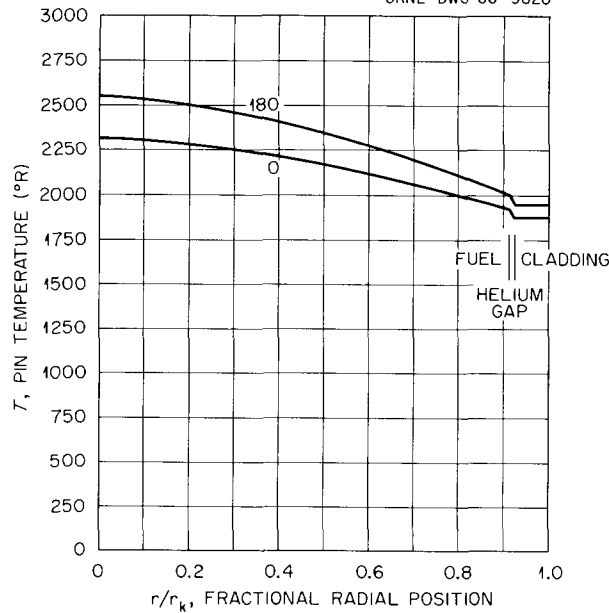


Fig. 2.12. Pin Temperature as a Function of Radial Position at Times  $t = 0$  and  $t = 180$  sec; Case 5.

It is expected that the turbine speed would not decrease with increasing condenser pressure. It should be noted that the cases involving operation at full power do not appear to have this sensitivity to condenser pressure changes; the condenser pressure starts an order of magnitude higher, where  $\Delta h_t(p_2, p_8)$  is a much weaker function of  $p_8$ .

The model is a first approximation to an accurate theoretical mockup of the MPRE, and many of the gross characteristics of the calculations appear to be consistent with the expected behavior of the system. Further development is needed, however, to remove known limitations. These revisions include (1) improvement of data describing the turbine pump characteristics, (2) inclusion of thermal effects in the condenser jet pump description, and (3) inclusion of pressure losses between the turbine pump and the condenser. Also, further comparison with experimental results is needed to confirm the validity of the model in detail or to point out aspects of it that require additional development. In any case it appears that a mathematical model can be developed that is capable of accurately predicting the dynamic behavior of the MPRE under a variety of conditions.

Reference Reactor

O. L. Smith

Information supplemental to the descriptions of the reference reactor presented in previous progress reports<sup>5,6</sup> was developed. The purpose of this information is to show as accurately as possible the power distribution along the irregular perimeter of the core. A sextant of the core is shown in Fig. 2.13. The core boundary is approximated by the solid line labeled "equivalent core boundary" in the figure. A DDK calculation in

---

<sup>5</sup>A. M. Perry, O. L. Smith, and J. V. Wilson, Reactor Physics, p. 35, Fig. 2.1, Space Power Program Semiann. Progr. Rept. June 30, 1964, USAEC Report ORNL-3683, Oak Ridge National Laboratory.

<sup>6</sup>O. L. Smith, Revision of MPRE Reference Design, p. 25, Medium-Power Reactor Experiment Quart. Progr. Rept. Mar. 31, 1965, USAEC Report ORNL-3818, Oak Ridge National Laboratory.

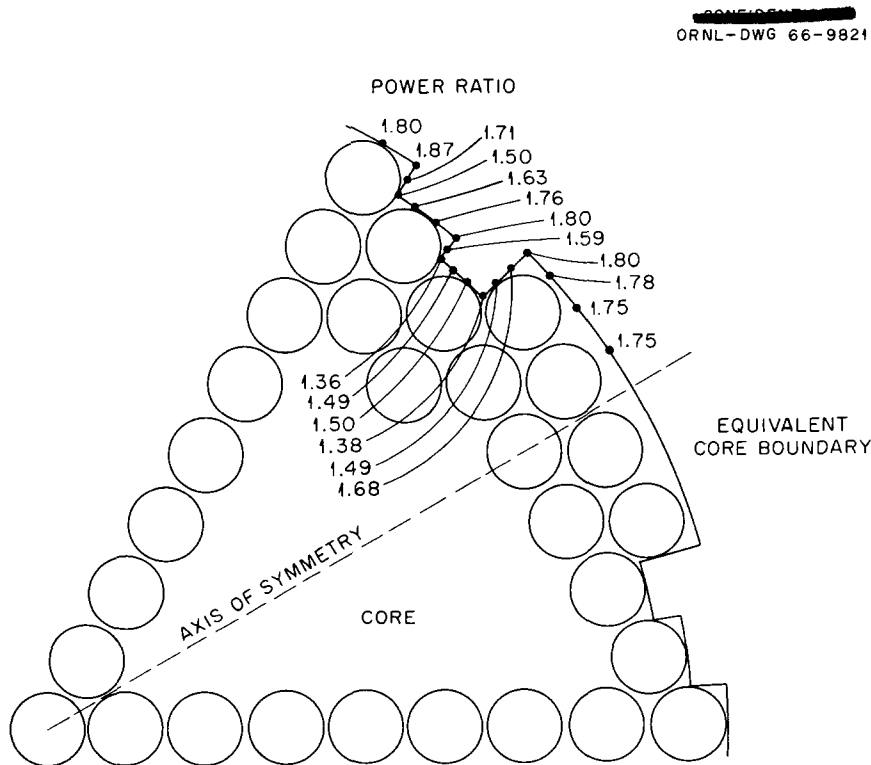


Fig. 2.13. Power Distribution Along Core Boundary of Reference Reactor.

$(r, \theta)$  geometry was performed to determine the power distribution of the numbered points along the boundary. The power distribution in the figure is expressed as the ratio of the power density at a given point to the density at the center of the core. It appears that no serious hot spots are produced by the irregularities, at least to the extent that the calculation reproduces the core boundary correctly.

## 3. DEVELOPMENT TESTS

A. P. Fraas      R. E. MacPherson

Liquid-Metal Jet Pump Test Loop

W. R. Huntley      M. E. LaVerne

Construction of the liquid-metal jet pump test loop shown schematically in Fig. 3.1 and installation of all related instrumentation were completed. This test loop<sup>1</sup> is to provide data on the hydraulic performance of jet pumps at MPRE service conditions with potassium as a working fluid. The electrical heating circuits were checked out, and all pressure-measuring equipment was calibrated at operating temperature. The loop dump tank was charged with potassium, and hot shakedown test operation was started. Preliminary noncavitating performance data were obtained and compared with water data for a similar pump.<sup>2</sup> Cavitating performance data have not yet been taken.

Figure 3.2 shows the noncavitating performance of a plastic model of the MPRE condenser jet pump operating with water. The figure is taken directly from Ref. 2 for comparison with the potassium data to be shown in Figs. 3.3 through 3.5.

Figures 3.3 and 3.4 show the corresponding performance of a full-scale stainless steel replica of the MPRE condenser jet pump operating with potassium as the working fluid. Figure 3.3 displays data taken with both the side and the nozzle streams at 1100°F; the data in Fig. 3.4 are for operation at 800°F. The curve from Fig. 3.2 has been superimposed on both figures for a comparison with the water data. The agreement may be seen to be excellent.

---

<sup>1</sup>W. R. Huntley and M. E. LaVerne, Liquid-Metal Jet Pump Test Loop, p. 23, Medium-Power Reactor Experiment Quart. Progr. Rept. Mar. 31, 1966, USAEC Report ORNL-3976, Oak Ridge National Laboratory.

<sup>2</sup>R. S. Holcomb et al., Radiator Jet Pumps, pp. 90-94, Medium-Power Reactor Experiment Quart. Progr. Rept. Mar. 31, 1965, USAEC Report ORNL-3818, Oak Ridge National Laboratory.

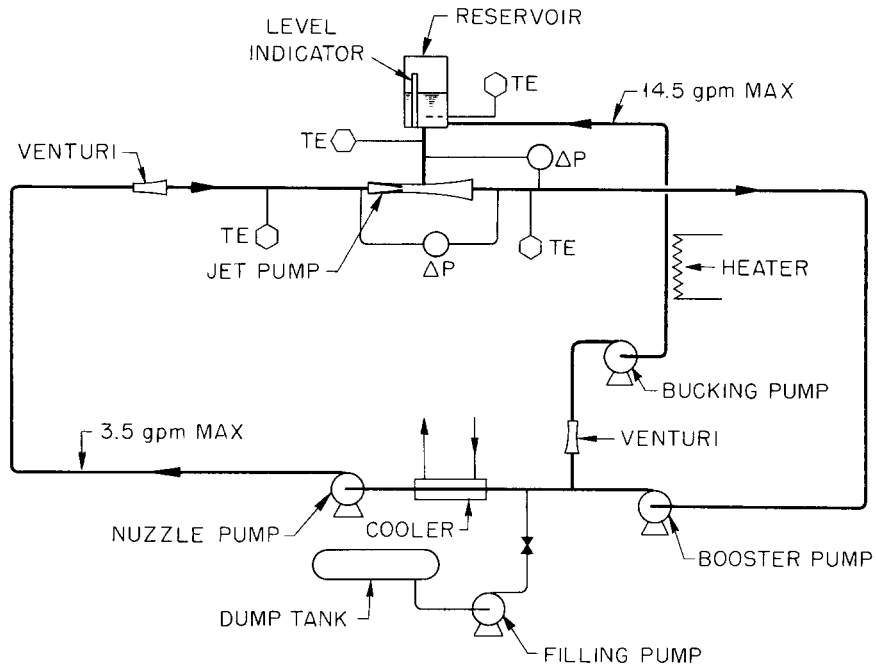


Fig. 3.1. Flow Diagram of Liquid-Metal Jet Pump Test Loop.

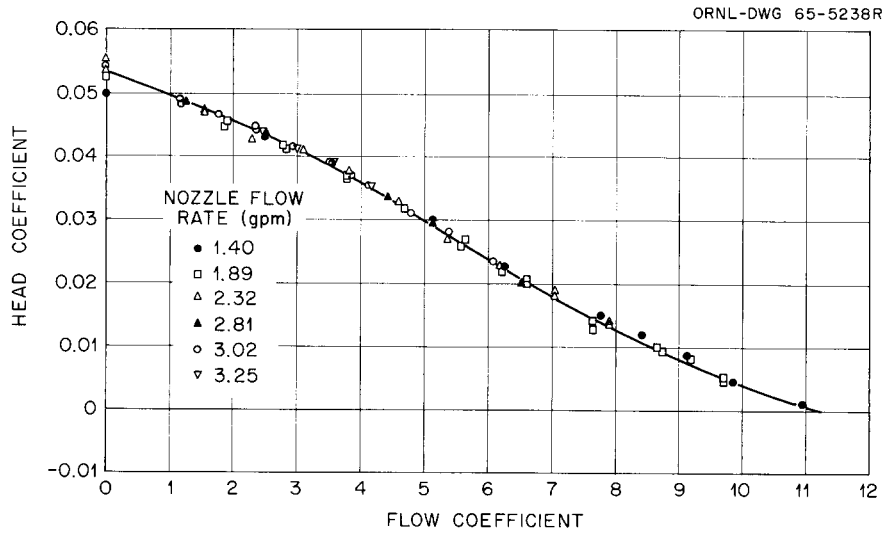


Fig. 3.2. Noncavitating Performance Data for Plastic Model of MPRE Condenser Jet Pump Operating with Water.

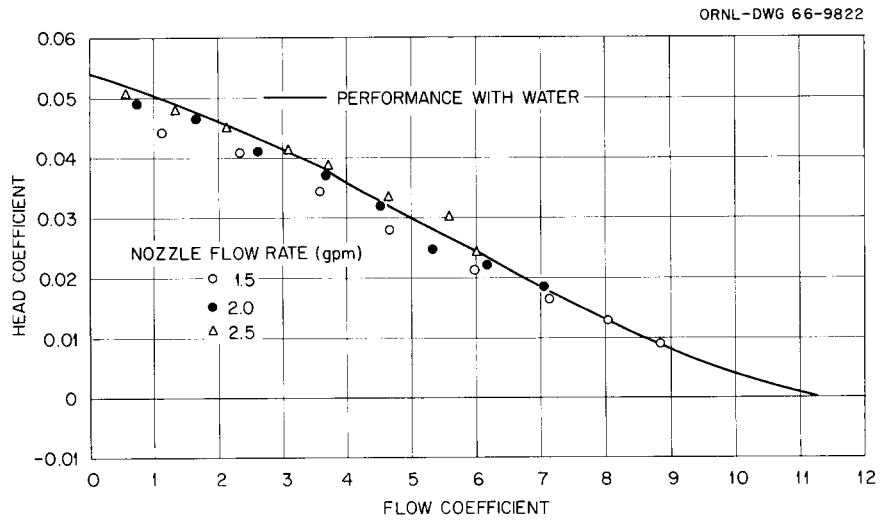


Fig. 3.3. Noncavitating Performance Characteristics of Condenser Jet Pump Operating with 1100°F Potassium.

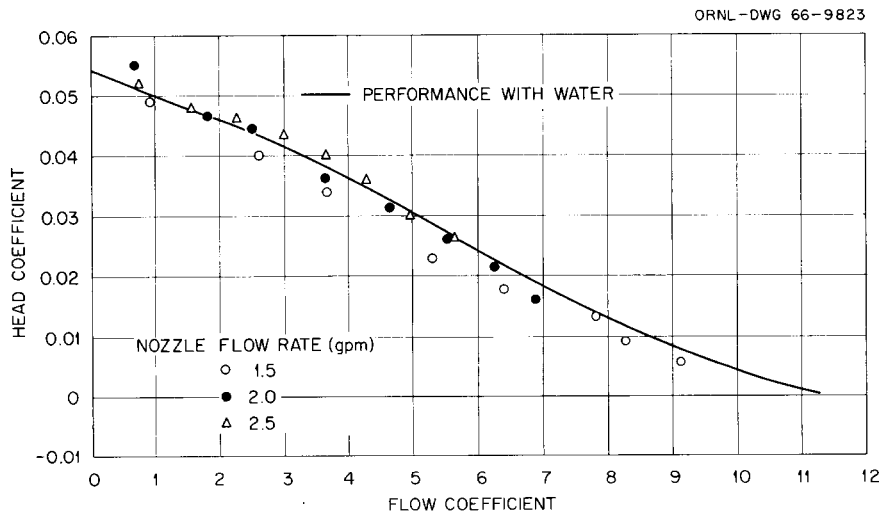


Fig. 3.4. Noncavitating Performance Characteristics of Condenser Jet Pump Operating with 800°F Potassium.

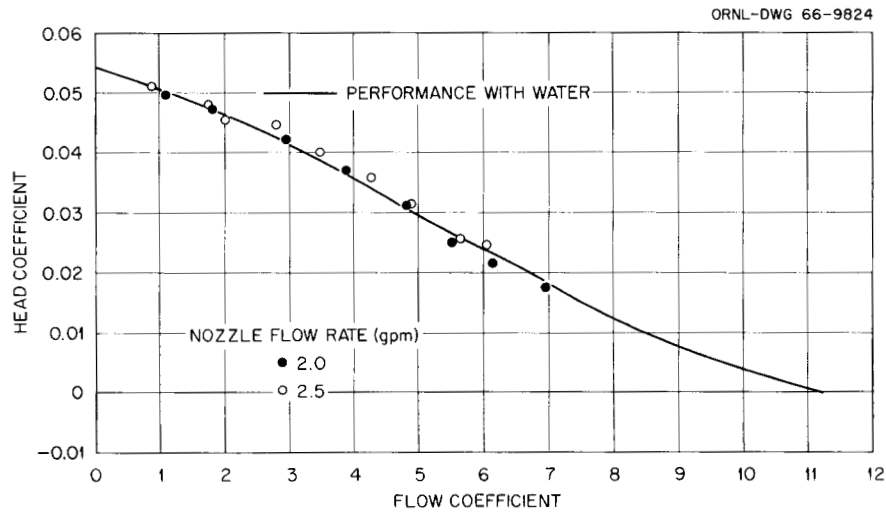


Fig. 3.5. Noncavitating Performance Characteristics of Condenser Jet Pump Operating with 800°F Potassium at Side Port and 750°F Potassium at the Nozzle.

The data in Fig. 3.5 were also taken with the side stream at 800°F but the nozzle stream at 750°F. Again, the potassium data compare favorably with the superimposed water-performance curve.

#### Tests of Ultrasonic Nucleation in Potassium

K. T. Jung      M. M. Yarosh

Tests for producing stable boiling of potassium at low heat fluxes and low temperatures were conducted with ultrasonic excitation for promoting nucleation in the liquid metal. The test apparatus consisted of a modified potassium reflux capsule fitted at the top with a force-insensitive mount to permit installation of the ultrasonic probe. The radiating surface was immersed 0.75 in. below the potassium liquid surface and thus was 1 in. above the end of the installed Watlow Firerod. The Firerod had no attachments for producing nucleation.

Liquid and vapor potassium temperatures were measured from within a thermocouple well installed in the capsule and were read on a two-channel Sanborn recorder. The potassium vapor pressure was also measured. A microphone was mounted on the capsule wall and boiling noises were

recorded simultaneously on magnetic tape and on a Sanborn chart. The occurrence of boiling was determined by observation of the temperature and noise traces and by audio monitoring of the boiling noises.

With the Firerod operating at a power of 1 kw and with the ultrasonic generator off, the potassium pool was raised to a maximum temperature of 1437°F in an effort to achieve stable boiling. The temperature trace recordings, shown in Fig. 3.6, indicate that stable boiling was never achieved. The sawtooth temperature pattern of the trace is characteristic of unstable boiling. The temperature difference between the liquid and vapor shows that the liquid was superheated as much as 125°F during the intervals in which boiling did not occur.

A comparison of the temperature trace of Fig. 3.6 with that of Fig. 3.7 illustrates the effect of operation of the ultrasonic probe. Figure 3.7 is a temperature trace for the capsule operating with a Firerod power of 1 kw but with the ultrasonic generator turned on. For the case shown, the system was operating with stable boiling at a pool temperature of approximately 1100°F. The temperature difference between the liquid and the vapor was less than 20°F.

Figure 3.8 is a temperature trace of the system operating with a Firerod power of 2 kw per rod at a pool temperature of approximately 1200°F. Turning the ultrasonic generator off (at point A) resulted in a return to intermittent boiling and temperature cycling. A restart of the generator (point B) again stabilized the temperature trace and indicated a steady boiling process.

A noise trace (shown in Fig. 3.9) and a sound tape of the boiling were made simultaneously during a test run similar to the run for Fig. 3.8. For this run the system was operating with the ultrasonic generator turned off until the point indicated on the chart. The absence of a signal up to this point indicated that no boiling occurred. A typical noise trace obtained when the system was operating in an unstable boiling mode with periodic "bumping" is shown in Fig. 3.10.

A vertical traverse of the potassium pool temperature was made to determine the magnitude of the temperature gradient in the pool and the effect of operation of the ultrasonic probe on the temperature gradient.

ORNL-DWG 66-9825

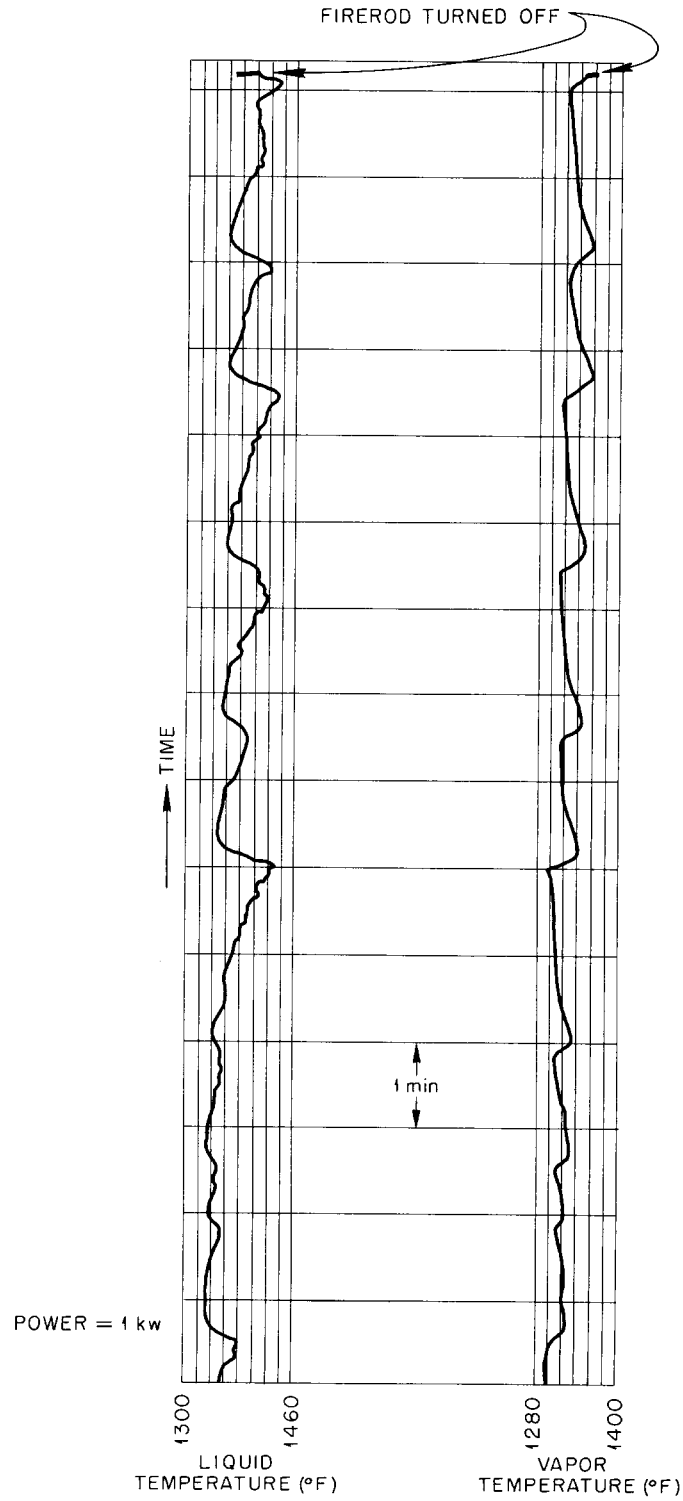


Fig. 3.6. Potassium Temperatures During Boiling Without Ultrasonic Generation at a Heater Rod Power of 1 kw.

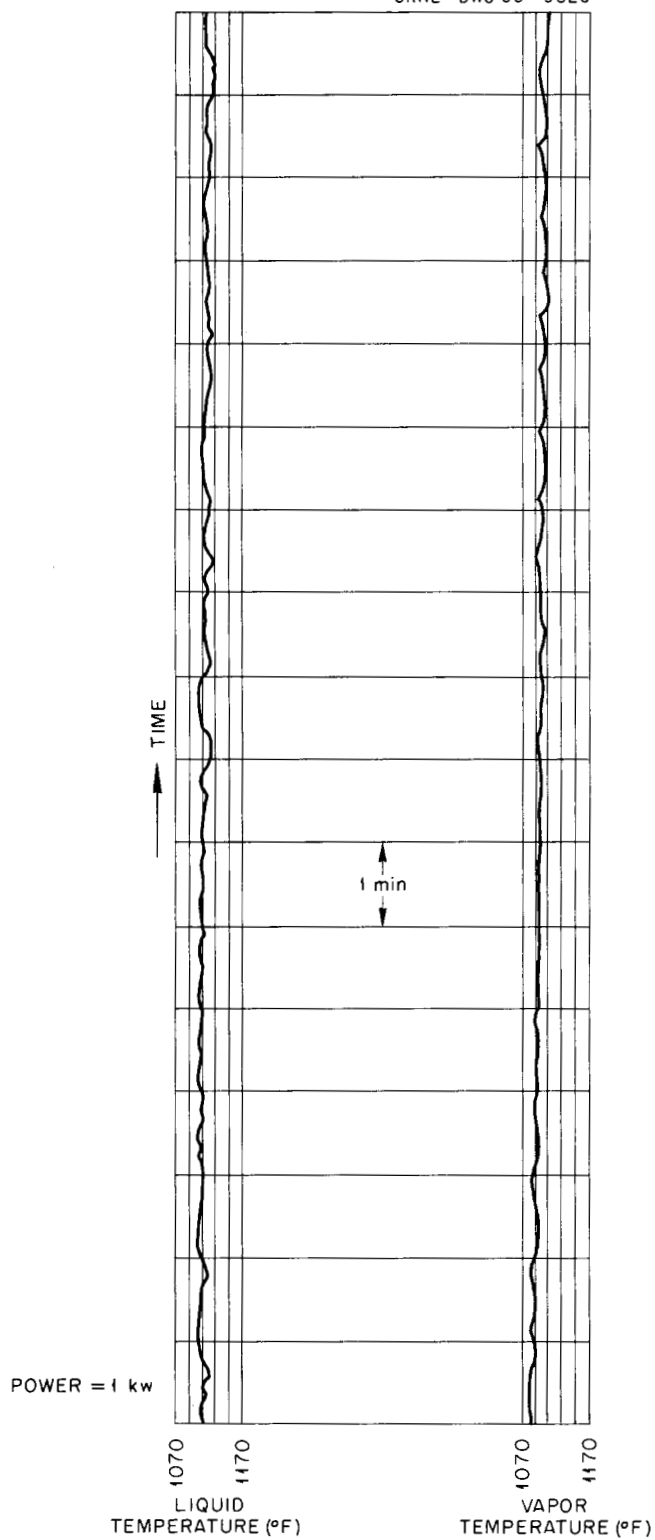


Fig. 3.7. Potassium Temperatures During Boiling with Ultrasonic Generation at a Heater Rod Power of 1 kw.

ORNL-DWG 66-9827

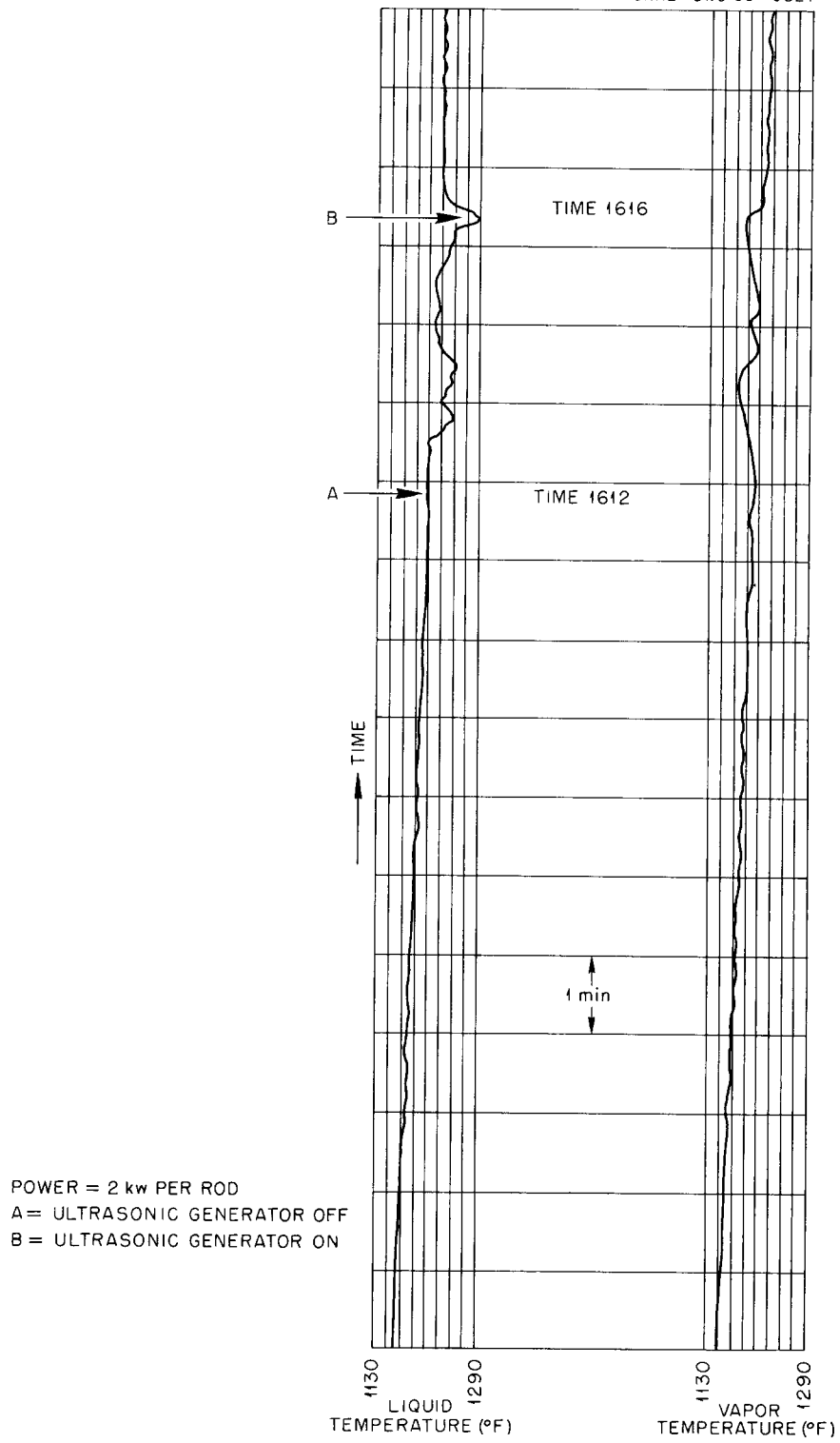


Fig. 3.8. Effect of Operation of Ultrasonic Generator on Boiling Potassium at a Heater Rod Power of 2 kw.

ORNL - DWG 66 - 9828

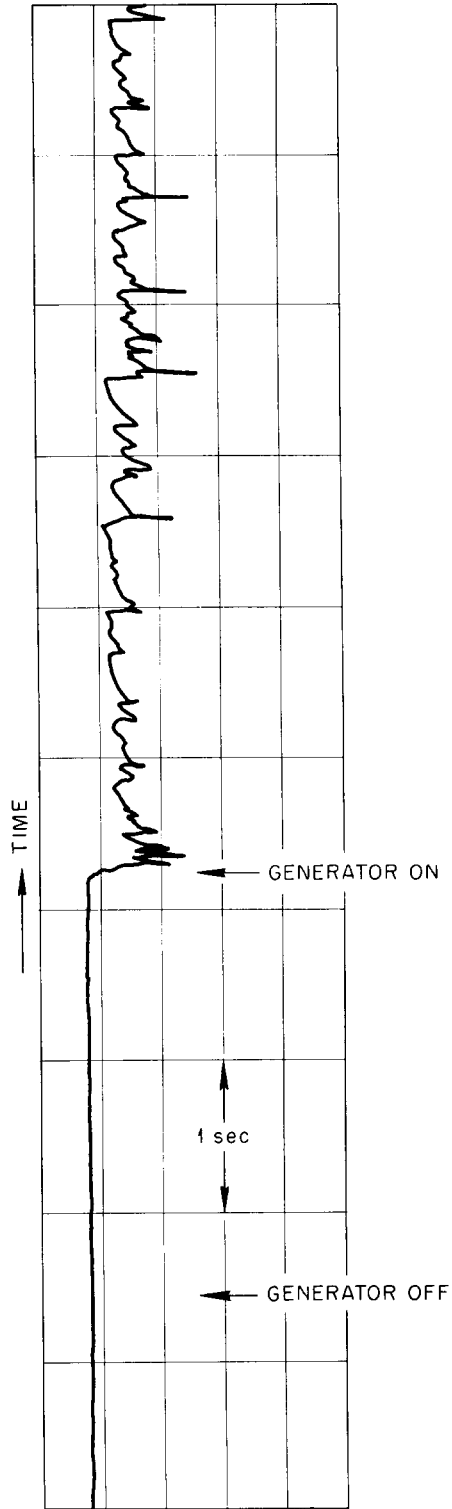


Fig. 3.9. Noise Trace for Boiling with Ultrasonic Generator On and Off at a Heater Rod Power of 2 kw.

ORNL-DWG 66-9829

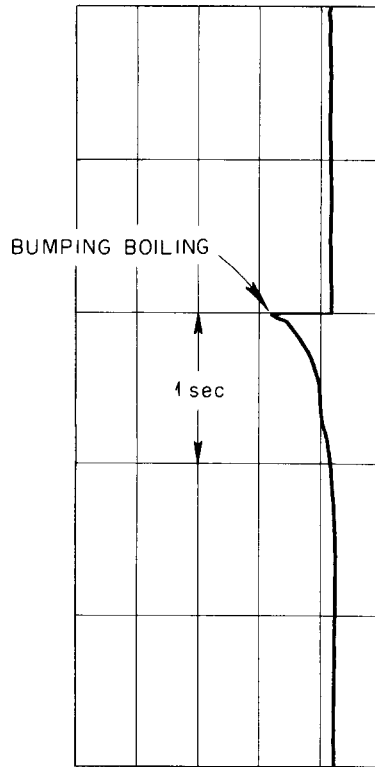


Fig. 3.10. Noise Trace During Unstable Boiling of Potassium at a Heater Rod Power of 2 kw.

Figure 3.11 is a graph of the pool temperature as a function of pool depth with and without the ultrasonic generator in operation. The break in slope for the curve at a depth of approximately 6 in. coincides with the top end of the heated length of the Firerod. As expected, energizing the ultrasonic probe has the effect of reducing the vertical temperature gradient in the pool. For the run shown, a maximum reduction in temperature gradient of approximately 50°F was obtained with operation of the ultrasonic generator.

At low pressures (less than 1 psia) the static head of the liquid has a significant effect on the local boiling point. If it is assumed that the surface of the potassium liquid is at saturation temperature, then higher temperatures are required at increasing pool depths to give saturation conditions. The dashed curve of Fig. 3.11 represents the temperature increase required. The effect of the variation of liquid density with temperature on the pool saturation temperature is small. The temperature

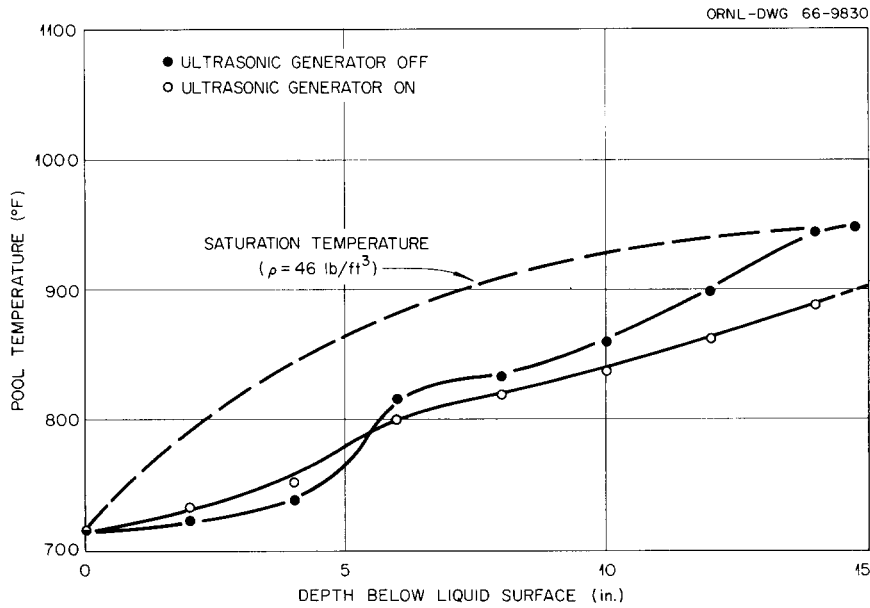


Fig. 3.11. Potassium Temperature Versus Pool Depth at a Heater Rod Power of 2 kw.

difference between the dashed curve and the solid curves shows that the bulk of the liquid was subcooled. From the results it is evident that a careful temperature mapping of the liquid potassium pool is necessary in order to define more clearly the effects of ultrasonic nucleation on the boiling process.

One of the objectives in the operation of the experiment was to determine whether a relationship could be established for detecting the degree of subcooling in the liquid potassium pool. The ultrasonic power required for the production of vapor voids in the potassium by a cavitation phenomena is believed to be sensitive to the degree of subcooling in the potassium liquid.<sup>3</sup> Erratic behavior of the ultrasonic probe during the beginning of this portion of the test led to a shutdown of the experiment. An x-ray of the capsule revealed that a failure had occurred in the mounting rod. Subsequent examination revealed that the failure occurred at a weld in the probe-extension rod.

Work on this experiment has been suspended, and work resumption is contingent on funding.

<sup>3</sup>Aeroprojects Progress Report No. 22, April 1, 1965 to May 31, 1965, USAEC Report NYO-2910-10.

Liquid-Metal Flowmeter Calibration Facility

W. F. Ferguson

The liquid-metal flowmeter calibration facility was designed and constructed to provide a means for calibrating flowmeters at elevated temperatures with potassium or other liquid metals as the working fluid. A zirconium hot trap and liquid-metal sampling system is provided in the facility to assure positive control of the oxide content of the inventory. Figure 3.12 is a photograph taken during construction of the facility. Testing of system controls and shakedown of the facility components are under way. Two flowmeters to be used in the SPS-1 facility will be calibrated.

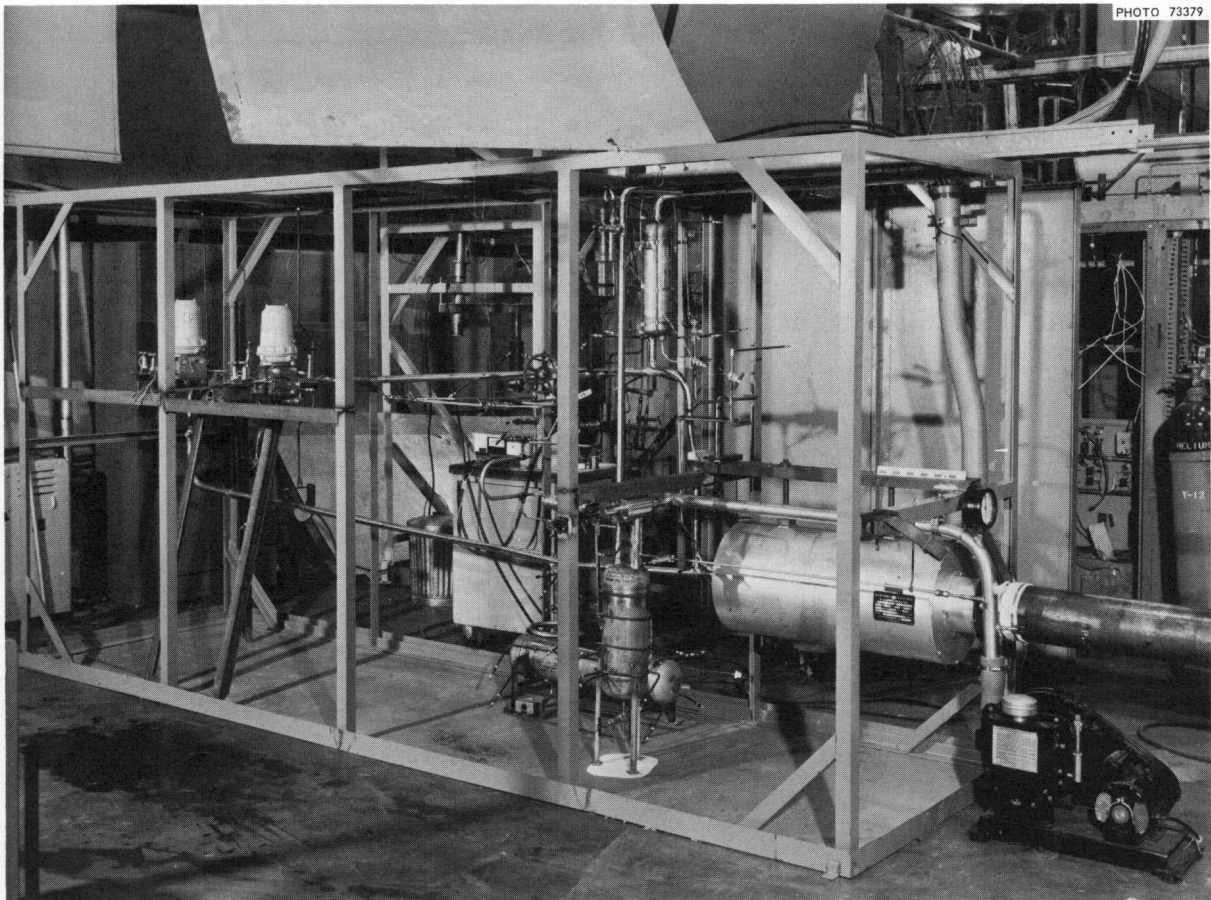


Fig. 3.12. General View of Liquid-Metal Flowmeter Calibration Facility.

Single-Rod Capsule Tests with Potassium

D. L. Clark

Fully compacted heaters were received from the manufacturer and are being installed for testing. In manufacturing these fully compacted heaters, the manufacturer attempted to achieve the maximum insulation density feasible for a cartridge-type heater. If this was achieved, the insulation density should be uniform throughout the unit.

The heaters obtained for the two SPS test facilities include two sets with Nichrome-V leads (in lieu of the standard nickel leads). Six heaters with beryllium oxide insulation are also being obtained, as well as six heaters with niobium-1% zirconium sheaths, BN insulation, and tantalum heater elements.

Insulation resistance tests on the fully compacted heaters at 1500°F at both the factory and ORNL show insulation resistances in excess of 1 megohm for all leakage paths. This value was verified by the two single-rod capsule tests (115 and 117) on these heaters.

Operation of two of the four heaters (110 and 113) with Nichrome-V leads is continuing at 5 kw and a 1600°F pool temperature in accelerated life tests. Heater 111 failed after 336 hr during a restart following a scheduled shutdown to allow it to drop to room temperature. Heater 113, in which the Nichrome-V leads had been nickel plated, failed after 1307 hr of operation at 5 kw and a 1600°F pool temperature when the leads melted near the end of a heater coil. Heater 112, the other heater with nickel-plated Nichrome-V leads, continues to operate after 1351 hr. Heater 110, which has bare Nichrome-V leads, continues to operate after 2073 hr. This test experience indicates no electrical contact problem between the Nichrome-V leads and the Nichrome-V heater element, at least within a 2000-hr interval. This is also indicated by tests conducted by the manufacturer in which the test heaters were temperature cycled thousands of times before failure of the Nichrome-V to Nichrome-V junctions occurred.

Test 103 was terminated because of a capsule leak. A high-purity argon cover gas had been provided for the interior of this heater, and the heater had operated for 1747 hr at 3 kw and 1540°F. The heater was not damaged and may be tested again at a later date. The leakage current

across the insulation was high (0.7 ma and above) throughout the test, but no damage from this is evident. Similar leakage currents occurred on the heater used in test 105. This heater was from the same manufacturer's lot as the one used in test 103; however, this heater was sealed with a silicone compound and failed after 2814 hr of operation at 5 kw and 1540°F.

The heaters used in tests 106, 107, and 108 were from the same manufacturer's lot, and the terminal end of each heater was sealed with a silastic compound (similar to heater 105). Heater 106 failed in the leads after 2052 hr at 3 kw and 1540°F. Heater 108 failed similarly after 2007 hr at 5 kw and 1540°F. Heater 107 continues to operate after 2937 hr at 5 kw and 1540°F. The leakage currents on these heaters were in the order of 0.2 ma throughout these operations. This value of leakage current indicates an insulation resistance of approximately 600,000 ohms. Failures were due to deterioration of the heater leads.

The Firerod heater tests conducted during this quarter are listed in Table 3.1.

Table 3.1. Firerod Heater<sup>a</sup> Tests in Potassium

Test No.	Nucleation Device <sup>b</sup> Radial Thickness (in.)	Firerod Power (kw)	Pool Temperature (°F)	Comments
103	0.060	3	1540	Capsule leaked; no heater failure in 1747 hr
105	0.060	5	1540	Failed after 2841 hr
106	0.030	3	1540	Failed after 2052 hr
107	0.030	5	1540	Operating; 2937 hr accumulated
108	0.030	5	1540	Failed after 2007 hr
110	0.030	5	1600	Operating; 2073 hr accumulated; Nichrome-V heater leads
111	0.030	5	1600	Nucleation failure after 336 hr; Nichrome-V leads
112	0.030	5	1600	Operating; 1351 hr accumulated; nickel-plated Nichrome-V leads
113	0.030	5	1600	Failed after 1307 hr; nickel-plated Nichrome-V leads
114	0.060			Special tests
115	0.060			Operating; 228 hr accumulated
117	0.060	5	1540	Operating; 444 hr accumulated

<sup>a</sup>MgO cores with BN between the windings; sheath rods tapered at lead end.

<sup>b</sup>Nucleation devices consist of three 0.250-in.-wide rings spaced 1/8 in. apart at bottom (inlet) of heated section.

Critical-Heat-Flux Tests of Seven-Rod Boiler with Water

J. K. Jones      J. K. T. Jung  
M. M. Yarosh

Installation of the seven-rod boiler with external wall heating in the critical-heat-flux test facility was completed. The boiler elements are instrumented with thermocouples swaged into the center of the heater rods. The critical heat flux tests conducted previously in this facility were dependent on the temperature signal received from this thermocouple. The detection system installed in the present boiler is designed to measure the leakage current from the lead wire to the thermocouple sheath. Since the resistance of the heater element insulation is sensitive to its temperature, a change in heater element temperature will be detected as a change in the leakage current measured.

In preliminary tests to determine the characteristics of the leakage-current detection system, the seven-rod boiler was operated without external heating. The six outer rods were operated at 3 kw/rod, and the center rod was operated at 4.5 kw/rod, with an average boiler exit vapor quality of less than 20%. A critical-heat-flux condition was initiated on the center rod by throttling the liquid flow to the boiler inlet until a rapid rise in leakage current indicated that a "burnout" condition had occurred. Simultaneous measurements of the rod central temperatures were also made, and power to the individual rods was tripped when either the current or the temperature exceeded the set points. The high-temperature shutdown system was set to cut off the power to each of the peripheral rods if a 50°C temperature excursion occurred and to the center rod if a 100°C temperature excursion occurred. The current trip settings were adjusted to approximately 1  $\mu$ a above the steady-state reading.

In the preliminary tests, the leakage-current detection system successfully shut down the heater element power on a high-current signal. The critical-heat-flux condition was confirmed by an almost simultaneous high-temperature trip from the thermocouple signal. The relative sensitivity of the current detection system can be adjusted so that the trip

set points can be tailored to the individual heater rod resistance characteristics.

After completion of the preliminary system checkout, it is planned to duplicate the heat flux measurements conducted previously on the 1/16-in.-spaced bundle and then examine the effect of the external shell heating on these earlier results. In the future this work will be carried out under the basic heat transfer program.

#### Small Water System

A. M. Smith      A. G. Grindell

The vapor and liquid piping configuration planned for the SPS-2 turbine-pump installation was used for a water test in the SWS with an Aeronutronic Mark-2 turbine pump. This system test was intended to verify the adequacy of the SPS-2 piping configuration<sup>4</sup> and to deduce satisfactory starting procedures and turbine pump operation limits. However, initial test operation was hampered by excessive leakage of lubricant (water) past the turbine-end journal bearing and into the turbine cavity. A new shaft was fabricated with reduced bearing running clearances that controlled the lubricant leakage satisfactorily.

Preliminary operation at 22-kw boiler power indicated that the turbine pump head was insufficient to provide a satisfactory boiler feed flow rate. A review of the data indicated that the speed of the unit was considerably lower than that achieved at similar steam conditions with the same unit in the steam-water turbine pump test rig. Visual examination of the Graphitar bearing revealed that it was cracked at the turbine end and that the bearing surfaces had sustained considerable scoring. As soon as a new bearing (fabricated of bearing brass) is installed the testing will be resumed.

---

<sup>4</sup>A. M. Smith and A. G. Grindell, Small Water System, pp. 27-28, Medium-Power Reactor Experiment Quart. Progr. Rept. Mar. 31, 1966, USAEC Report ORNL-3976, Oak Ridge National Laboratory.

Small Potassium Systems

A. M. Smith    A. G. Grindell

System No. 1

A series of tests (No. 11)<sup>5</sup> of heater rod bundle 9 was terminated after 241 hr at a maximum power level of 3.5 kw per rod because of the loss of internal thermocouples in all seven heater rods, electrical failures in two heater rods, and a continuously high ground current indication in one of the remaining five rods at a power level of 1.0 kw. Following shutdown of the facility, the heater rod bundle and all piping that operated with liquid potassium, except the condenser and the Electrodynamic pump, were removed from the facility for detailed examination.

It was decided to obtain burnout heat flux data with a new 1/16-in.-spaced boiler and to perform initial tests of a potassium vapor quality meter designed and built by Westinghouse-Astronuclear Corporation. This test program required major revision of the test facility.

The designs of a new boiler, vapor separator, hot well, and heat exchangers were completed, and fabrication was initiated. Revised piping drawings and electrical and instrumentation flow sheets were completed. Field installation of all components, except the test boiler and electromagnetic flowmeters, was completed. The boiler barrel is being fabricated, and the flowmeters are being calibrated with potassium at operating temperatures.

The test program will be directed toward a determination of the effects of vapor exit quality on the burnout heat flux and pressure drop at various boiler pressures. An attempt will be made to deduce satisfactory operating procedures for the vapor-quality meter.

System No. 2

A total of 71 hr of boiling operation at a power level of approximately 3 kw per rod was accumulated before the system was shut down by

---

<sup>5</sup>S. E. Bolt, A. M. Smith, and A. G. Grindell, Small Potassium Systems, pp. 28-30, Medium-Power Reactor Experiment Quart. Progr. Rept. Mar. 31, 1966, USAEC Report ORNL-3976, Oak Ridge National Laboratory.

numerous false power scrams caused by failure of the internal thermocouples in the heater rods.<sup>5</sup>

During the test period, two system startups were made in which boiling was initiated without using the hot finger. In each case, potassium was added to the boiler, the boiler inlet and outlet valves were closed, and the boiler power was raised slowly to 1 kw per rod. As the power was increased, large temperature excursions in the heater rods were observed that indicated unstable boiling. The magnitude and frequency of the excursions gradually decreased with increase in the boiler temperature and pressure. The Electrodynamic boiler feed pump was then turned on, the boiler inlet valve was opened, and the boiler outlet (vapor) valves were opened slowly. As forced boiler feed was started, the temperature fluctuations in the heater rods followed a regular pattern with an amplitude of about 10°F.

During the second test, which had a duration of approximately 48 hr, a scram that resulted from an internal thermocouple failure automatically shut down the loop. This was the fifth heater rod thermocouple lost since the initial startup. Test operation was terminated because the thermocouple in a sixth rod was giving indications of failure.

During the shutdown to change the heater rods an Aeronutronic Mark-2 turbine pump was installed in the system (see Fig. 3.13) for endurance testing. The installation of the turbine pump and all necessary piping, heaters, and instrumentation was completed. Heater rods were received, and a boiler bundle is being fabricated. In the event the turbine pump does not provide an adequate boiler feed pressure, the Electrodynamic pump, which is installed in a parallel boiler feed line, will be used.

Tests of Turbine Pumps for Boiling-Potassium Systems

H. C. Young      A. G. Grindell

After replacement of the MgO-insulated boiler heater rod bundles in the intermediate potassium system, the second unit of the Aeronutronic

PHOTO 73412

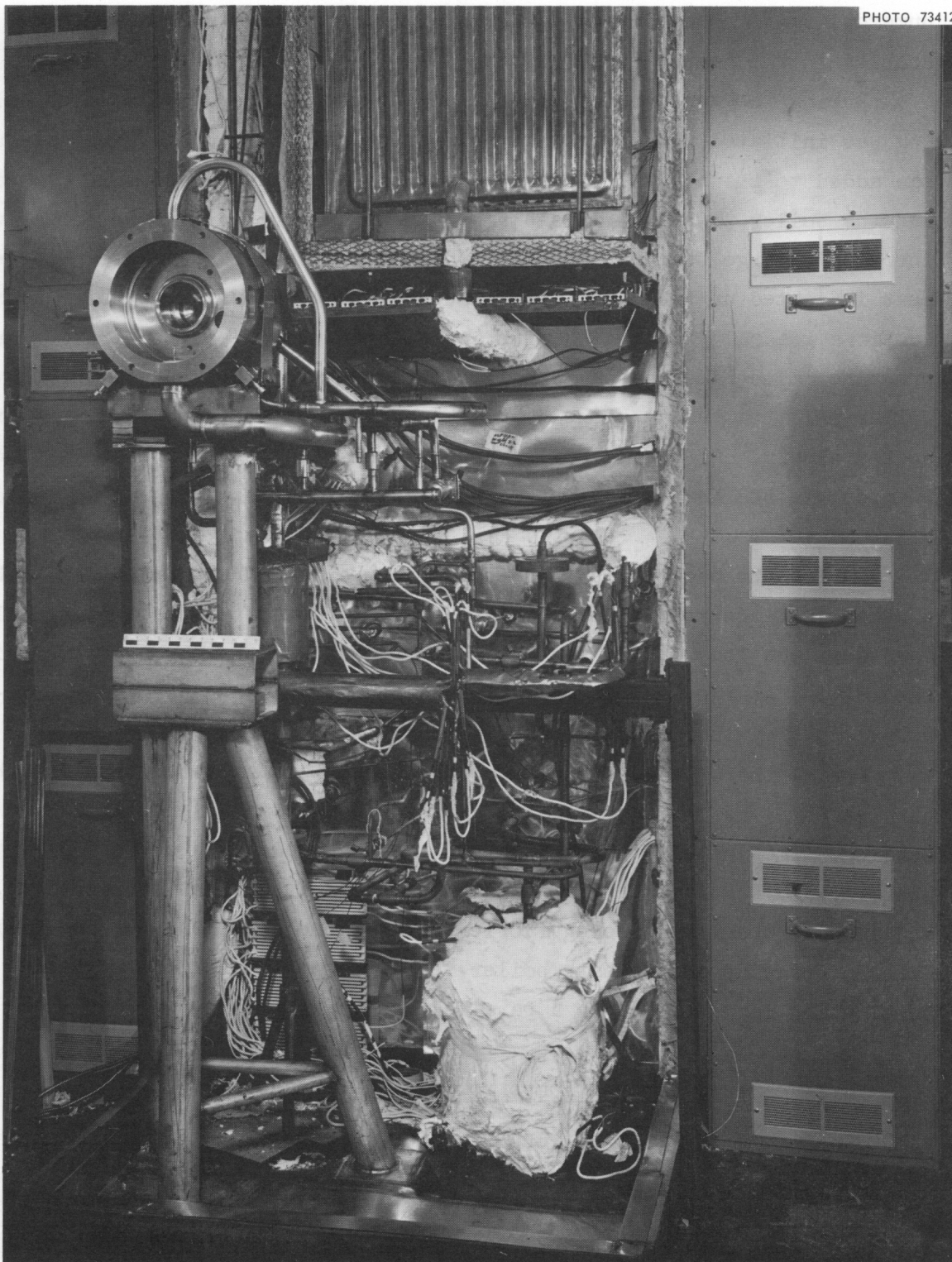


Fig. 3.13. View of SPS-2 Looking into the Aeronutronic Mark-2 Turbine-Pump Housing.

Mark-1 turbine pump was restarted.<sup>6</sup> During the first restart, bearing-lubricant flow was not established. Frozen potassium in an electromagnetic flowmeter had plugged the lubricant line. After the plug was thawed, flow was established, and the pump was started. It operated satisfactorily even though the boiler heater rods demonstrated such low electrical resistivity that only 18 of the 91 rods were operable. The system was shut down to replace the boiler heater bundle again, and the turbine pump was removed for inspection. Although it had operated nearly 2600 hr with 46 starts and stops, the pressure drop across the nozzle required to start rotation remained essentially the same as that observed during earlier starts.

When the pump was disassembled there were no signs of the galling of TZM parts experienced with the first unit.<sup>7</sup> This may be due to the use of Aqua-Dag, a carbon-water solution, on close-fitting static surfaces and shaft threads. Despite operation in cavitation for most of the 2600 hr at up to 1000°F, the pump impeller showed no signs of damage (see Fig. 3.14). Similarly, the turbine wheel showed no evidence of bucket erosion (see Fig. 3.15). According to visual observations, the bearings were in good condition. The turbine-end journal had approximately 0.2-mil taper, and the diametral clearances for both bearings had increased by 0.3 mil (from 2.8 to 3.1 mils). Some very light metallic pickup was visible on both journal surfaces (see Fig. 3.16). The journal runouts were in the order of 0.4 mil. In view of the large diametral clearances and measurable wear in the bearings, it was decided to replace pump unit 2 with unit 1, which had been rebuilt with a new shaft and bearings.

Water testing<sup>6</sup> of the Aeronutronic Mark-2 turbine pump was started in the steam-water test rig. During initial tests, air leaked into the test loop at threaded stainless steel pipe joints and through the leads to the inductance probes, which are used to measure the journal position

---

<sup>6</sup>H. C. Young and A. G. Grindell, Test of Turbine Pumps for Boiling-Potassium Systems, pp. 32-33, Medium-Power Reactor Experiment Quart. Progr. Rept. Mar. 31, 1966, USAEC Report ORNL-3976, Oak Ridge National Laboratory.

<sup>7</sup>H. C. Young and A. G. Grindell, Turbine Pump Development for Potassium Systems, p. 60, Medium-Power Reactor Experiment Quart. Progr. Rept. Mar. 31, 1965, USAEC Report ORNL-3818, Oak Ridge National Laboratory.

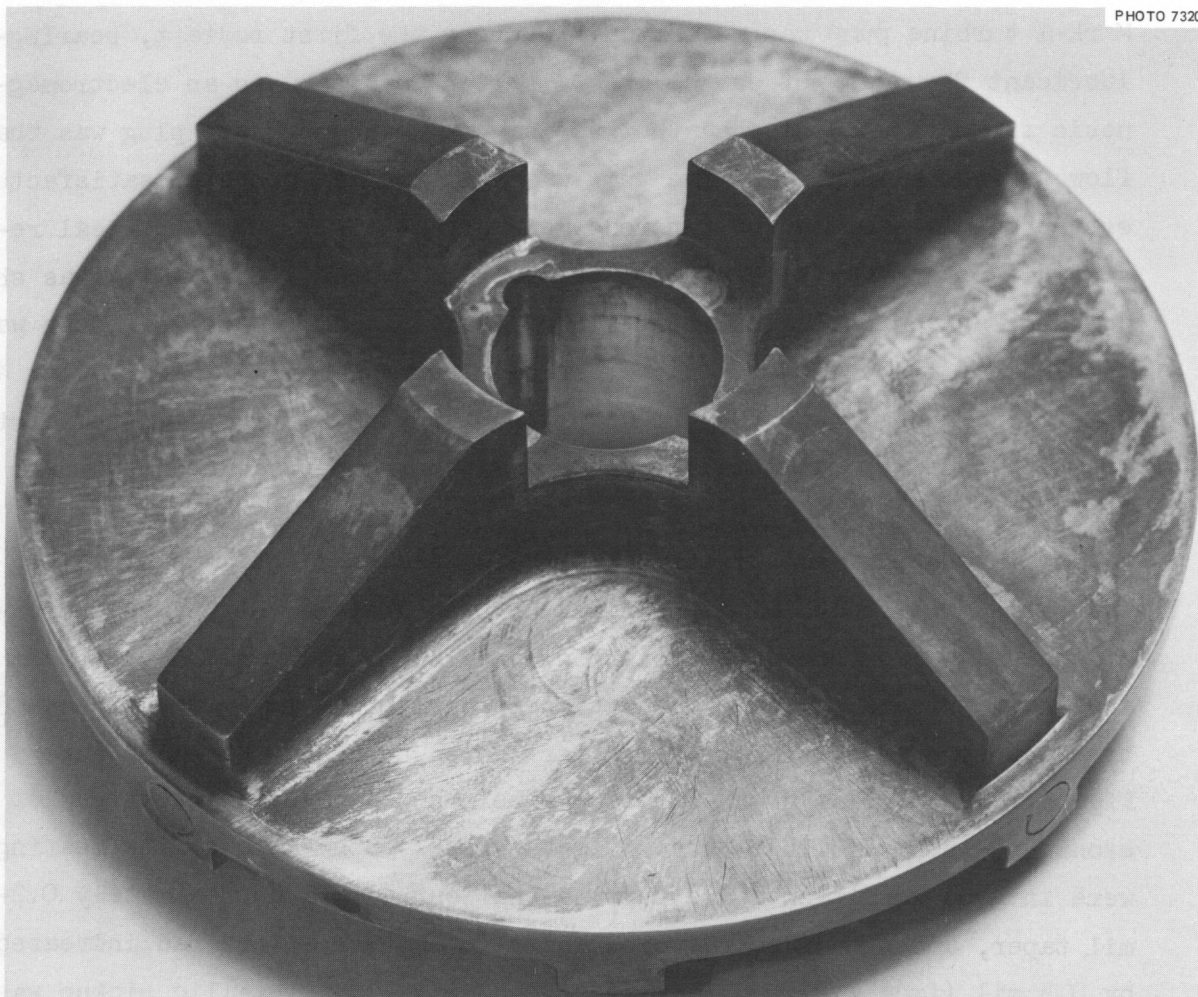
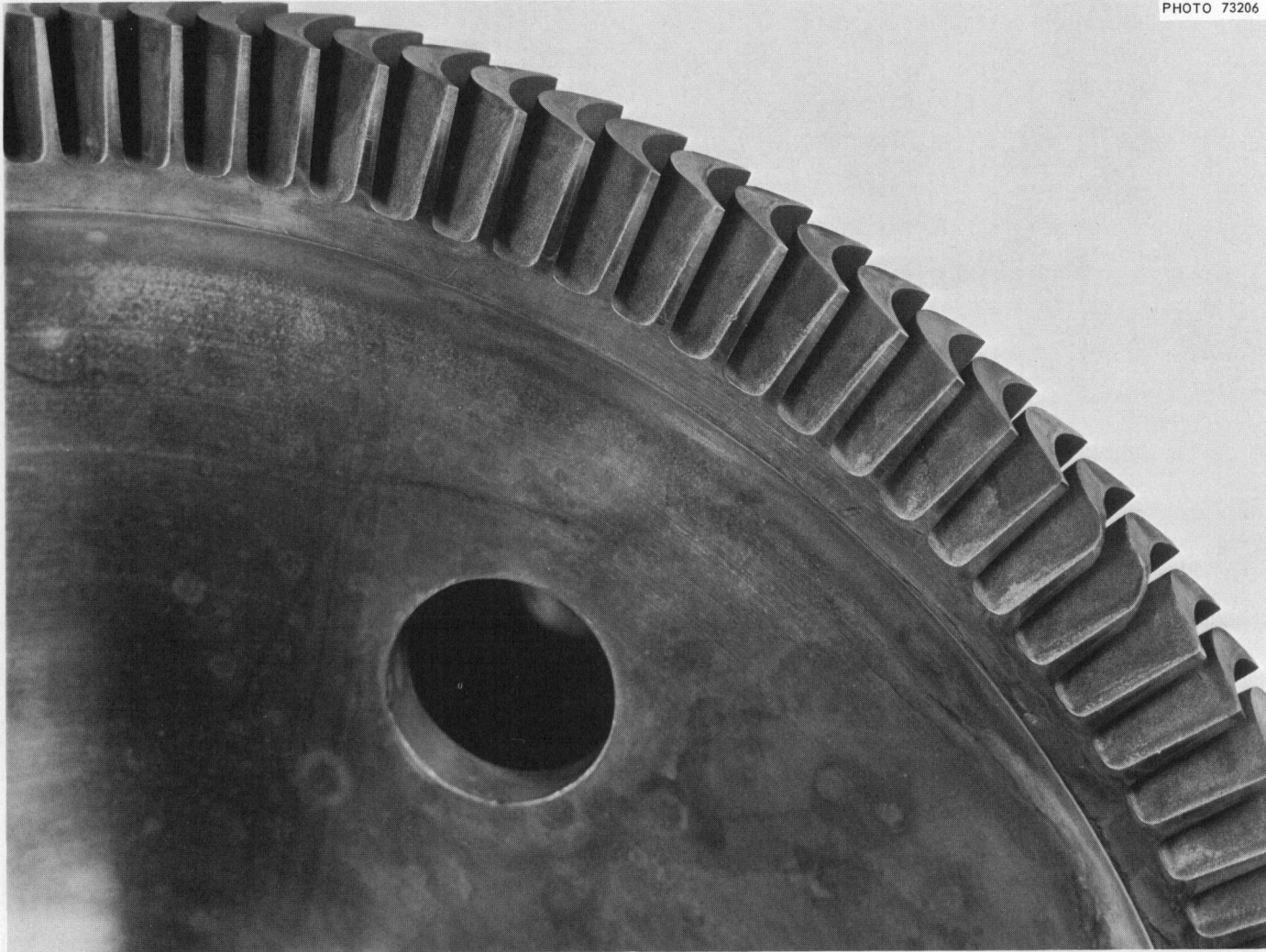


Fig. 3.14. Aeronutronic Mark-1 Turbine Pump. Pump impeller from unit 2 after 2576 hr of operation with potassium in the intermediate potassium system.

in the bearing. All threaded joints were welded, the pipe threads at all flowmeters were soldered or brazed, and the probe leads were sealed by forcing silastic between the lead wire and the Teflon insulation for the full length of the lead wire. Having achieved a leaktight system, preliminary head-flow and cavitation-inception data were obtained at low speeds.

The Mark-2 rotary assembly with the instrumented bearing holder and the first- and second-stage turbine nozzle blocks is shown in Fig. 3.17. The bearing was made of bearing bronze, and the journal and thrust surfaces on the stainless steel shaft were plated with chromium. Bearing

PHOTO 73206



~~CONFIDENTIAL~~

~~CONFIDENTIAL~~

73

Fig. 3.15. Aeronutronic Mark-1 Turbine Pump. Turbine wheel from unit 2 after 2576 hr of operation with potassium in the intermediate potassium system.



Fig. 3.16. Aeronutronic Mark-1 Turbine Pump. View of journal and thrust-bearing surfaces from unit 2 after 2576 hr of operation with potassium, including 47 starts and stops, in the intermediate potassium system.

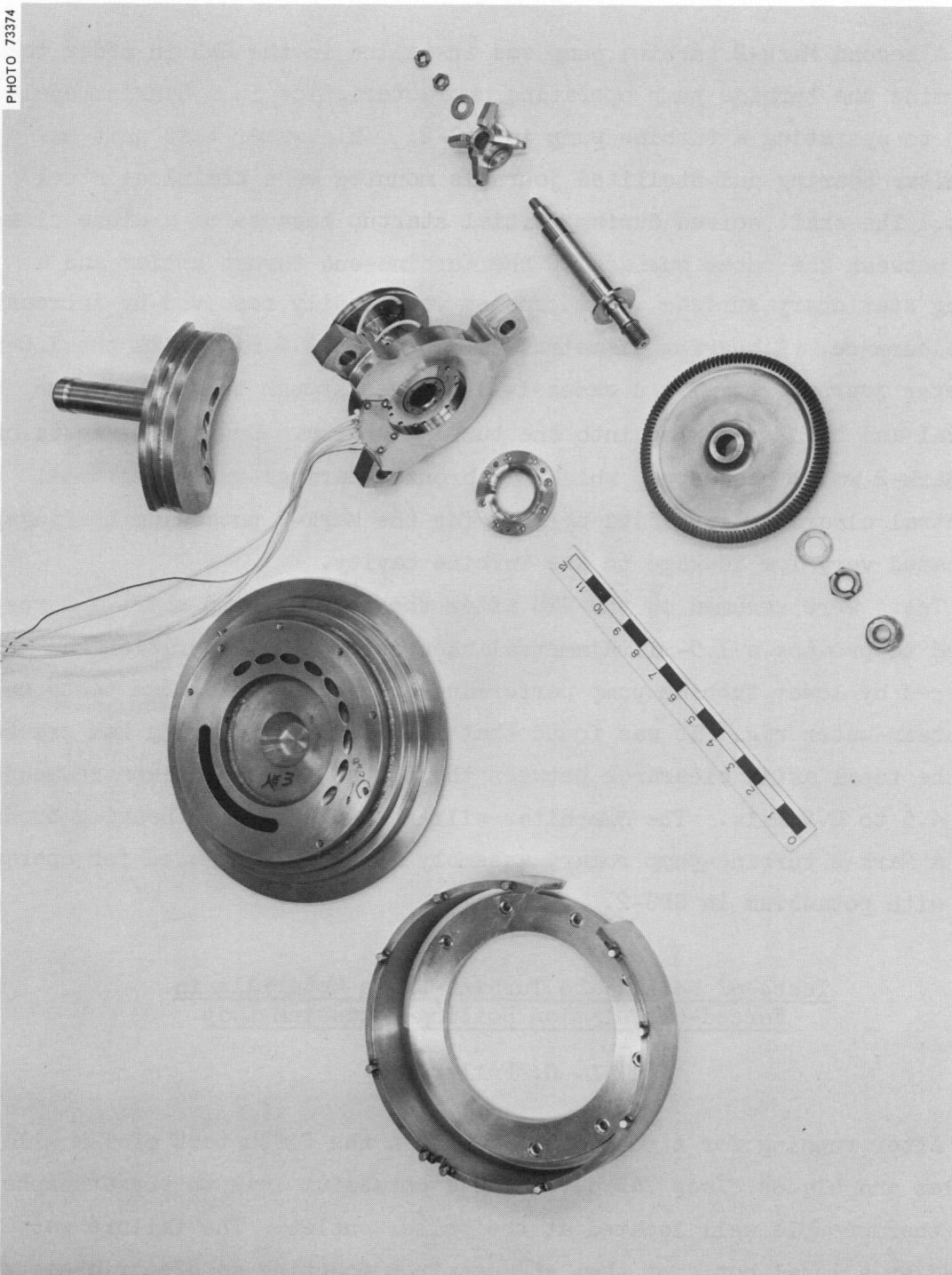


Fig. 3.17. Parts for Steam-Water Test of Aeronutronic Mark-2 Turbine Pump. Nozzle blocks, bearing holder, turbine wheel, shaft, and impeller are shown.

bronze was substituted for the tungsten carbide of the journals used in the potassium unit to indicate more readily the presence of bearing problems.

A second Mark-2 turbine pump was installed in the SWS in order to determine the turbine pump operating characteristics in a Rankine cycle prior to operating a turbine pump in SPS-2. This water test unit had a Graphitar bearing and Stellite journals mounted on a stainless steel shaft. The shaft seized during initial startup because of a close clearance between the outer surface of the turbine-end thrust collar and a mating stationary surface. The problem was readily resolved by increasing the clearance. A bearing diametral clearance of 3.6 mils with the 1.0-in.-diameter journals permitted excessive leakage through the turbine-end journal and thrust bearing into the turbine cavity. Concurrent tests of the Mark-2 water prototype, which has bronze bearings and the 1.5-mil diametral clearance specified by ORNL for the Mark-2 potassium bearings, indicated very low leakage to the turbine cavity.

Tests were resumed on the SWS after the turbine pump shaft was replaced to provide a 1.5-mil diametral clearance. Test operation was then hampered by lower turbine pump performance than predicted from tests on the steam-water rig. It was found that the Graphitar bearing had cracked and the total axial clearance between the thrust faces had been reduced from 4.5 to 0.5 mils. The Graphitar will be replaced with bearing bronze.

A Mark-2 turbine-pump rotary assembly is being assembled for operation with potassium in SPS-2.

Tests of Nozzle and Turbine-Blade Materials in  
Forced-Circulation Boiling-Potassium Loop

L. C. Fuller

After running for a total of 3600 hr in the fifth test of TZM alloy nozzles and blades, loop 7A3 developed a potassium leak to the atmosphere at a thermocouple well located at the boiler outlet. The failure was caused by a local hot spot that stemmed from mounting an electric heater too close to the joint between the thermocouple and the adapter sleeve used to attach it to the boiler. Argon was admitted to the loop in time

to protect the test section from oxidation. The test section was removed, examined, rebuilt, and reinstalled. The loop has been repaired and is awaiting startup to complete its scheduled total operation of 10,000 hr.

Intermediate Water System Operation

A. M. Smith      M. E. Lackey  
M. M. Yarosh    A. G. Grindell

The IWS was operated very little during the quarter because attention of the available personnel was centered mainly on the alteration and rebuilding of the small water system and the two small potassium systems. However, near the end of the quarter, the heater rod bundle was removed from the facility and a dummy heater rod containing pressure taps for measuring the boiler pressure drop was installed. The dummy was substituted for a heater rod in the row next to the outermost row of rods. The boiler bundle will be reinstalled, and data on the boiler pressure drop will be obtained over a wide range of boiler operating conditions.

Intermediate Potassium System

M. M. Yarosh    P. A. Gnadt  
                  J. Zasler

IPS operating run 2 was terminated on December 27, 1965, because of Firerod heater failures,<sup>8</sup> and the nature of these failures indicated that a reevaluation of the fabrication techniques was in order.<sup>9</sup> In the interim period the first MgO-insulated heater bundle was reconditioned and installed in the boiler. This bundle had been removed after operating run 1 because internal insulation resistance of the rods limited the power to approximately 1 kw per rod.

---

<sup>8</sup>P. A. Gnadt, J. Zasler, and M. M. Yarosh, Intermediate Potassium System, pp. 65-76, Medium-Power Reactor Experiment Quart. Progr. Rept. Mar. 31, 1965, USAEC Report ORNL-3818, Oak Ridge National Laboratory.

<sup>9</sup>N. C. Cole, Firerod Development, pp. 131-134, Medium-Power Reactor Experiment Quart. Progr. Rept. Mar. 31, 1965, USAEC Report ORNL-3818, Oak Ridge National Laboratory.

The system was reflux cleaned, and when power was applied to the boiler, attempts to exceed the original 1-kw level were unsuccessful. As power was increased, the insulation resistance dropped to values considered unsafe for further operation. The turbine pump was then started and allowed to run at low power levels for 6.5 hr to establish that the system and the turbine pump unit were still operating satisfactorily.

Since a delay was expected before new boiler heater rods were available, a decision was made to remove the turbine pump (unit 2) for examination. This pump had operated in the cavitating mode for approximately 2577 hr and had been started 46 times. The results of examination of the turbine pump are covered in a preceding section on "Tests of Turbine Pumps for Boiling-Potassium Systems."

A new group of heater rods has now been obtained, and a new boiler bundle has been fabricated and installed. A high-temperature screening test of the resistance of the electrical insulation was made on each heater. Any heater with an insulation resistance less than 1.0 megohm at 1500°F was rejected. This screening test should eliminate the early failures encountered previously. The original Mark-1 turbine pump (unit 1) was modified to include the changes made to the second unit<sup>10</sup> and installed in the system. A 0- to 30-in. H<sub>2</sub>O pressure transmitter was installed on the turbine pump suction line to provide better accuracy in the measurement of this low pressure. A differential pressure transmitter was added to measure the pressure drop between the radiator jet pump outlet and the turbine pump suction to determine whether vapor bubbles are being carried through the lines to the turbine pump suction.

The system is scheduled for startup early in July 1966. The forthcoming operation will attempt to demonstrate the performance characteristics of the system at power levels up to the full rated output of 4 kw per rod.

---

<sup>10</sup>H. C. Young and A. G. Grindell, Tests of Turbine Pumps for Boiling Potassium Systems, pp. 59-65, Medium-Power Reactor Experiment Quart. Progr. Rept. Mar. 31, 1965, USAEC Report ORNL-3818, Oak Ridge National Laboratory.

Large Potassium System

W. F. Ferguson

The program for a large potassium system<sup>11</sup> was terminated because no funds were provided for FY-1967. System design was completed to provide design packages suitable for resumption of the program if the funding is restored in the future. Purchased materials and fabricated components were stored in marked containers and will be held until further notice.

Reactor Control-Plug Drive System

J. Foster      J. T. Meador

Measurements of the time-displacement relationship during scram drops of the control-plug assembly were continued. Modifications of the shock-absorber system were completed to eliminate the unsatisfactory deceleration characteristics observed in early drop tests. Some of the photographs of the time-displacement oscilloscope traces for the dropped assembly have been redrawn in Fig. 3.18 to exhibit the improvement in the decelerating action of the shock absorbers. These particular curves are for a drop of a 125-lb control-plug assembly from a height of about 5.6 in. The maximum velocity and deceleration values for curve A ( $v_A$  and  $a_A$ ) are 3.253 ft/sec and 55.4 ft/sec<sup>2</sup>, respectively, for the original shock absorbers. The corresponding values for curve B ( $v_B$  and  $a_A$ ) in Fig. 3.18 are 3.567 ft/sec and 42.6 ft/sec<sup>2</sup> for the modified shock absorbers. The shock absorber has a stroke of 2 in. and acts over the lower 2 in. of the control-plug travel. The performance exhibited by curve B is satisfactory and free from undesirable impact loads and noises.

The drop tests described above were made from a height of 5.65 in. because adjustments made in the Fabreeka pad thickness, in the design of the shock-absorber yoke and impact-spring assembly, and in the shock-absorber mounting reduced the full travel from 8 in. to this lower figure.

---

<sup>11</sup>S. I. Kaplan, Large Potassium System, pp. 44-45, Medium-Power Reactor Experiment Quart. Progr. Rept. Mar. 31, 1966, USAEC Report ORNL-3976, Oak Ridge National Laboratory.

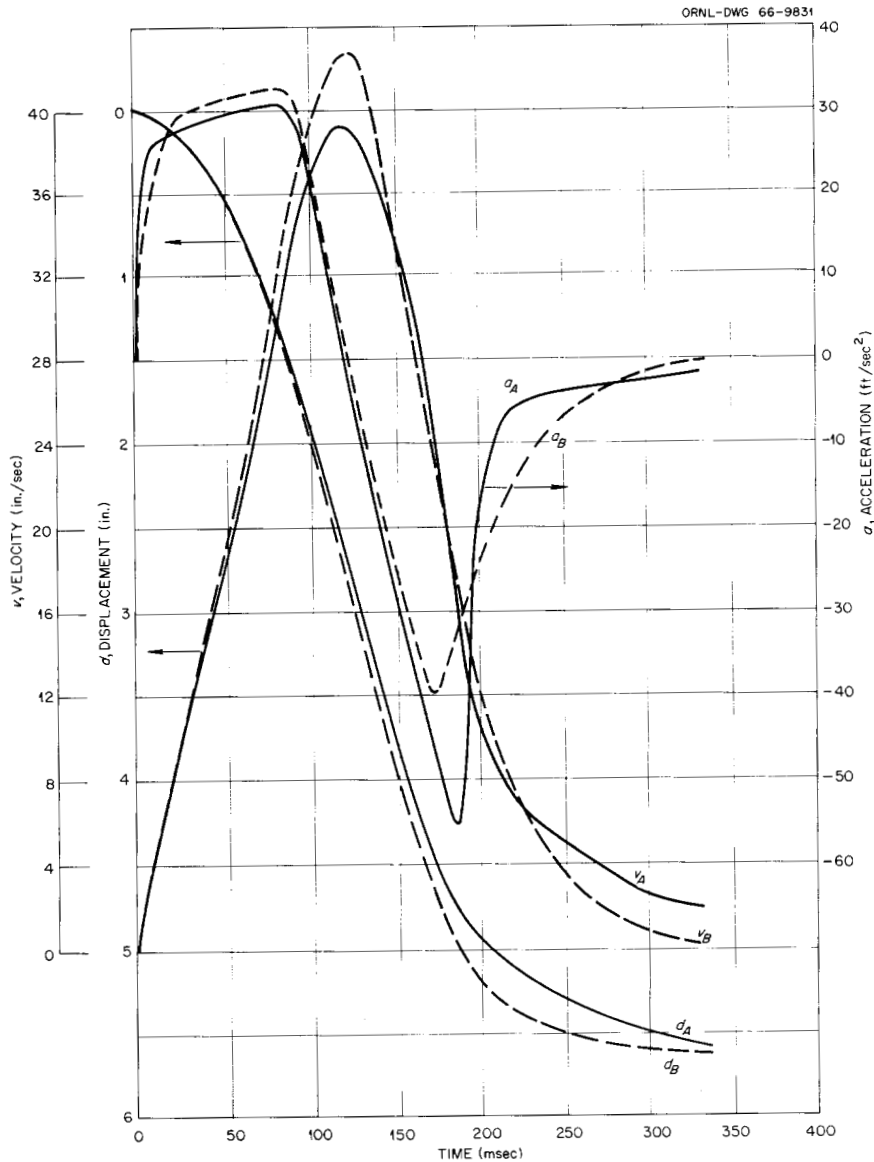


Fig. 3.18. Displacement, Velocity, and Acceleration Versus Time for Scram Tests of Reactor Control-Plug Assembly When Dropped 5.65 in.

Upon completion of these modifications and the tests described above, a spacer was made and installed to permit drop tests from the full 8-in. height, and such tests were made. Performance was satisfactory, as shown in the oscilloscope time-displacement trace data in Fig. 3.19. The maximum velocity and acceleration ( $v_C$  and  $a_C$ ) values are 4.95 ft/sec and 69.3 ft/sec<sup>2</sup>, respectively.

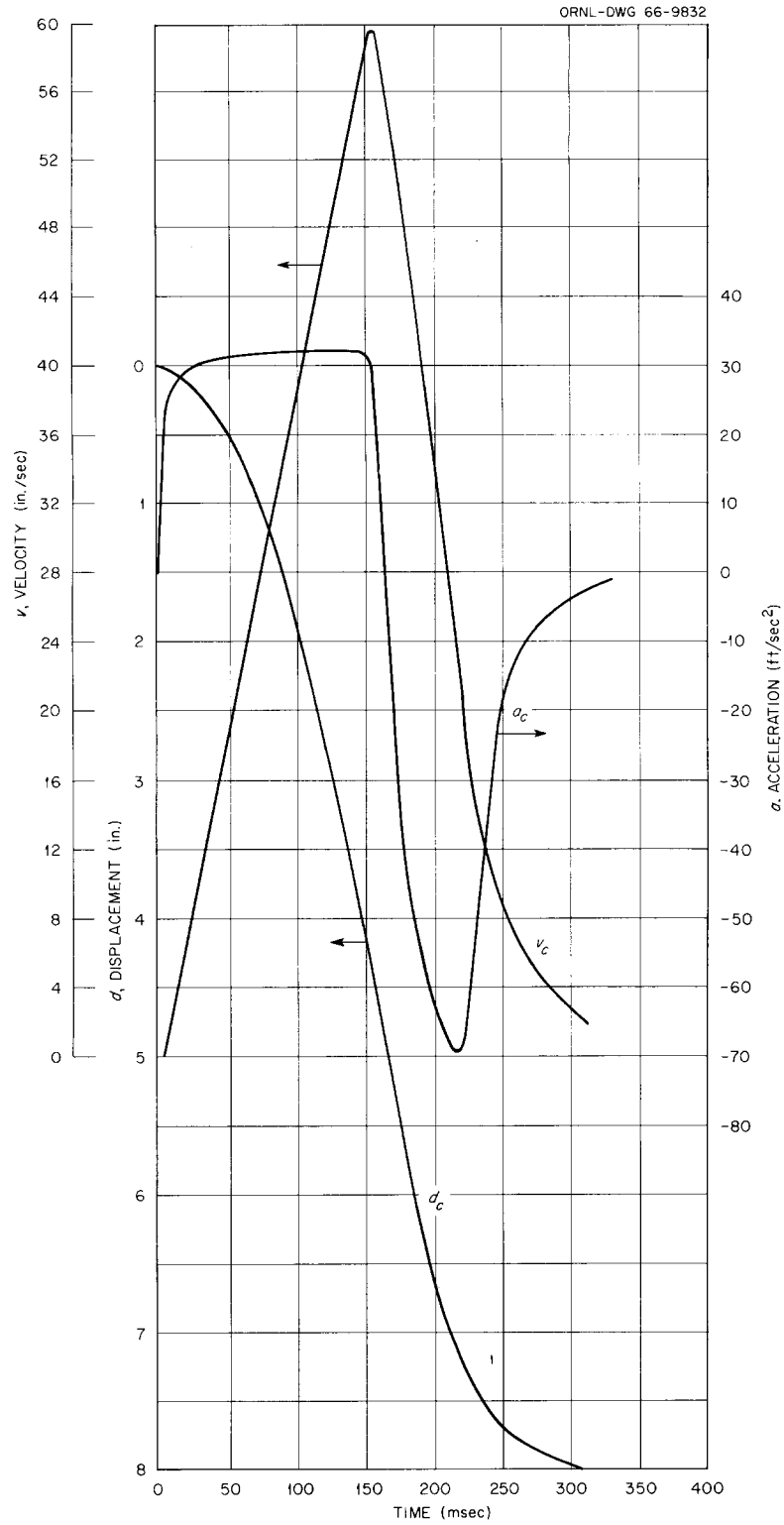


Fig. 3.19. Displacement, Velocity, and Acceleration Versus Time for Scram Tests of Reactor Control-Plug Assembly When Dropped 8.0 in.

A series of oscilloscope traces was also made to evaluate the magnet release time. The magnet used was the new one provided by the Instrumentation and Controls Division for this control drive system. For magnet currents ranging from 0.6 to 1.0 amp, the observed magnet release times varied from 60 to 80 msec. Release-time values for this magnet determined by the Instrumentation and Controls Division before installation were about 4.5 msec at 0.7 amp. It is believed that the difference is due largely to delays in the electrical system used in making the oscilloscope measurements. This belief is consistent with the fact that magnets developed in the past have had release times of less than 10 msec.

The Bendix synchro transmitters for coarse and fine control-plug position indication were received and installed on the gear box of the lead-screw drive. The assembly is shown in Figs. 3.20 and 3.21. Figure 3.22 shows a dismantled control drive and synchro-transmitter assembly.

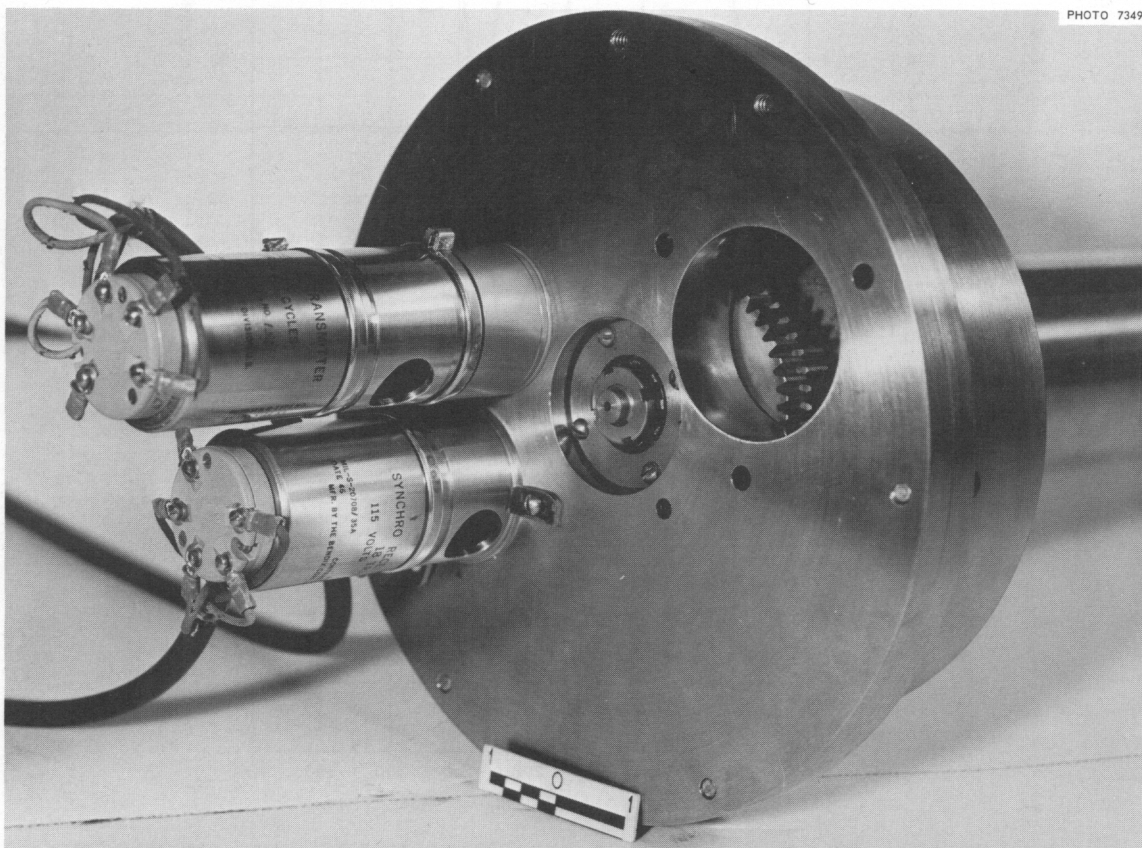


Fig. 3.20. Position Transmitters Mounted on Control-Plug Drive Gear Box.

~~CONFIDENTIAL~~  
PHOTO 73492

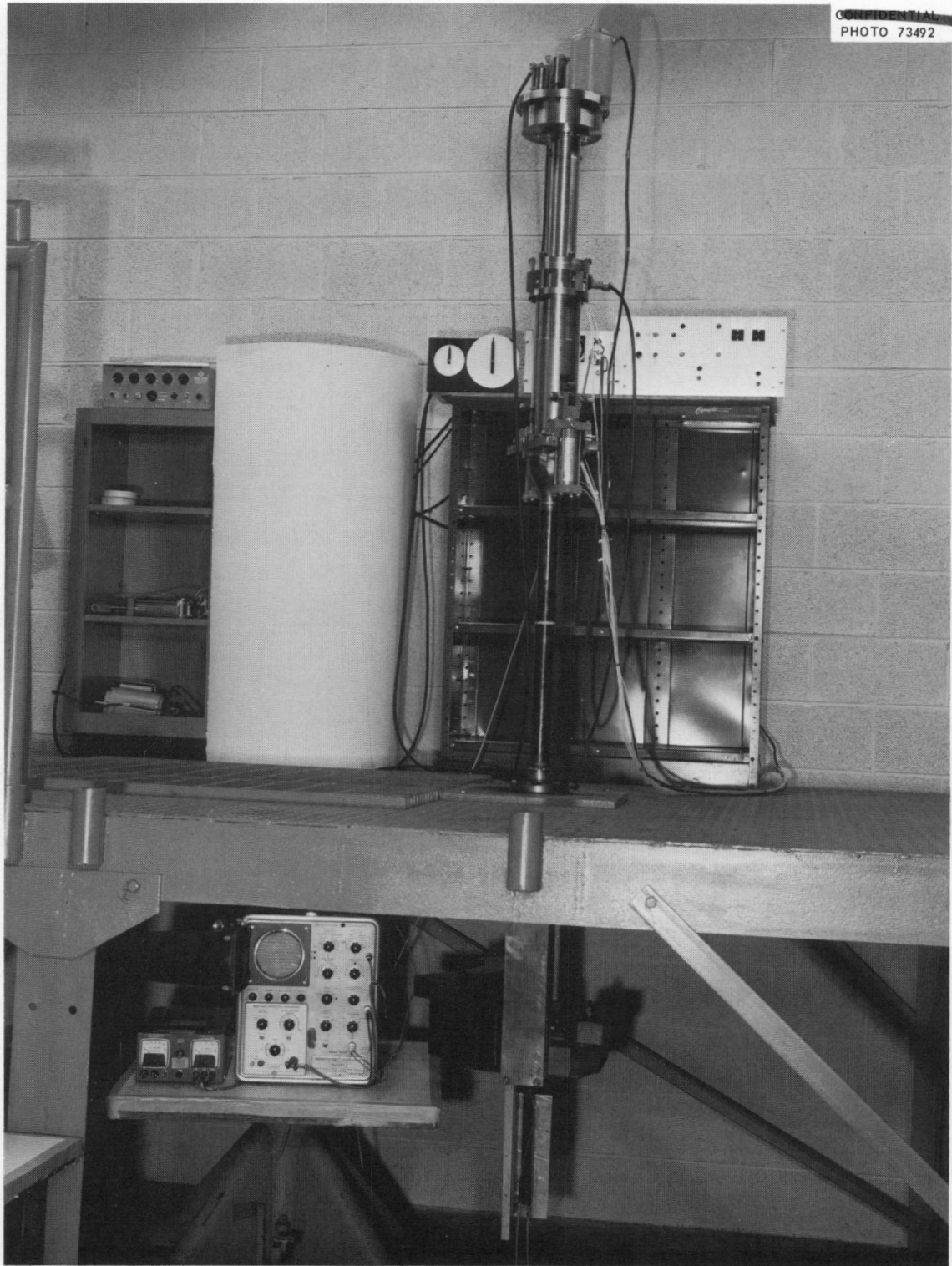


Fig. 3.21. Control-Plug Drive Assembly with Position Transmitters Mounted on Top.

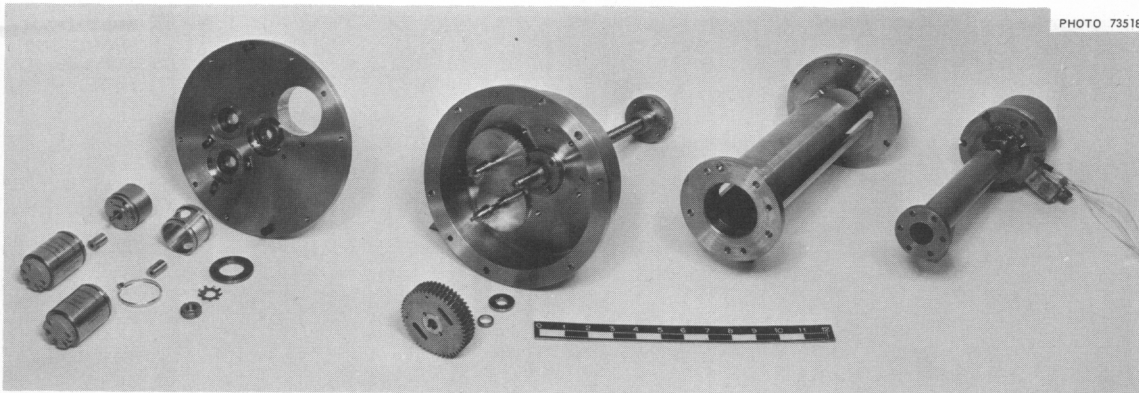


Fig. 3.22. Dismantled Control-Plug Drive Mechanism.

The transmitters worked satisfactorily in operating tests, and the read-out synchros gave good indications of control-plug position. The readout units with temporary dials and pointers attached are shown in Fig. 3.21.

#### Fuel Element Irradiation Tests

F. R. McQuilkin

Irradiation is continuing on extensometer test assembly 07-10 and on MPRE prototype fuel element capsules 03-9 and 06-9. Typical temperatures for the specimens in each of the assemblies, as indicated by thermocouples loosely banded to the specimen cladding surface, are listed in Table 3.2.

The extensometer capsule 07-10 is being power and temperature cycled once a week by retracting or inserting the capsule. Periodic measurements of the fuel stack height are being made when the capsule is inserted and retracted with the reactor at 30 Mw and when the reactor is at zero power. A summary of the test data is given in Fig. 3.23. (Similar data for the prior period were given in the previous report.<sup>12</sup>) The measurements suggest that the decreasing height of the UO<sub>2</sub> fuel stack has leveled off at a total shrinkage of the 9-in. fuel column of approximately 46 mils

---

<sup>12</sup>V. A. DeCarlo, F. R. McQuilkin, and R. L. Senn, Fuel Element Irradiation Tests, pp. 53-55, Medium-Power Reactor Experiment Quart. Progr. Rept. Mar. 31, 1966, USAEC Report ORNL-3976, Oak Ridge National Laboratory.

Table 3.2. Cladding Temperatures in Capsules 03-9, 06-9, and 07-10

Cladding Thermocouple Location	Temperature Element Designation	Temperature <sup>a</sup> (°F)		
		Capsule 03-9	Capsule 06-9	Capsule 07-10
At top end of capsule	TE X08	160 (71°C)	(b)	205 (96°C) <sup>c</sup>
At bottom end of spring	TE X07	210 (99°C)	223 (106°C)	238 (114°C) <sup>d</sup>
At top of fuel stack, front <sup>e</sup>	TE X06	823 (439°C)	717 (381°C)	1145 (618°C)
Between top and middle of fuel stack, back <sup>e</sup>	TE X03	1460 (793°C)	1398 (759°C)	1462 (794°C)
At middle of fuel stack, front	TE X04	1548 (842°C)	1462 (794°C)	1550 (843°C)
At middle of fuel stack, back	TE X01	(f)	1550 (843°C)	1554 (846°C)
Between middle and bottom of fuel stack, front	TE X05	1490 (810°C)	1445 (785°C)	1530 (832°C)
At bottom of fuel stack, back	TE X02	1222 (661°C)	1278 (692°C)	1235 (668°C)

<sup>a</sup>Temperatures were read June 28, 1966 when the capsules were at the positions given below. The thermal-neutron flux at these positions, measured with argon in a loop on the back outer surface of the capsules, is also given.

Capsule	Distance from Reactor Face (in.)	Thermal-Neutron Flux (neutrons/cm <sup>2</sup> ·sec)
03-9	5.36	$1.2 \times 10^{13}$
06-9	3.60	$8.7 \times 10^{12}$
07-10	3.60	$7.0 \times 10^{12}$

<sup>b</sup>Thermocouple failed June 1, 1965. The last temperature indicated prior to failure was 180°F (82°C).

<sup>c</sup>Near air gage.

<sup>d</sup>At upper bulkhead.

<sup>e</sup>Back denotes side away from reactor; front denotes side facing reactor.

<sup>f</sup>Thermocouple failed January 20, 1966. The last temperature indicated prior to failure was 1500°F (816°C).

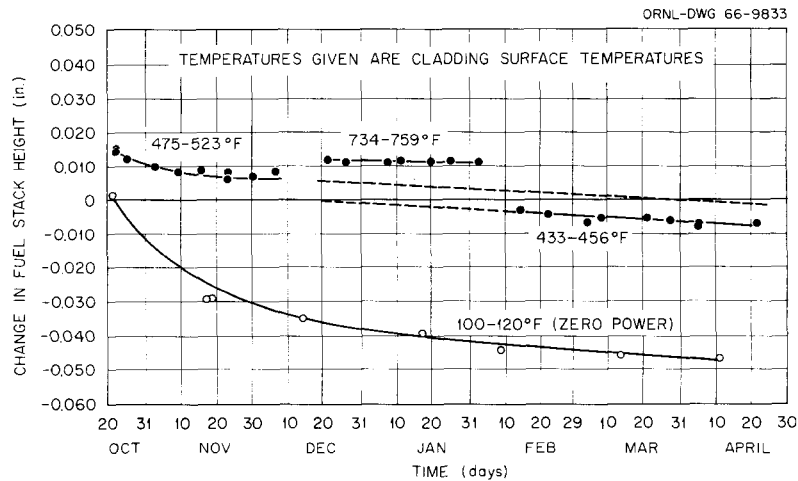


Fig. 3.23. Change in Fuel Stack Height with Irradiation Time for Capsule 07-10.

after 155 days of exposure. The exposure and burnup data for the three experiments are given in Table 3.3.

Table 3.3. Exposure and Burnup of Capsule  
03-9, 06-9, and 07-10 as of June 27, 1966

Capsule	Exposure at 30 Mw (equivalent days at full power)	Burnup (Mwd/MT of UO <sub>2</sub> )
03-9	407	5922
06-9	407	5922
07-10	220	3201

### Zero-Gravity Experiments

R. B. Korsmeyer

Separator 3, described previously,<sup>13</sup> was flown by Wright-Patterson Air Force Base in zero-gravity trajectories on April 26, May 11, and May 17, 1966 for a total of 26 maneuvers. The first 13 maneuvers, on April 26, were of a preliminary nature and provided the basis for selection of the operating conditions for the subsequent flights. The 14th and 15th maneuvers were performed on the May 11 flight and failed to yield useful data. The flight was aborted for reasons not related to the experiment. However, the final 11 maneuvers performed May 17 yielded the information desired and demonstrated that the separator design is basically sound. The direction of improvement is clearly indicated, and only straightforward development is required.

The separator design applies, of course, to the removal of liquid entrainment from its own vapor, whereas the zero-gravity experiment utilized a mixture of air and water for simplicity and economy. The utilization of a noncondensable fluid complicated the performance in that

<sup>13</sup>R. B. Korsmeyer, Zero-Gravity Vapor-Separator Experiments, pp. 79-81, Medium-Power Reactor Experiment Quart. Progr. Rept. Dec. 31, 1965, USAEC Report ORNL-3937, Oak Ridge National Laboratory.

dispersion of air bubbles in the liquid maintained in the expansion tank became a problem peculiar to this experiment.

Since no particular difficulty in zero-gravity experiments had been previously encountered with slinging of the droplets out of the air stream by centrifugation in the separator proper, the problem in the present experiment was the control of the free liquid in the expansion tank where the liquid removed was collected. Previous experiments had shown that this liquid had to be swirled in order to establish a stable free-liquid surface, and this was done by means of tangential water jets. Entrainment was provided by a full-cone water spray injected into the air stream just below the separator. Air flow was between 600 and 700 cfm, and the spray and swirl flows were separately variable up to a maximum of 13.5 gpm each.<sup>14</sup>

#### Flight Objectives

In the April 26 preliminary flight the bubble entrainment in the swirling liquid, caused by right-angle impingement of the entering water sheet (generated by water removed from the air stream) with the swirling liquid in the expansion tank, was generally cumulative in zero-gravity until the expansion tank became completely filled with a two-phase bubbly mixture. At this point the mass of bubbles was sufficient to decouple a large part of the liquid from the tangential jets. This resulted in loss of swirl and therefore loss of control over the liquid. The effect was regenerative in that the quantity of bubbles passing into the water pump eventually caused the pump to lose prime and the apparatus become inoperative. The objectives of the May zero-gravity flights were therefore to determine

1. the behavior of quiescent liquid in the expansion tank, mainly under the effect of surface tension, in view of the unusual tank geometry (no water flow),

---

<sup>14</sup>R. B. Korsmeyer, Zero-Gravity Experiments, pp. 94-96, Medium-Power Reactor Experiment Quart. Progr. Rept. Mar. 31, 1965, USAEC Report ORNL-3818, Oak Ridge National Laboratory.

2. a rough measure of the minimum swirl required to stabilize the liquid and to prevent excessive creeping at the feathered edges of the spinning fluid in the absence of interference from the impinging water sheet (i.e., no water spray),
3. a rough measure of the maximum water entrainment (i.e., lowest quality simulated vapor) that could be handled without loss of control of the free-liquid surface in the expansion tank through bubble accumulation.

### May 17 Flight Results

Quiescent Liquid Behavior. With the expansion tank filled nearly full (8 liters) and the liquid surface subject to some air buffeting, the free-liquid surface went out of control with the onset of weightlessness, as was expected. The air buffeting seemed to cause large masses of liquid to flop around, aided by random acceleration perturbations of the order of a few hundredths g, and to spill over into the air stream at the separator lip where the water sheet is normally skimmed from the air stream. To a lesser extent, some liquid escaped through the 3/8-in. holes provided to vent air from the expansion tank. This run definitely showed the need for swirl stabilization.

Behavior of Swirling Liquid Alone. Five runs were made in which the liquid inventory in the expansion tank was varied from 4 liters (about the minimum amount that will keep the tank drains well covered) to 8 liters and the swirl flow was varied from 9 to 13.5 gpm. The lowest average swirl velocity occurred with the combination of 8 liters and 9 gpm, and conversely the highest velocity occurred with minimum inventory and 13.5-gpm swirl flow. At low inventory the liquid was completely stable, with no observable creep away from the main rotating body at the edges where the velocity approaches zero. At high inventory some liquid occasionally detached itself from the main rotating body and crept along the wall under the action of surface tension to regions of greater curvature. In no event, however, did the liquid leave the expansion tank, even though it was subjected to the unavoidable random acceleration perturbations characteristic of aircraft zero-gravity flight.

Behavior of Swirling Liquid with Inflow of Separated Liquid. The remaining five runs were performed with both swirl and radial inflow of water to the expansion tank. Separated liquid flow (and removal rate) was varied from 9 to 13.5 gpm; this corresponded to vapor qualities entering the separator of about 34% down to 25%. In all cases the total water carryover in the air stream, including that which was reentrained, did not exceed about 0.5 liter/min, except in a few instances where excessive perturbations occurred from rough flying conditions. Separated liquid removal was about 99% effective, and the air stream leaving the separator had an equivalent vapor quality of between 97 and 98%.

As already indicated, the water sheet skimmed from the air stream aspirated enough bubbles into the swirling liquid to decouple part of the inventory from the swirl jets and thus reduce the swirl to almost nothing at the top (i.e., the part of the inventory farthest removed from the jets). As a result the two-phase mixture filled the tank completely, and some spillover occurred at the inside lip, in spite of the entering water sheet. It could not be determined whether the spillover was due, at least in part, to a known air flow assymetry in the region where it occurred.

In the runs with low inventory the bubble accumulation in the expansion tank eventually stopped the swirl jets because of excessive air entrainment into the water pump and its consequent loss of prime. With high inventory, however, run failure did not occur within the duration of the zero-gravity environment.

### Conclusions

The flight of May 17 demonstrated that the separator-expansion tank design is basically sound. Improvements in tank geometry are indicated to the end that the swirl velocity may be reduced and still maintain a stable liquid in the expansion tank, particularly at low inventory.

Although at high inventory the system operated with reasonable stability during the 25- to 30-sec zero-gravity available, the results do not establish that the free-liquid surface would remain stable for long periods in a zero-graviey environment even though small, random acceleration perturbations did not interfere.

~~CONFIDENTIAL~~

The question of long-term stability seems to be connected with the bubble entrainment problem since passage of the bubbles in quantity through the liquid circulating system degrades the system's performance, even to the point of shutting it down. While it appears feasible to alter the expansion tank geometry to eliminate virtually all bubbles in the liquid leaving the expansion tank, a more direct and satisfactory solution is to do away with the circulating air all together. A liquid in contact with only its own saturated vapor in the expansion tank will not support such bubbles because the liquid is of necessity at a slightly lower temperature by virtue of the cooler flow emanating from the swirl jets. This condition is the one for which the separator is designed and needed.

Although a flight-qualified experiment with water and steam in place of water and air is substantially more complex than the very simple package that was flown, the power requirements are modest and the design appears to be practical if the vapor is circulated by a blower instead of by boiling.

## 4. MATERIALS

G. M. Adamson

Natural-Circulation Boiling-Potassium Loop Tests

J. H. DeVan      D. H. Jansen

Compatibility tests of small stainless steel loops operated with boiling potassium were continued. The current series of tests is being conducted to determine the effects of oxygen contaminants deliberately added to the potassium bath on the corrosion rate of the various loop components.<sup>1</sup> The status of this series of tests is indicated in Table 4.1.

Loop NCL-10

Preliminary results of test NCL-10 were reported previously.<sup>2</sup> The loop was constructed of type 316 stainless steel and contained alternate types 316 and 347 stainless steel sleeve-type inserts in the condenser-subcooler leg. Operation of the loop, which was scheduled for 3000 hr, was terminated after 2750 hr by a potassium leak in the lower boiler region.

A chemical analysis of a portion of the boiler wall exposed to the potassium bath was performed to ascertain the nature of the Widmanstätten precipitate lining the surface. Results indicated carbon depletion similar to that observed in other tests operated under these conditions, although a higher carbon content was detected at the surface; this is attributed to carburization from CO<sub>2</sub> and CO during the ingress of air at the time of the failure. Chemical analyses on a second series of incremental turnings taken from the failure region indicate a heavy concentration of nitrogen, 0.76 wt %, at the inside loop surface. The nitrogen

---

<sup>1</sup>J. H. DeVan and D. H. Jansen, Corrosion of Conventional High-Temperature Alloys in Natural-Circulation Boiling-Potassium Loop Tests, pp. 82-84, Medium-Power Reactor Experiment Quart. Progr. Rept. June 30, 1965, USAEC Report ORNL-3860, Oak Ridge National Laboratory.

<sup>2</sup>J. H. DeVan and D. H. Jansen, Natural-Circulation Boiling-Potassium Loop Tests, pp. 59-64, Medium-Power Reactor Experiment Quart. Progr. Rept. Mar. 31, 1966, USAEC Report ORNL-3976, Oak Ridge National Laboratory.

Table 4.1. Status of Stainless Steel  
Boiling-Potassium Test Loops

Loop	Type of Stainless Steel Loop Material	Insert Material	Status	Miscellaneous Information
NCL-9	316	Alternate types 316 and 347 stainless steel	Test terminated at 3000 hr as scheduled	3500 ppm O <sub>2</sub> added to bath
-10	316	Alternate types 316 and 347 stainless steel	Test terminated at 2750 hr; loop leaked	Purified potassium used; 20 ppm O <sub>2</sub>
-11	304	Alternate type 304 stainless steel and TZM	Test terminated at 3000 hr as scheduled	Purified potassium used
-12	304	Alternate type 304 stainless steel and TZM	Loop operating	3100 ppm O added as K <sub>2</sub> O
-13	304	Alternate type 304 stainless steel and TZM	Loop operating	4550 ppm O added as K <sub>2</sub> O
-14	304	Alternate type 304 stainless steel and TZM	Loop fabricated and ready for assembly	Potassium to be spiked; 10,000 ppm O <sub>2</sub>
-15	316	Alternate types 316 and 347 stainless steel	Planned	To replace loop NCL-10

content dropped off uniformly with depth into the pipe wall (0.24 wt % at a depth of 20 mils). These results indicate that the heavy Widmanstätten structure concentrated at the inner surface is a nitride formed by the ingress of nitrogen during the leak. This nitride structure was not observed in other portions of the loop some distance from the failure site.

#### Loop NCL-11

Loop NCL-11 was fabricated from type 304 stainless steel and contained tight-fitting alternate type 304 stainless steel and TZM alloy sleeve-type inserts in the condenser-subcooler leg. The loop was charged with purified potassium, and it operated for a scheduled 3000 hr at design conditions.

The weight change profile of the stainless steel inserts is shown in Fig. 4.1, along with values for the weight changes in the TZM alloy. A weight loss in the condensing region and a weight gain in the subcooler,

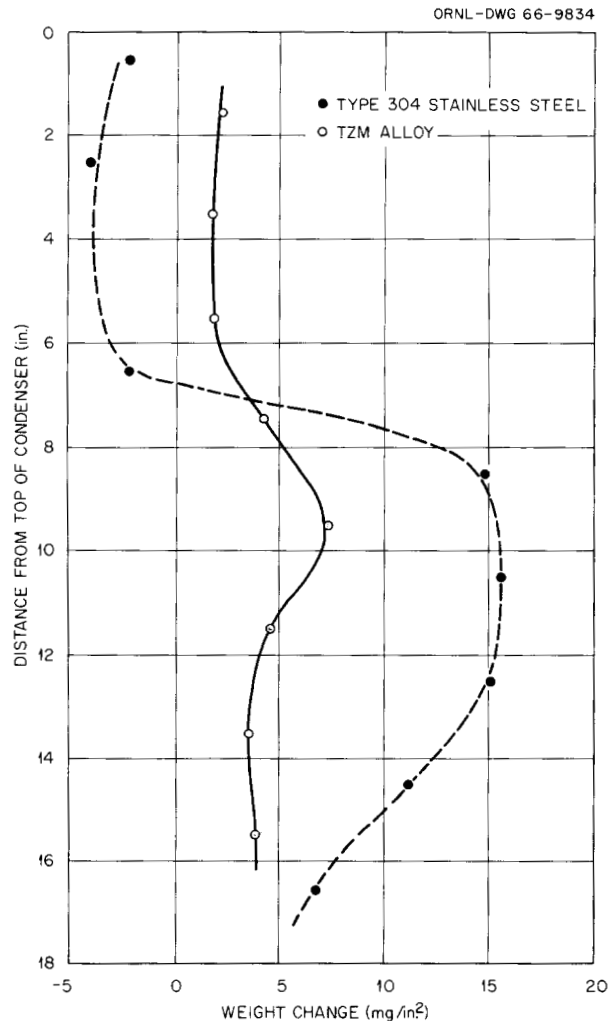


Fig. 4.1. Profile of Weight Changes of Type 304 Stainless Steel and TZM Alloy Inserts from the Condenser and Subcooler Leg of a Type 304 Stainless Steel Boiling-Potassium Loop Operated at a Condenser Temperature of 1600°F for 3000 hr. Purified potassium was used.

characteristic of tests of this type, were detected on the stainless steel insert specimen. All the TZM alloy inserts showed uniform weight gains that were apparently caused by deposition of components of the stainless steel, as described below.

The inner surfaces of the TZM alloy inserts from the condenser, liquid surface, and subcooler regions were checked spectrographically in an effort to determine the nature of the weight gains illustrated in Fig. 4.1. These

specimens all picked up small amounts of silicon, iron, nickel, and chromium. The major contaminant was chromium, and it was heaviest at the liquid level in the condenser. This is in accord with the higher weight gain exhibited by specimens in this region. The exposed surface of the TZM insert with the greatest weight gain is shown in Fig. 4.2.

Results of metallographic examination of the other stainless steel components (boiler, vapor line, and subcooler) indicate very limited corrosion or dissolution attack. The site of heaviest corrosion was on the lower boiler wall in the vicinity of the nucleator (shown in Fig. 4.3).

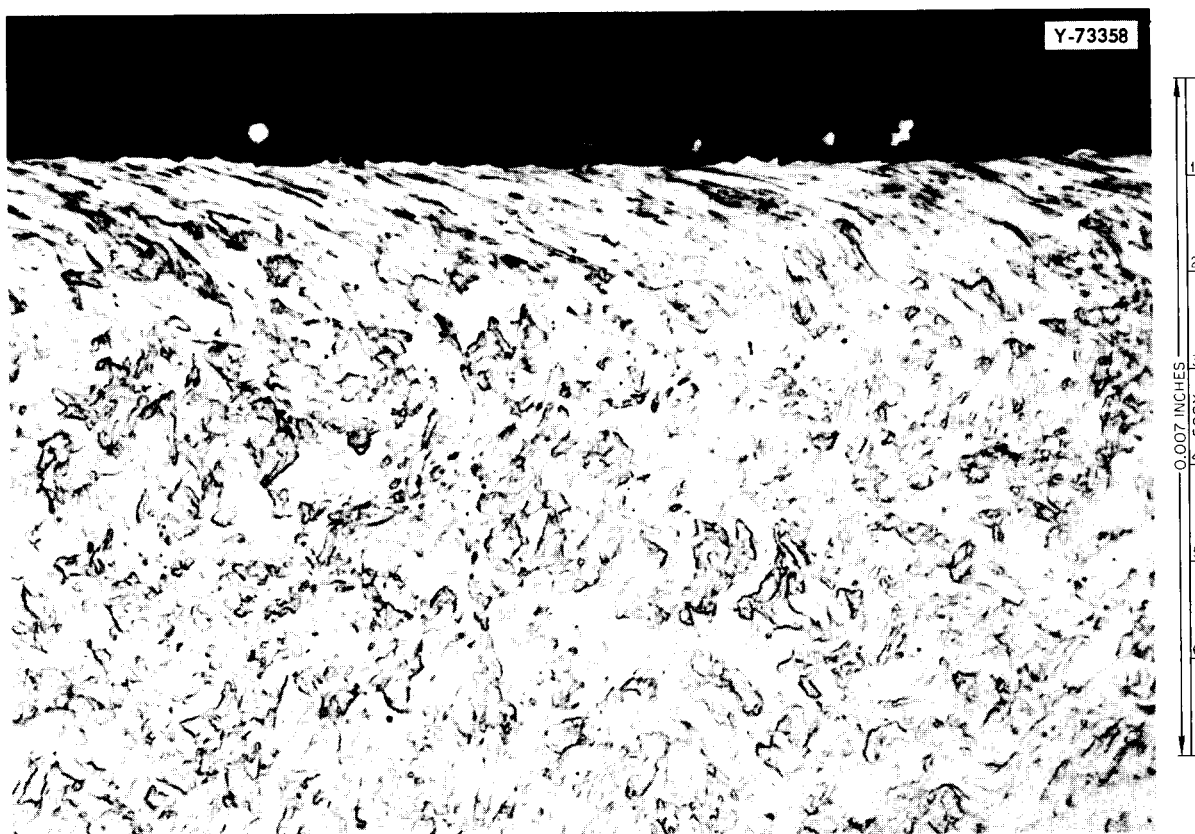


Fig. 4.2. Inner Surface of TZM Alloy Insert Taken from the Vicinity of the Liquid Surface in the Condenser-Subcooler Leg of the Boiling-Potassium Loop. The weight gain of this specimen is attributed to the slight crystalline deposit at the edge. Etchant:  $H_2SO_4-H_2O_2-H_2O$ . (Confidential with caption)

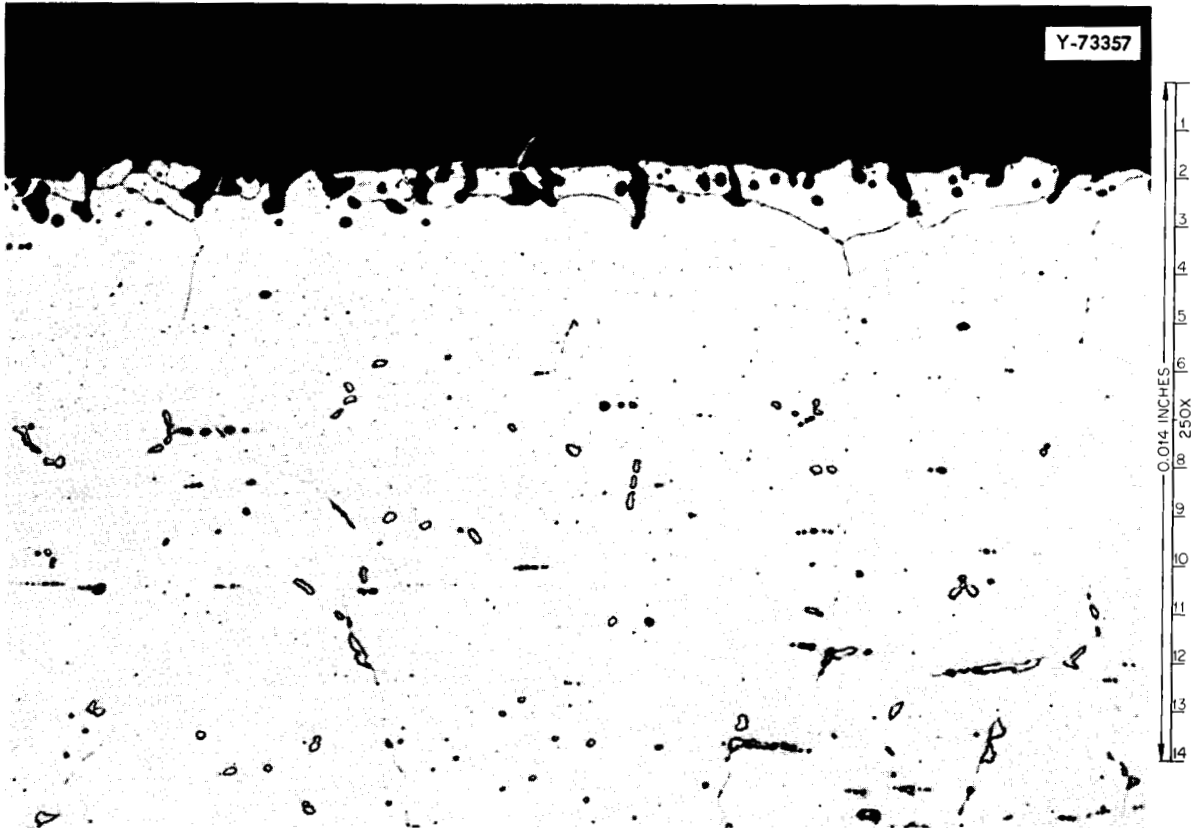


Fig. 4.3. Inner Surface of Type 304 Stainless Steel Boiler Wall Adjacent to the Nucleator Showing Heaviest Corrosion Found on Any Portion of the Boiling-Potassium Loop. Etchant:  $\text{HNO}_3$ -HCl-lactic acid. (Confidential with caption)

Brazing Alloy Development

C. W. Fox

The development and evaluation of experimental nickel-base brazing alloys is continuing. Results of additional Miller-Peaslee shear tests are shown in Table 4.2. These tests complete the series discussed previously.<sup>3</sup> During this period, the four different alloys being considered were tested after aging for 1000 hr at 1500°F. The results reported previously for as-brazed specimens are also listed in Table 4.2.

<sup>3</sup>C. W. Fox, Brazing Alloy Development, pp. 75-76, Medium-Power Reactor Experiment Quart. Progr. Rept. Mar. 31, 1966, USAEC Report ORNL-3976, Oak Ridge National Laboratory.

Table 4.2. Results of Miller-Peaslee Shear Tests of Type 316  
Stainless Steel Brazed with Nickel-Germanium Type Alloys  
and Tested at Room Temperature

Alloy Composition (wt %)	Flow Point (°F)	Room-Temperature Shear Strength <sup>a</sup> (psi)		Shear Strength <sup>a</sup> at 1500°F, As Brazed (psi)
		As Brazed	Aged 1000 hr at 1500°F	
65 Ni-20 Ge-5 Fe-5 Cr-5 Si	1940	37,250	40,000	14,500
70 Ni-20 Ge-5 Fe-5 Si	1995	34,100	49,000	14,000
65 Ni-25 Ge-5 Cr-5 Fe	1995	32,500	49,950	9,000
55 Ni-25 Ge-20 Nb	2012	29,600	25,700	14,300

<sup>a</sup>Average for two specimens.

These alloys exhibit good strength in the as-brazed condition at room temperature and at 1500°F and even better strength in the as-brazed-and-aged condition. Three of the four alloys show a strengthening effect as a result of the high-temperature aging treatment.

An additional series of nickel-base brazing alloys has been formulated with slightly modified compositions. This series constitutes an attempt to optimize the desirable characteristics in this alloy system. Melting-point determinations and metallographic evaluations of these alloys are in progress.

#### Behavior of Stainless Steel Welds Under Cyclic Loading

D. A. Canonico      R. W. Swindeman

A fatigue study of stainless steel weldments is continuing. Since the data were last reported,<sup>4</sup> the fatigue properties of the wrought type 304 stainless steel used in the program have been accumulated. These data, along with those for the as-welded and postweld heat-treated specimens, are given in Table 4.3 and are plotted in Fig. 4.4.

<sup>4</sup>D. A. Canonico and R. W. Swindeman, Behavior of Stainless Steel Welds Under Cyclic Loading, pp. 111-113, Medium-Power Reactor Experiment Quart. Progr. Rept. Dec. 31, 1965, USAEC Report ORNL-3937, Oak Ridge National Laboratory.

Table 4.3. Summary of Fatigue Data for Wrought Type 304  
Stainless Steel at Room Temperature

Test cycle frequency - 10 cps

Specimen No.	Specimen Type	Average Plastic Strain (in./in.)	Stress (psi)	Cycles to Failure	Failure Location
13	Base metal	0.013	85,000	2,195	Radius
1	Base metal	0.0086	70,000	7,776	Radius
12	Base metal	0.0049	57,500	18,640	Radius
2	Base metal	0.0049	60,500	20,200	Radius
16	Base metal	0.00325	69,000	33,400	Radius
8	Base metal	0.0032	56,500	56,790	Gage length
15	Base metal	0.00325	55,500	144,110	Radius
10	Base metal	0.00195	55,500	236,330	Gage length
13A	As-welded joints	0.0059	81,000	2,440	Gage length
15A	As-welded joints	0.0044	82,000	4,600	Radius
5A	As-welded joints	0.0035	81,000	3,900	Radius
3A	As-welded joints	0.0034	81,000	10,500	Radius
5B	As-welded joints	0.0026	80,000	15,900	Radius
15B	As-welded joints	0.0021	79,000	14,820	Radius
3B	As-welded joints	0.0017	74,500	76,200	Radius
14A	Welded and postweld heat-treated joints	0.0098	81,000	1,860	Gage length
12B	Welded and postweld heat-treated joints	0.0059	75,000	5,370	Gage length
4A	Welded and postweld heat-treated joints	0.0044	60,500	10,500	Gage length
8B <sup>a</sup>	Welded and postweld heat-treated joints	0.0035	63,000	25,050	Gage length
10B <sup>a</sup>	Welded and postweld heat-treated joints	0.0034	62,000	17,900	Gage length
6B	Welded and postweld heat-treated joints	0.0026	60,500	30,000	Gage length
8	Welded and postweld heat-treated joints	0.022	58,000	62,190	Gage length
2B	Welded and postweld heat-treated joints	0.0019	73,000	70,470	Gage length
10A	Welded and postweld heat-treated joints	0.0017	58,500	496,000	Weld

<sup>a</sup>Failed in heat-affected zone.

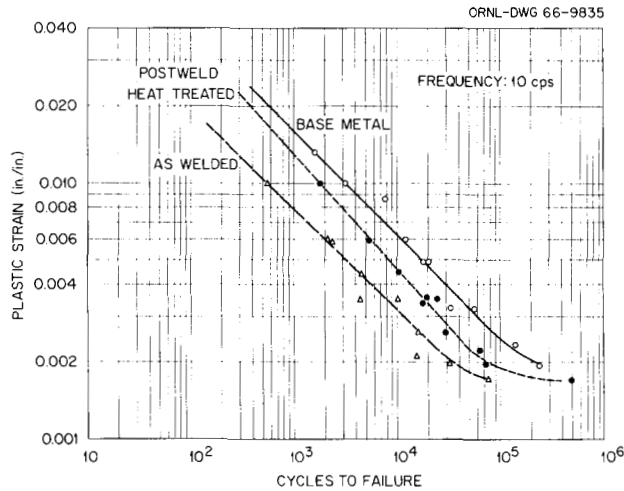


Fig. 4.4. Results of Fatigue Tests of Type 304 Stainless Steel Weldments at Room Temperature. Filler metal was type 308 stainless steel.

It may be seen that the fatigue life of the base metal is over five times greater than that of the as-welded specimens for the same plastic strain. A postweld heat treatment of the specimens improves the fatigue life of the weldment to the point where there is a difference of less than a factor of 2.

These results are startling in that the failures (except for specimen 10A, which failed in the weld metal, and specimens 8A, 8B, and 10B, which failed in the heat-affected zone) all occurred in the base metal. The results of this study seem to indicate that the presence of the weld metal tends to concentrate the strain in the base metal and thereby cause premature failure. The postweld heat treatment tends to normalize the properties across the weldment and relieve this condition.

The study has been expanded to include the effect of temperature on the fatigue life of the weldments. Data are being gathered for 1000°F and 1200°F at 2-cps as well as the 10-cps test frequency. Preliminary data are available and are reported in Table 4.4. Only two elevated-temperature tests have been run at 10 cps. Base-metal specimens were used, and both had fatigue lives corresponding to those obtained at room temperature. Data for the as-welded condition were collected for 0.006-in./in. plastic strain at a frequency of 2 cps. Data have also been obtained at the same strain and frequency for the postweld heat-treated

Table 4.4. Results of Tests to Determine the Effect of Elevated Temperatures on the Fatigue Life of Type 304 Stainless Steel Weldments

Material	Average Plastic Strain (in./in.)	Cycles to Failure				
		At Room Temperature and 10 cps	At 1000°C		At 1200°F	
			2 cps	10 cps	2 cps	10 cps
Base metal	0.01	3,200				
As-welded joints		550				
Postweld heat-treated joints		1,800				
Base metal	0.006	12,000		13,000		12,000
As-welded joints		2,200	9,600		2,300	
Postweld heat-treated joints		5,500	20,000		13,600	
Base metal	0.0035	50,000				
As-welded joints		9,000				
Postweld heat-treated joints		19,000				

specimens. These data show definite temperature effects, and more data must be collected to substantiate the results.

Bore-Seal Development

N. C. Cole

One of the major limitations at present in the development of electrical generators for use in potassium vapor is the lack of a corrosion-resistant seal between the ceramic bore seal and the stainless steel components of the stator to isolate the potassium vapor in the rotor cavity from the windings of the stator. A generator being considered for study in potassium systems has a bore of AD-99 Al<sub>2</sub>O<sub>3</sub>. The seal joint is made by metallizing the ceramic and copper brazing it to Ceramvar, which, in turn, is welded to the stainless steel. The only corrosion protection for the joint is a nickel electroplate. Two types of metallizing are used as the first step in building this complex assembly. In the areas to be brazed, a molybdenum-manganese-silicon solution is applied and then fired to form a glassy phase. Over other areas of the ceramic,

a molybdenum-manganese-titanium solution is used to promote adherence of the nickel plating.

Small specimens representing several different seal manufacturing processes were obtained to permit potassium-vapor compatibility tests. After exposure to vapor, the specimens were helium leak tested for seal soundness. A description of the various samples was presented in a previous report,<sup>5</sup> and the results of testing are summarized in Table 4.5.

It is apparent that molybdenum-manganese metallizing, regardless of whether silicon or titanium is used in the solution, is highly vulnerable to potassium vapor at temperatures of 600°F or higher. The nickel electroplate cannot be expected to furnish sufficient protection as it now exists on the LMCD-2 bore seal because of its thin and incomplete coverage. Based on these tests, it is concluded that a 3-mil tungsten vapor plate applied over the nickel electroplate should provide adequate protection from potassium vapor up to 1000°F for 1000 hr. The active metal braze, 82% Ti-18% Cu, should also be applicable for potassium service at test temperatures.

#### Analysis of IPS Filter Deposit

##### B. Fleischer

The filter in the bearing feed line of the IPS turbine pump circuit was removed and opened for routine inspection at the end of test run 3. The filter had been in the system for approximately 2600 hr during test runs 2 and 3, and there was no evidence of filter plugging prior to removal.

Visual examination of the filter element, Fig. 4.5, showed the presence of a thin layer of a fine-grained grayish deposit that covered most of the filter-screen surface, except that portion directly in front of the inlet line. To assess the nature of the deposit and the reason for its presence, several analyses were performed. Approximately 35 mg of

---

<sup>5</sup>N. C. Cole, Bore-Seal Tests, pp. 107-109, Medium-Power Reactor Experiment Quart. Progr. Rept. Sept. 30, 1965, USAEC Report ORNL-3897, Oak Ridge National Laboratory.

Table 4.5. Effect of Potassium Vapor on Various Bore-Seal Prototypes  
After 1000 hr of Exposure at 600 and 1000°F

Description of Bore-Seal Prototype	Corrosive Attack <sup>a</sup>				Helium Leakage			
	Test 1		Test 2		Test 1		Test 2	
	At 600°F	At 1000°F	At 600°F	At 1000°F	At 600°F	At 1000°F	At 600°F	At 1000°F
Metallized AD-99 Al <sub>2</sub> O <sub>3</sub> copper brazed to Ceramvar	C	C			Yes	Yes		
Metallized AD-99 Al <sub>2</sub> O <sub>3</sub> copper brazed to Ceramvar and covered by nickel electroplate	C	B	B	B	Yes	No	No	No
Metallized AD-99 Al <sub>2</sub> O <sub>3</sub> copper brazed to Ceramvar, covered with nickel electroplate, and then vapor plated with tungsten <sup>b</sup>	C	B	A	A	Yes	No	No	No
Metallized AD-99 Al <sub>2</sub> O <sub>3</sub> copper brazed to Ceramvar, covered with nickel electroplate, and then plasma sprayed with nickel aluminide	C	C	Corroded from side not tungsten plated		Yes	Yes		
Lucalox Al <sub>2</sub> O <sub>3</sub>	A	A			No	No		
General Atomic's Columbian to Lucalox, exposed, copper-brazed joint		A				No		
Ei-3 Al <sub>2</sub> O <sub>3</sub> brazed with 82% Ti-18% Cu brazed to Ceramvar (active metal braze)			A	A			No	No

<sup>a</sup>A = No apparent corrosion.

B = corroded through most of thickness via metallized layer.

C = Corroded through entire thickness via metallized layer.

<sup>b</sup>Test 1 specimen had only one side coated with tungsten.

Test 2 specimen had both sides tungsten plated.



Fig. 4.5. Filter Element and Canister from Bearing Feed Line of IPS Turbine-Pump Piping.

deposit was mechanically dislodged from the filter, and several samples were analyzed by x-ray diffraction. The major portion of the deposit was used to determine the fraction of water-soluble elements present and the composition of the water-soluble species and insoluble portions by quantitative analysis.

The composition of the water-soluble and insoluble portions of the deposit are shown in Table 4.6. The water-soluble portion accounted for about 29% of the sample weight and was primarily composed of  $K_2CO_3$  and  $KHCO_3$ . The undissolved portion was composed primarily of chromium and significant fractions of oxygen, potassium, iron, and molybdenum.

Table 4.6. Composition of Water-Soluble  
and Undissolved Portions of  
Deposit on IPS Filter

Species in Deposit	Water-Soluble Portion (%)	Undissolved Portion (%)	Total (%)
$K_2CO_3$	23.4		23.4
$KHCO_3$	14.2		14.2
K	0.3	4.5	4.8
Cr	0.5	33.7	34.2
Mo	0.5	3.4	3.9
Si	0.2		0.2
Fe	0.1	10.2	10.3
Ni		0.6	0.6
O		5.9	5.9
C		1.1	1.1

The oxygen content of the insoluble fraction is of particular interest. A review of oxygen analysis data for potassium samples taken during cleanup and operation failed to reveal any definite incidence of contamination. The failure to detect contamination, however, does not rule out its occurrence. An insufficient number of data points, inadequate sampling techniques, or erroneous analysis could prevent its detection. Also, rapid reaction of oxygen with the construction materials and deposition of oxygen in another portion of the system in the form of a corrosion

product oxide(s) could render sampling ineffective for detection of contamination. Experience from the SNAP-8 corrosion loop program<sup>6</sup> indicates that the reaction rate is fast with oxygen-contaminated NaK and stainless steel at 1300°F. At 1000°F, which is the temperature used for reflux cleaning of the IPS, it is conceivable that reaction rates are also rapid. Since a significant fraction of oxygen was found in the deposit, it is believed that oxygen contamination occurred during some phase of repair, cleanup, or operation, and this was responsible for inducing the corrosion reactions that lead to the deposits.

---

<sup>6</sup>H. W. Savage et al., SNAP-8 Corrosion Program Summary Report, USAEC Report ORNL-3898, p. 90, Oak Ridge National Laboratory.

Previous reports in this series are:

- ORNL-3270 Space Power Program Progress Report for Period Ending December 31, 1961
- ORNL-3337 Space Power Program Progress Report for Period Ending June 30, 1962
- ORNL-3420 Space Power Program Progress Report for Period Ending December 31, 1962
- ORNL-3489 Space Power Program Progress Report for Period Ending June 30, 1963
- ORNL-3534 Medium-Power Reactor Experiment Progress Report for Period July 1, 1963 to September 30, 1963
- ORNL-3571 Space Power Program Progress Report for Period Ending December 31, 1963
- ORNL-3641 Medium-Power Reactor Experiment Progress Report for Period January 1, 1964 to March 31, 1964
- ORNL-3683 Space Power Program Progress Report for Period Ending June 30, 1964
- ORNL-3748 Medium-Power Reactor Experiment Progress Report for Period Ending September 30, 1964
- ORNL-3774 Medium-Power Reactor Experiment Progress Report for Period Ending December 31, 1964
- ORNL-3818 Medium-Power Reactor Experiment Progress Report for Period Ending March 31, 1965
- ORNL-3860 Medium-Power Reactor Experiment Progress Report for Period Ending June 30, 1965
- ORNL-3897 Medium-Power Reactor Experiment Progress Report for Period Ending September 30, 1965
- ORNL-3937 Medium-Power Reactor Experiment Progress Report for Period Ending December 31, 1965
- ORNL-3976 Medium-Power Reactor Experiment Progress Report for Period Ending March 31, 1966



ORNL-4018

C-93a -- Advanced Concepts for Future  
Application -- Reactor Experiments  
M-3679 (49th ed., Rev.)

Internal Distribution

- |                         |   |
|-------------------------|---|
| 1. G. M. Adamson        | 35. R. N. Lyon                            |
| 2. S. E. Beall          | 36. H. G. MacPherson                      |
| 3. M. Bender            | 37. R. E. MacPherson                      |
| 4. D. S. Billington     | 38. F. C. Maienschein                     |
| 5. A. L. Boch           | 39. H. C. McCurdy                         |
| 6. R. B. Briggs         | 40. J. T. Michalczo                       |
| 7. A. D. Callihan       | 41. J. W. Michel                          |
| 8. C. E. Center (K-25)  | 42. A. J. Miller                          |
| 9. C. J. Claffey        | 43. K. Z. Morgan                          |
| 10. W. B. Cottrell      | 44. M. L. Nelson                          |
| 11. F. L. Culler        | 45. A. M. Perry                           |
| 12. J. H. DeVan         | 46. P. H. Pitkanen                        |
| 13. E. P. Epler         | 47. A. Rupp                               |
| 14. J. Foster           | 48. G. Samuels                            |
| 15. A. P. Fraas         | 49. A. W. Savolainen                      |
| 16. L. C. Fuller        | 50. E. D. Shipley                         |
| 17. W. R. Grimes        | 51. O. Sisman                             |
| 18. A. G. Grindell      | 52. M. J. Skinner                         |
| 19. E. Guth             | 53. O. L. Smith                           |
| 20. W. O. Harms         | 54. A. H. Snell                           |
| 21. M. R. Hill          | 55. I. Spiewak                            |
| 22. H. W. Hoffman       | 56. R. L. Stephenson                      |
| 23. R. S. Holcomb       | 57. G. M. Tolson                          |
| 24. A. Hollaender       | 58. D. B. Trauger                         |
| 25. L. B. Holland       | 59. J. J. Tudor                           |
| 26. R. F. Hyland        | 60. A. M. Weinberg                        |
| 27. W. H. Jordan        | 61. J. C. White                           |
| 28. S. I. Kaplan        | 62. M. M. Yarosh                          |
| 29. J. J. Keyes         | 63. F. C. Zapp                            |
| 30. M. E. Lackey        | 64-65. Y-12 Document Reference<br>Section |
| 31. C. E. Larson (K-25) | 66-68. Central Research Library           |
| 32. M. E. LaVerne       | 69-118. Laboratory Records Department     |
| 33. R. S. Livingston    | 119. Laboratory Records, LRD-RC           |
| 34. M. Lundin           |   |

External Distribution

120. Division of Research and Development, AEC, ORO  
121-122. Reactor Division, AEC, ORO  
123-240. Given distribution as shown in M-3679 (49th ed., Rev.) under  
Advanced Concepts for Future Application -- Reactor Experiments  
category

[REDACTED]

~~RESTRICTED DATA~~

This document contains Restricted Data as defined in the Atomic Energy Act of 1954. ~~Its transmission, disclosure, or its contents in any manner to an unauthorized person is prohibited.~~

~~CONFIDENTIAL~~